SPANBETON

TU Delft

FINITE ELEMENT MODELLING OF SKEW SLAB-GIRDER BRIDGES

Thesis
Submitted in partial fulfillment of the requirements for the degree
Master of Science

Faculty of Civil Engineering and Geosciences
Technical University of Delft

By: Kassahun K. Minalu
August, 2010

ACKNOWLEDGEMENTS

First and foremost, I would like to express my deepest appreciation to my graduation committee members: Prof.dr.ir. J.C. Walraven, dr.ir. C. van der Veen, dr.ir. P. C.J. Hoogenboom. ir. C. Quartel and ir. L.J.M. Houben. Thank you for directing me with your knowledge and experience in many long discussions on various topics related to my research.

I would like to express my thankfulness to all people of Spanbeton prefab company. Individual heartfelt appreciation is extended to Spanbeton engineers, Den Hertog Sander, Pluis Math, Oosting Diederik, Papampouklis Konstantinos and Broeze Maarten for their constructive comments and great contribution to this work.

I am indebted to express my gratitude to all members of G5 for their assistance throughout this journey. I will always cherish the memories of our time together as a group in Roland. Special thanks to Kass the Biomass for your exceptional contribution.

Finally, I would like to express my gratitude to my family, for their unconditional support and prayers at all times. And to my beloved girlfriend Meron, she was right next to me throughout the course of this work, thank you.

Kassahun K. Minalu
Delft, August 2010

TABLE OF CONTENTS

LIST OF FIGURES

LIST OF TABLES

LIST OF GRAPHS

ABSTRACT

Presently constructed bridges are often skew. The configuration of such a structure is the result of natural or man-made obstacles such as, complex intersections, space limitations, and/or mountainous terrains. Loads in many skew bridges take a different path towards the support than right bridges. In very skew bridges this brings about significant torsion moments near the obtuse corner, decrease in longitudinal bending moments and increase in transverse moments in the deck. Analytical calculations or conventional two-dimensional plate analysis only cannot provide sufficient accuracy for engineering practice. Therefore, in this study, an appropriate finite element modelling technique is looked for, which capable of predicting the three-dimensional behaviour of high skew bridges consisting of a cast in-place concrete deck on precast prestressed inverted T-girders.

Five different numerical models have been created and compared using SCIA engineer and ATENA 3D finite element packages. Special attention has been paid to torsion moments near the obtuse corner. The comparison of the results is based on the accuracy for engineering design, the modelling efficiencies and the post processing effort. It was found that the model consisting of shell elements for the deck and eccentric beam elements for the girders is the best for engineering practice.

In some of the analysis made with the orthotropic plate modelling method, the contribution of the girders to the torsion stiffness has been ignored. This was performed to see the sensitivity of the load distribution to the torsion stiffness of the girders, which have little torsion inertia. The resulting load distribution showed slightly increased bending moments. However, this increase in bending moment is insignificant. This shows that for ultimate limit state equilibrium, it is possible to leave out the torsion reinforcement at all.

The effect of the angle of skewness on the internal force distribution was investigated using two finite element modelling techniques. Four skew angles of 0^o, 30^o, 45^o, and $60°$ were considered for each finite element model. The results show that, live load maximum bending moments in girders of skew bridges are generally smaller than those in right bridges of the same span and deck width. On the contrary, the torsion moment in the obtuse corner of the bridge and the transverse moments in the deck increase with skew angel.

Finally, the sensitivity of the skew bridge performance to the presence of end diaphragm beams in the FE model was studied by considering and leaving out the end diaphragm beams. For models with end diaphragm beams, 900mm wide full depth cast in place reinforced concrete diaphragms were provided at both supports of the bridge. It was concluded that for the presence of end diaphragm beams decreases the live load bending and twisting moments in the girders and the deck. However, this reduction was not significant as compared to the torsion moment in the diaphragms.

CHAPTER 1, INTRODUCTION

1.1 Background

Newly designed bridges are often skew. This is due to space constraints in congested urban areas. Skew bridges allow a large variety of solutions in roadway alignments. This contributes to a small environmental impact for new road construction projects. It can also be needed due to geographical constraints such as mountainous terrains. However, the force flow in skew bridges is much more complicated than in right-angle bridges. Analytical calculations alone do not provide sufficient accuracy for structural design. Numerical analysis needs to be performed, in which a skew bridge can be modelled in several ways with different degrees of sophistication.

In right-angle bridges the load path goes straight towards the support in the direction of the span. In skew bridges this is not the case. For a solid slab skew bridge the load tends to take a short cut to the obtuse corners of the bridge as shown in Figure 1.1. In bridge decks supported by longitudinal girders this effect occurs too, although less pronounced. This change in direction of the load path in very skew bridges brings about the following special characteristics (1).

- Significant torsional moments in the deck slab
- Decrease in longitudinal moment
- Increase in transverse moment
- Concentration of reaction forces and negative moments at the obtuse corners
- Small reactions and a possibility of uplift reaction forces at the acute corners

These special characteristics of skew bridges make their analysis and design more intricate than right bridges.

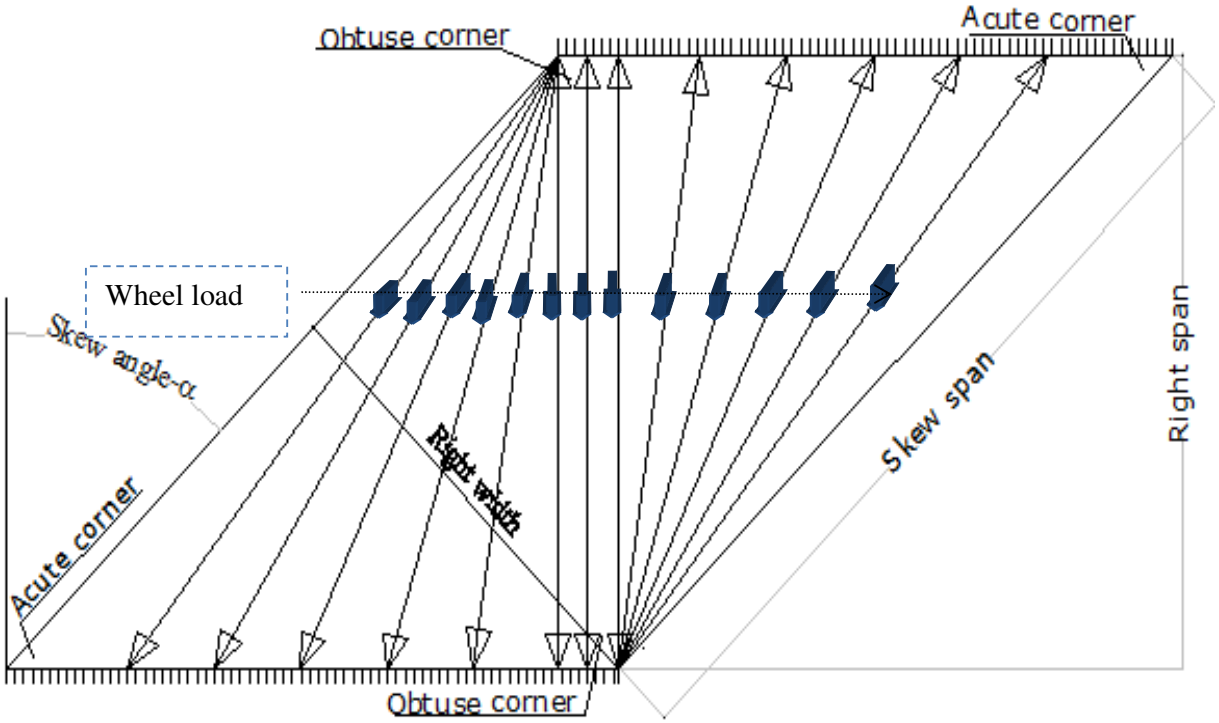

Fig1. 1, Load paths in torsion stiff skew bridges

A very successful bridge type nowadays is constructed out of a series of prefabricated concrete girders with a cast in-situ reinforced concrete deck. For simply supported medium to long span bridges many engineers choose prestressed girders that have an inverted T shape (ZIP) (Fig. 1.2). For bridges of this kind with a small skew angle less than 20^{o}, it is frequently considered safe to ignore the skew angle and analyze the bridge as a right-angle bridge with a span equal to the skew span [(1)]. This approximate modeling overestimates the longitudinal moments and underrates torsion and shear when the skew angle will be large. Consequently, for bridges with a skew-angle greater than 20^{o} a more accurate numerical method to determine the internal response of the bridge is recommended [(2)].

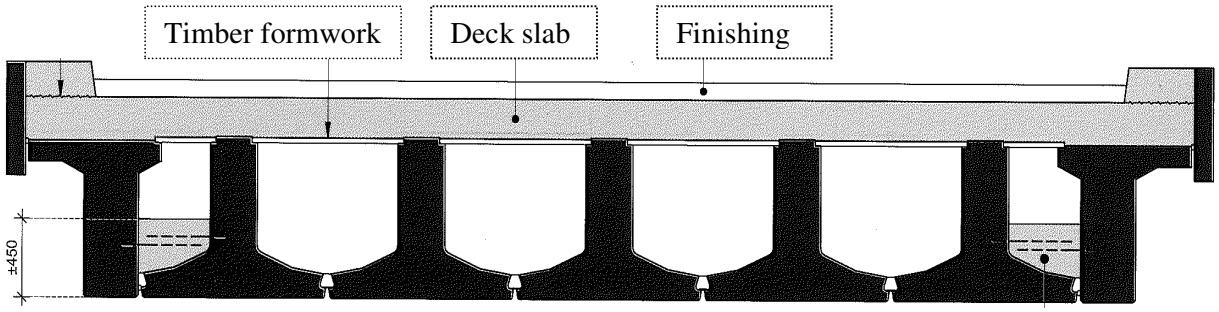

Fig1. 2, Cross-section of a typical Inverted T-girder bridge (ZIP Bridge, Spanbeton)

The torsion moments in a skew girder bridge are particularly interesting. The computed torsion moments strongly depend on the torsion stiffness of the girders. If large torsion stiffness is used in the analysis (uncracked stiffness) then the torsion moments will be large and much torsion reinforcement is required. On the contrary, when small torsion stiffness is assumed (cracked stiffness) then the torsion moments absorbed by the structure will be small and little torsion reinforcement will be required. In this case the loading will predominantly be carried by bending moments. As a result, more bending reinforcement and/or prestressing cables will be required. In this case the twisting moment is the result of deformation (compatibility torsion). Consequently, in design for the ultimate limit state, torsion reinforcement might be left out altogether. On the other hand, without torsion reinforcement severe cracking can develop well beyond the allowable serviceability limits.

The internal force distribution calculation and the general behavior of skew slab-girder bridges can be simulated in several ways.

I. **Orthotropic plate**. In this model, slab and girder are assumed to be plate structures stiffened by girders. It is the study of an equivalent elastic system obtained by transforming the stiffness of a number of girders and deck into a uniformly distributed system of same over all stiffness to the original one. At the end, the bridge structure is idealized as an orthographic plate of different stiffness in the longitudinal and transverse direction.

II. **Isotropic plate with concentric beam elements.** It consists of thin shell elements and beam elements. The Shell elements represent the bridge deck. The beam elements represent the girders. The beam elements are directly connected to the shell elements sharing the same node.

III. **Isotropic plate with eccentric beam elements.** This model consists also of thin shell elements and beam elements. In contrast to the previous model, the beam elements are eccentrically connected to the shell elements by rigid links which account for the distance between the center of the deck and the girder centre line.

IV. **Shell elements for both girders and deck.** In this model both girder and deck slab are modeled by quadrilateral shell elements.

V. **Volume elements.** This model is a truly three dimensional using volume elements to simulate the behavior of the girders and concrete deck accurately.

The question which modeling technique is appropriate for the particular bridge type at hand is typically answered by considering the following important aspects.

- The desired level of accuracy in results for daily practice in the construction industry.
- Time-efficiency of the analysis, which is a function of the modeling time for the engineer and the time needed for the computer to give results (waiting time).
- Application friendliness of the model and susceptibility in making errors. Simplicity of interpreting the results of the model, availability and user friendliness of the software and the required educational level of the engineer can be considered in this aspect.

In this study, the advantages and disadvantages of each of the above models in the analysis of cast in-situ deck on precast prestressed inverted T-girders skew bridges was thoroughly examined. The effects of the skewness on the general behavior of this type of bridge were also studied in depth. Additionally, different ways to calculate reinforcement for torsion and shear was studied using Euro-code of recommendations.

1.2 Objective of the Research

The primary objectives of this research are the following:

1. To provide information regarding the advantages and disadvantages of various structural modelling approaches for skew girder bridges (in particular, longitudinally skewed, concrete inverted T (ZIP) girder bridges) and to select the best modelling technique.
2. To provide information regarding the consequences of different methods for designing torsion reinforcement especially for no torsion design.
3. To give some idea on the effect of skewness on the general behaviour of this kind of bridges.
4. Assess the potential failure mode when modeling a high skew bridge as a right-angle bridge and comment which part of the design will be compromised.
5. Provide information about the advantage and disadvantages of considering end diaphragm beams in the FE model.

1.3 Approach to the work

The objectives of this work will be achieved by thoroughly examining the results of the above finite element modelling techniques. The one which is the simplest and accurate enough for daily practice will be chosen and recommend for use in the construction industry. The current practice in the construction industry shows that orthotropic plat modelling approach is prominent. As the result, special attention was given for this modelling method and the following six different studies were performed.

a. Considering the stiffness of end diaphragm beams in the transverse direction and with full torsional stiffness for the girders in the serviceability limit state.
b. Considering the stiffness of end diaphragm beams in the transverse direction and with reduced (cracked) torsional stiffness for all structural elements in the ultimate limit state.
c. Disregarding the stiffness of the transverse end beams in the transverse direction and with full torsional stiffness for the girders in the serviceability limit state.
d. Disregarding the stiffness of the transverse end beams and with reduced (cracked) torsion stiffness of all structural elements in the ultimate limit state.
e. Considering the stiffness of the end diaphragm beams and disregarding the torsion stiffness of the girders at all.
f. Disregarding the stiffness of the transverse end beams and torsion stiffness of the girders at all.

For modelling techniques II-V mentioned above, the following two models for each were performed.

I. Considering the stiffness of end diaphragm beam and with full torsion stiffness for the girders in the serviceability limit state.
II. Considering the stiffness of end diaphragm beams and with reduced (cracked) torsional stiffness for all structural elements in the ultimate limit state.

1.4 Description of the case study

The bridge shown in the Figure 1.3 and 1.4 is selected by Spanbeton (Precast Company in the Netherlands, which has own design department) as a representative bridge for daily practice. This bridge has the following attributes:

- One simply supported span.
- 4 lanes of 20m right-width deck.
- 15 ZIP 1300 (Inverted T-girders) and 2 TRA 1300 (End (Spandrel) girders), 36m long with 1.2m center to center spacing between inverted T-girders (ZIP).
- 230mm thick cast in place reinforced concrete deck slab.
- The supports at each end of the bridge are parallel to each other and have a 45^{o} longitudinally configured skew angle.
- Concrete quality of C53/65 (B65) for precast prestressed girders and C28/35 (B35) for cast in place reinforced diaphragms and deck slab.
- Precast beams are connected to cast in place deck using shear reinforcement. As a result, it is assumed that the precast prestressed concrete girders and the deck slab experience fully composite action.
- 900mm full end diaphragm beams at each support is provided to help the lateral load distribution and decrease the mid span moment. Torsionally stiff end diaphragms inhibit end rotation of the loaded girder at the expense of causing some end rotation in the adjacent unloaded girders. The negative end moment so introduced in the loaded girder reduces the positive mid span moment. This behavior corresponds to a reduction in the live load distribution factors as well.
- Due to the high labour cost of cast in place concrete diaphragms in prestressed concrete bridges, use of intermediate diaphragms (IDs) is considered as an added and perhaps unnecessary cost to bridge construction and often omitted in daily practice. Consequently, intermediate diaphragm beams are not provided in this work.

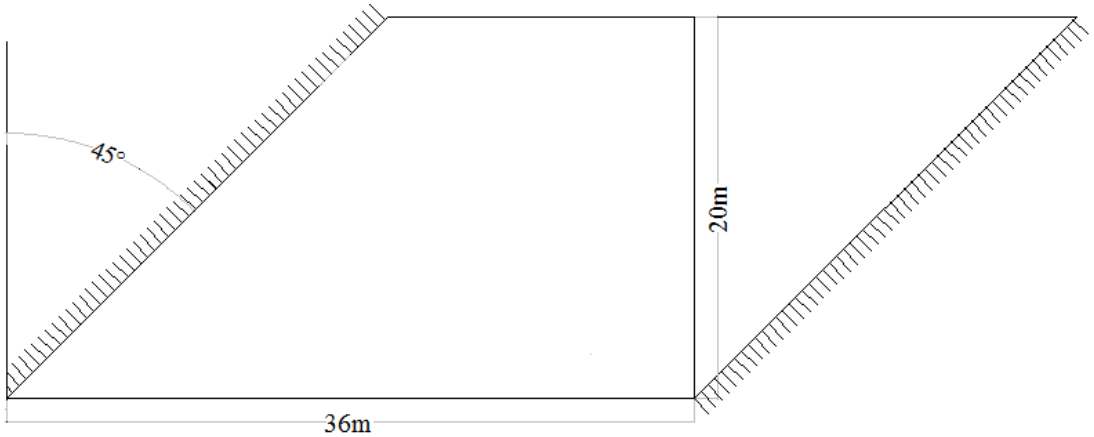

Fig 1.3 a, plan view of the selected bridge type

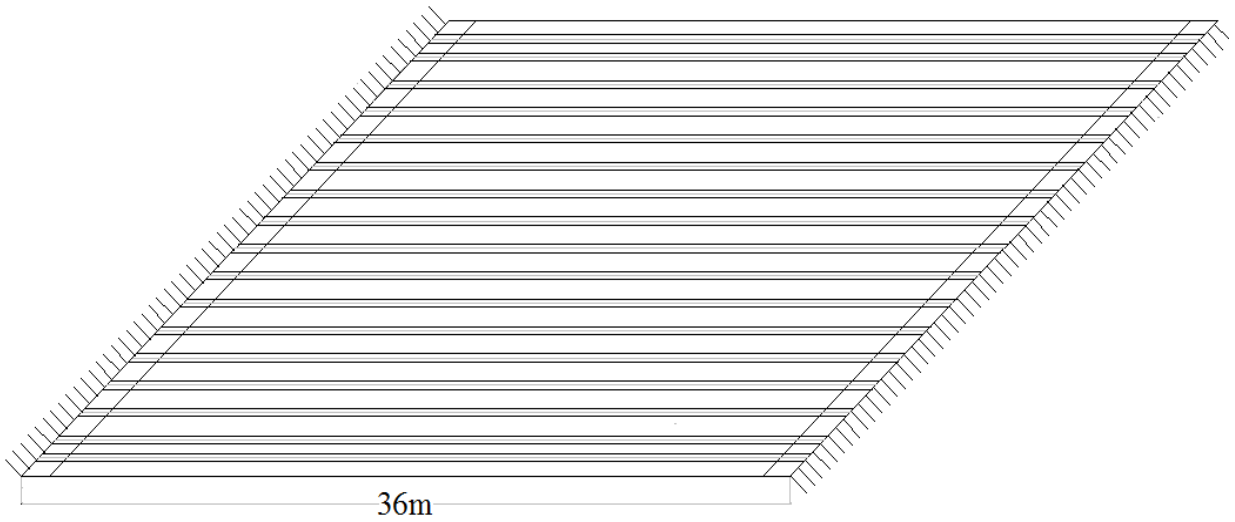

Subject skew bridge plan with precast girders

Figure 1.3 (b), plan view

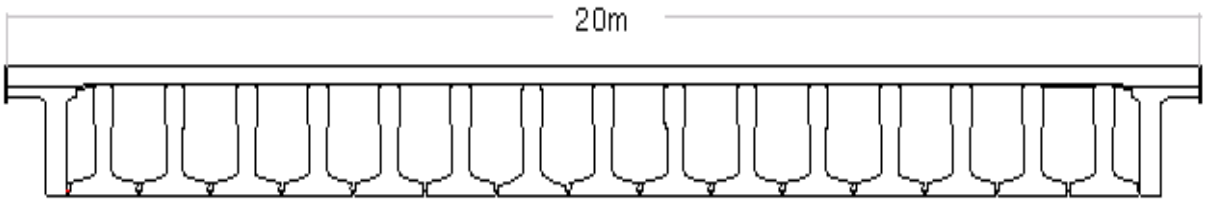

Fig1.3, (c) Arrangement of beams

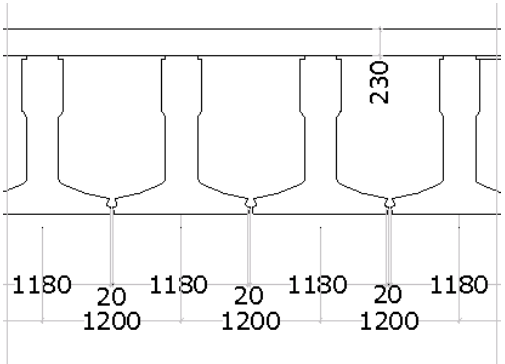

Fig 1.3 (d) Internal beams

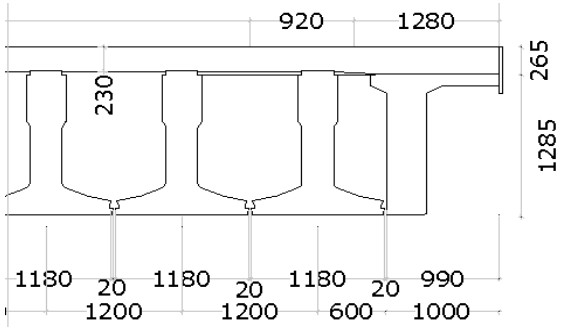

Fig 1.3 (e) internal and End beams together

Fig1. 3, plan and cross section of the typical bridge type

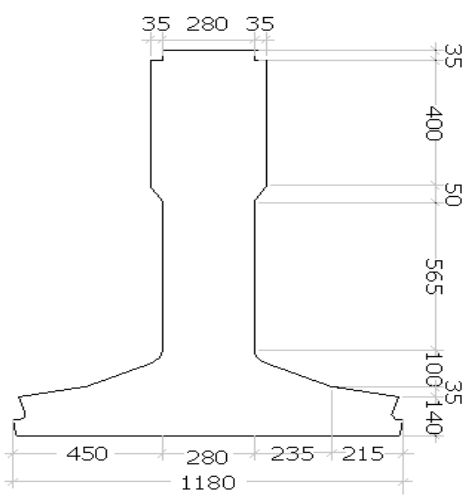

Inverted T- (ZIP) beam

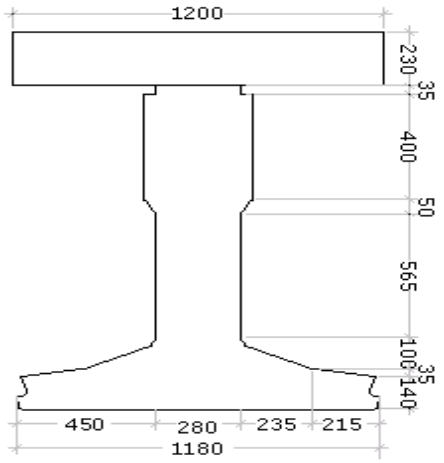

Inverted T-(ZIP) girder and portion of cast in place deck

Figure 1.3 (e)

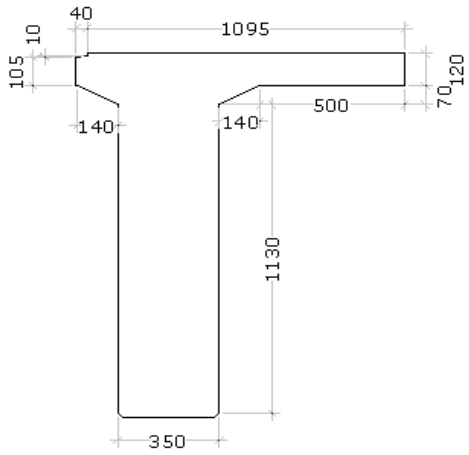

Spandrel (TRA) girder

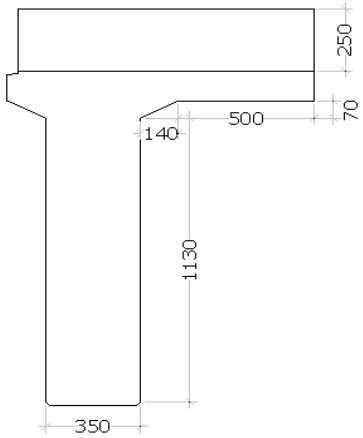

Spandrel (TRA) girder and portion of cast in-situ deck slab

Figure 1.3 (f)

Fig1. 4, cross sections of the girders

1.5 Literature review

In order to contextualize the current work, related works from literature is discussed. In addition a thorough review of literatures on various aspects of intermediate diaphragms for skewed prestressed concrete (PC) girder bridges is presented. This was done with the purpose of gaining a better understanding on the advantages and disadvantages of providing ID in skew prestressed girder bridges and other related issues. A literature review was also done on lateral live load distribution factors in skew bridges and the effect of diaphragms on the load distribution factors.

1.5.1 Lateral load distribution using finite element analysis

Many studies of skewed bridges using finite element analysis have been made in the past years especially on live load distributions in the transverse direction. For instance,
Mohammad, Khaleel and Rafik (1990) [(3)] conducted finite-element analysis to determine moments in continuous right and skew slab-and-girder bridges due to live loads. They analyzed 112 continuous bridges, each having five pretensioned I girders. The spans vary between 24.4 and 36.6 m and are spaced between 1.8 and 2.7 m on center. The skew angle varies between 0 and 60°. The finite element analysis makes use of a skew stiffened plate which consists of two thin shell elements and one beam element. The two thin shell elements are connected to the beam element by rigid links. The element used to model the reinforced concrete deck slab is an 8 node isoperimetric thin shell element with six degrees of freedom at each node. In this study it is concluded that larger skew angle significantly reduces the design longitudinal moment. The reduction of maximum positive and negative moments in the interior girders is less than 6% for skewness of less than 30° and as much as 29% when skew angle is 60°. The reduction of the maximum positive or negative bending moments in the exterior girders is less than 10% for angles of skew less than 45° and as much as 20% when skew angle is 60°.

Mabsout et al. (1997) [(4)] compared four finite-element modeling methods to determine load distribution factors for a one-span, two-lane, simply supported, composite steel girder bridge. In the first method, the concrete slab was modeled with quadrilateral shell elements, and the steel girders were idealized as space frame members. The centroid of each girder coincided with the centroid of the concrete slab. In the second model, the concrete slab was modeled

with quadrilateral shell elements and eccentrically and rigidly connected to space frame members, which represented the girders. In the third method, the concrete slab and steel girder web were modeled with quadrilateral shell elements. Girder flanges were modeled as space frame elements, and flange-to-deck eccentricity as modeled by imposing a rigid link. In the fourth method, the concrete slab was modeled with isotropic, eight-node brick elements; the steel girder flanges and webs were modeled with quadrilateral shell elements. All of the four finite-element models produced similar load distribution factors. The results indicated that the concrete slab could be modeled with sufficient accuracy as quadrilateral shell elements and the girders as concentric space frame elements.

Khaloo and Mirzabozorg(2003) [(5)] have also conducted three-dimensional analysis for skew simply supported bridges of concrete decks with five concrete I-section precast prestressed girders using ANSYS. Span lengths, skew angles, girder spacing, and arrangements of internal transverse diaphragms were the basic variables. In all models two end diaphragms and different arrangements of internal transverse diaphragms are considered. They analyzed Bridges with three span lengths of 25, 30, and 35 m. Girder spacings of 1.8, 2.4 and 2.7 m and skew angles of 0^o, 30^o, 45^o, and 60° are chosen in the skew bridge models. Three different arrangements for internal transverse diaphragms are considered. In the first pattern the models do not include any internal transverse diaphragms. In the second pattern, internal transverse diaphragms are parallel to the axis of the support, and in the third pattern internal transverse diaphragms are perpendicular to the longitudinal girders. In their study, they showed that the skew angle of the deck is the most influential factor on load distribution. The load distribution factors of skew bridges are always less than those of right bridges. The load distribution factor of external girders reduces by 24% for a skew angle of 60° as compared with right bridges. In addition the study showed the sensitivity of load distribution factors of internal girders with respect to skew angle. For decks with a skew angle of 60° the distribution factors decrease by 26.3% as compared with right bridges. However, for decks with a skew angle up to 30°, this effect is insignificant. In this study for system without internal transverse diaphragms, the load distribution factors of external girders are not influenced significantly when skew angle increases; however, these factors decrease up to 18% in internal girders. When the transverse diaphragms are parallel to the axis of the support, load distribution factors of external girders decrease up to 19% and those of the internal girders are approximately constant when skew angle increases. When the internal transverse diaphragms are perpendicular to the girders, distribution factors of both internal

and external girders decreases as skew angles increases and are more sensitive than the other two systems with respect to skew angles. In general, for large skew angles, the effect of internal diaphragms parallel to the supporting lines is insignificant. Also, in various skew angles, the effect of spacing between internal transverse diaphragms perpendicular to longitudinal girders is insignificant.

Huang, Shenton, and Chajes (2004) [(6)] carried out field testes and theoretical analyses using finite element methods for two span continuous slab-on-steel girder composite Bridge with a skew angle of 60°. The main objectives of this study were to experimentally evaluate the load distribution for the highly skewed bridge, compare the predictions resulting from the AASHTO formulas with the field test results, and verify the theoretical analyses using the finite element method with the field test results. A three-dimensional finite element model of the bridge was developed using the commercial program ANSYS. In the numerical model, the influence of the transverse diaphragms and diaphragm stiffness was analyzed by considering three different cases: diaphragms with the stiffness calculated from the real cross frames, diaphragms with one-half the calculated stiffness, and finally, no transverse diaphragms at all. The effect of end diaphragms is revealed at the pinned ends of the girder. Without diaphragms, the strain at the support was exactly zero. However, for the case with diaphragms at the pinned ends of girders at the acute corner side of the bridge, positive strains appeared, and at the pinned ends of girders at the obtuse corner side of the bridge, negative strains appeared. Due to these negative strains at the pinned ends, positive strains at the middle of the span are reduced. Results of this research also showed that the strains in the girders away from the load decreased and the strains in the girders under the load increased when the stiffness of the diaphragms was reduced. However, comparing the case with the full stiffness to the case with half the stiffness, the difference in the peak strains is not significant. That mean, the peak strains change more slowly as the stiffness of the diaphragm increases, showing that the influence of the diaphragms is not linear. This study additionally showed that, the analytical results are in good agreement with the measured data. The numerical model is slightly stiffer than the real structure; i.e., the model predicts smaller strains than recorded in the girders farthest from the load.

Menassa, Mabsout, Tarhini and Frederick (2007) [(7)] have conducted FEA for simply supported, one-span, multilane skew reinforced concrete slab bridges. Four span lengths were considered in this parametric study as 7.2, 10.8, 13.8, and 16.2 m with corresponding solid

slab thicknesses of 450, 525, 600, and 675 mm respectively. One, two, three, and four lane bridges without shoulders at both free edges were investigated. The effect of skewness is studied by combining the spans and lanes considered with skew angles varying between 0^o and 50° by increments of 10^o. Right bridges, zero skew angles, served as a reference for comparison with skewed bridges. The general FEA program, SAP2000 (1998), was used to generate the three-dimensional (3D) finite-element models. The concrete slabs were modeled using quadrilateral shell elements with 6 degree of freedom at each node. From this study, they concluded the following:

1. The ratio between the FEA longitudinal moments for skewed and straight bridges was almost one for bridges with skew angle less than 20°. This ratio decreased to 0.75 for bridges with skew angles between 30^o and 40°, and further decreased to 0.5 as the skew angle of the bridge increased to 50°
2. This decrease in the longitudinal moment ratio is offset by an increase by up to 75% in the maximum transverse moment ratio as the skew angle increases from 0^o to 50°.
3. The ratio between the FEA maximum live-load deflection for skewed bridges and right bridges decreases in a pattern consistent with that of the longitudinal moment. This ratio decreases from one for skew angles less than 10° to 0.6 for skew angles between 40 and 50°.

The above research finally recommends that engineers should perform three-dimensional finite-element analysis when the skew angle is greater than 20°.

Trilok Gupta and Anurag Misra (2007) [(8)] studied the effect of skew on the behavior of T-beam bridges of short to medium range of spans where the span and width are of the same order. The study was carried out for two lane T-Beam girder bridges of 8m, 16m, 24m and 32m right spans and 0^0, 10^0, 20^0, 30^0, 40^0, 50^0 and 60^0 skew angles using grillage analogy method. This research has concluded the following.

a. The maximum support reaction is occurred at the support near obtuse corner with the exception of 0^0 skew angle, for which the maximum reaction was occurred at the support of the middle girder.
b. For skewness of greater than 30^o, the minimum reaction force is negative (uplift reaction). For large span bridges, this negative reaction starts at 20^o skewness and increases with the angle of skew.

1.5.2 Importance of diaphragms for precast prestressed girder bridges using finite element analysis

Griffin (1997) [(9)] researched the influence of intermediate diaphragms on load distribution in prestressed concrete I-girder bridges. The studies included two bridges with a 50^o skew angle. One of the bridges has concrete intermediate diaphragms. Bridge with IDs has experienced unusual concrete spalling at the interface of the diaphragms and the bottom flange of girders. The IDs appeared to be contributing to the increased rate of deterioration and damage instead of reducing the moment coefficient and distributing the traffic loads as expected. Experimental static and dynamic field testing were conducted on both bridges. Once the calibration of the finite element models was completed using the test data, analysis was conducted with actual truck traffic to investigate load distribution and the cause of the spalling at the diaphragm-girder interface. Based on the results obtained in the research study, IDs did not create a significant advantage in structural response. The finite element analysis also revealed the cause of concrete spalling in the diaphragm girder interface region. The tendency of the girders to separate as the bridge was loaded played a large role in generating high stress concentrations in the interface region. Other explanatory factors with the presence of the diaphragm are anchor bars. It also stated that to resolve this problem would require the removal of the concrete ID.

Cai *et al.* (1998) [(10)] investigated six prestressed concrete bridges, and the results were compared with field measurement of these bridges. It was found that the finite element prediction that did not consider IDs had better agreement with field test results, implying that the effectiveness of IDs of these bridges are insignificant in distributing the live loads. Further examination of the details of these bridges found that the diaphragm connections are weak. The diaphragms would have more significant effects on vertical live load distribution if a full moment connection is ensured between the diaphragms and girders.

Barr et al. (2001) [(11)] studied the evolution of flexural live-load distribution factors in a three span prestressed concrete girder bridge, where a bridge with three spans with lengths of 24.4m, 41.8m, and 54.9m, and a skew angle of 40^o was tested. A finite element model was developed to assess the live-load distribution procedures recommended by the AASHTO code. For both interior and exterior girders, the addition of IDs had the least effect on the live-load distribution factor among the variables investigated in this study. For the exterior girders,

IDs slightly increased the live-load distribution factor for low skew angles. For skew angles larger than 30^o, the addition of IDs was slightly beneficial. According to this study, for design consideration from a structural standpoint, the largest changes would be credited to the addition of end diaphragms, while almost no changes would occur due to the addition of intermediate diaphragms, since these showed almost no change in the distribution factors.

Khaloo and Mirzabozorg (2003) [(5)] have taken skew angle, girder spacing, and span length for bridges as the parameters for carrying out a parametric study for skew bridges. They considered four kinds of configurations of bridges in their study, with the first type being without ID, the second type having an ID parallel to the supporting lines, and for the third and fourth configurations, the diaphragms were perpendicular to the girders. The following conclusions were drawn from this study:

1. The arrangement of IDs in the bridges has a significant effect on the load distribution pattern. This effect varies for different askew angles, such that in low skew angles the effects of IDs are relatively significant. While in the high skew bridge the effect of IDs parallel to the support is small.
2. IDs perpendicular to the longitudinal girders of the bridge are the best arrangement for load distribution.
3. Bridges with intermediate transverse diaphragm perpendicular to longitudinal girders, the effect of spacing between IDs on load distribution is insignificant.

Aziz Saber, Freddy Roberts, Walid Alaywan and Joseph Toups (2007 [(12)] have also made detail investigation on the need for continuity diaphragms in skewed, precast, prestressed concrete I-girder bridges; to study the load transfer mechanism through full-depth continuity diaphragms. A three dimensional finite element model was developed to simulate the behavior of skewed continuous-span bridges. GTSTRUDL structural design and analysis software, version 25 is employed to generate this model. The diaphragms are modeled as space truss members between the precast prestressed girders. This study concluded that the effect of continuity diaphragms on the maximum stress and deflection of the girders was negligible. As a result, continuity diaphragms could be eliminated from skewed, continuous, precast prestressed concrete girder bridges because continuity diaphragms are ineffective and full-depth diaphragms are not needed to control deflections or reduce member stresses but may be needed for construction, lateral stability during erection, or resisting/transferring earthquake or other transverse loads.

CHAPTER 2, ANALYSIS APPROACH

Linear elastic analysis which assumes linear material behavior, that the stress of a member is proportional to its strain and material having identical stress-strain properties in both tension and compression was adopted in this study.

2.1 Division of the carriageway into notional lanes

The bridge considered in this case study has 20m right width. The carriageway is 17.2m after deducting 1.4m hard strip each side of the bridge. For design purpose a theoretical lane width of 3m is considered. The number of notional lanes is then:

Ing(17.2/3)=5, and 2.2m remaining area.

2.2 Load cases

2.2.1 Dead loads (self weight of the bridge)

Load case 1, Self weight of the deck: thickness of the deck is 230mm

$P_{deck} = 0.23 * 25 = 5.75 kN / m^2$

Load case 2, Self weight of the girders:

Inverted T Girders, cross sectional area =0.599m^2

Spandrel Girders (End Beam), cross sectional area=0.559m^2

$P_{Zip} = 0.599 * 25 = 14.975 kN / m$

$P_{End} = 0.559 * 25 = 13.975 kN / m$

2.2.2 Permanent loads

Load case 3, Edge Elements: the following elements were provided on both sides of the bridge deck.

Handrails: 2kN/m, placed at 0.17m from the edge.

Strip grazing: 0.4*25=10kN/m^2, uniformly distributed to a width of 0.380m.

Safety barrier: 1kN/m, placed at 0.973m from edge of the bridge

Footbath =0.5*(0.215+0.23)*25=5.56kN/m ^{2}

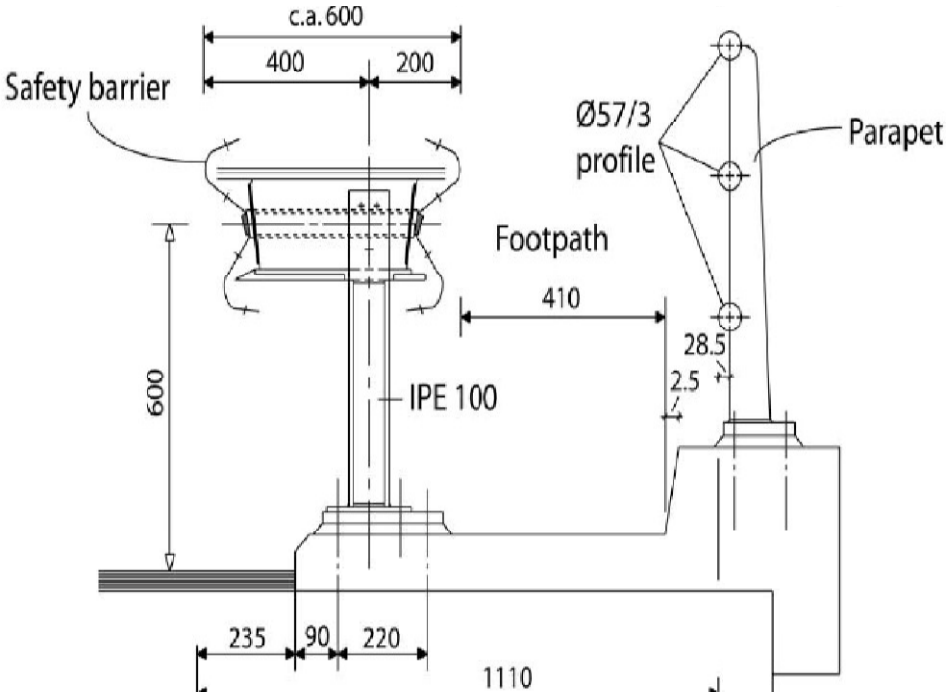

Fig2. 1, edge elements attached to the bridge deck

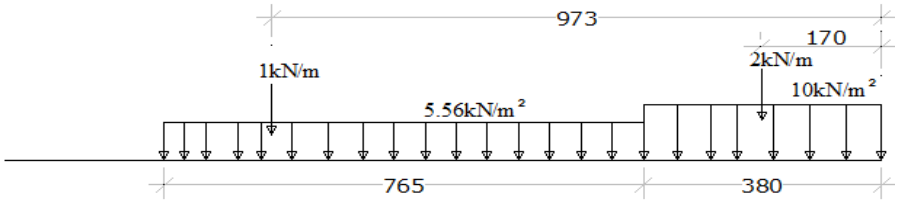

Fig2. 2, edge element loads

Load case 2, Asphalt layer:

Not only as a wearing surface but also to level the initial camber of the prestressed girders, 140 mm asphalt layer is provided for the whole carriage way.

$$P_{asphalt} = 0.14 * 23 = 3.22 kN/m^2$$

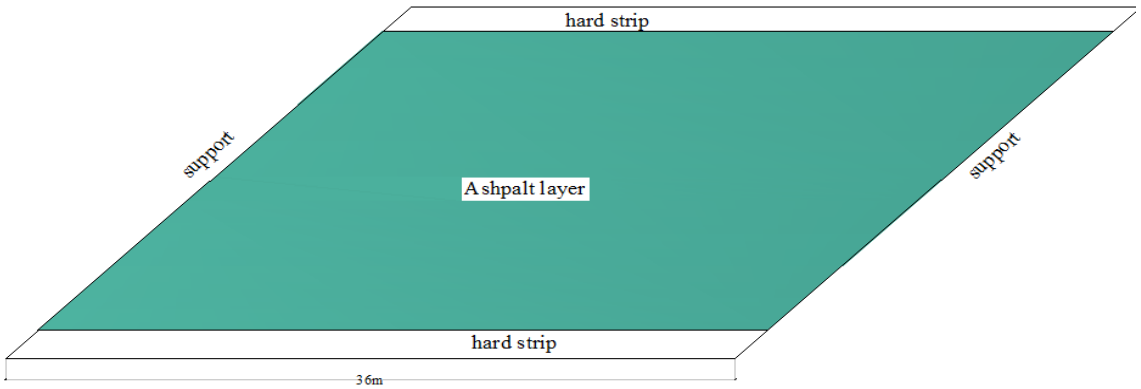

Fig2. 3 edge element loads

2.2.3 Variable loads

Load models according to Euro code (Load model 1)

Load Model 1: concentrated and uniformly distributed loads, which covers most of the effects of the traffic of Lorries and cars is used for general and local verification. The concentrated axle loads were applied at a contact surface of 400x400mm to simulate the wheel of the tracks.

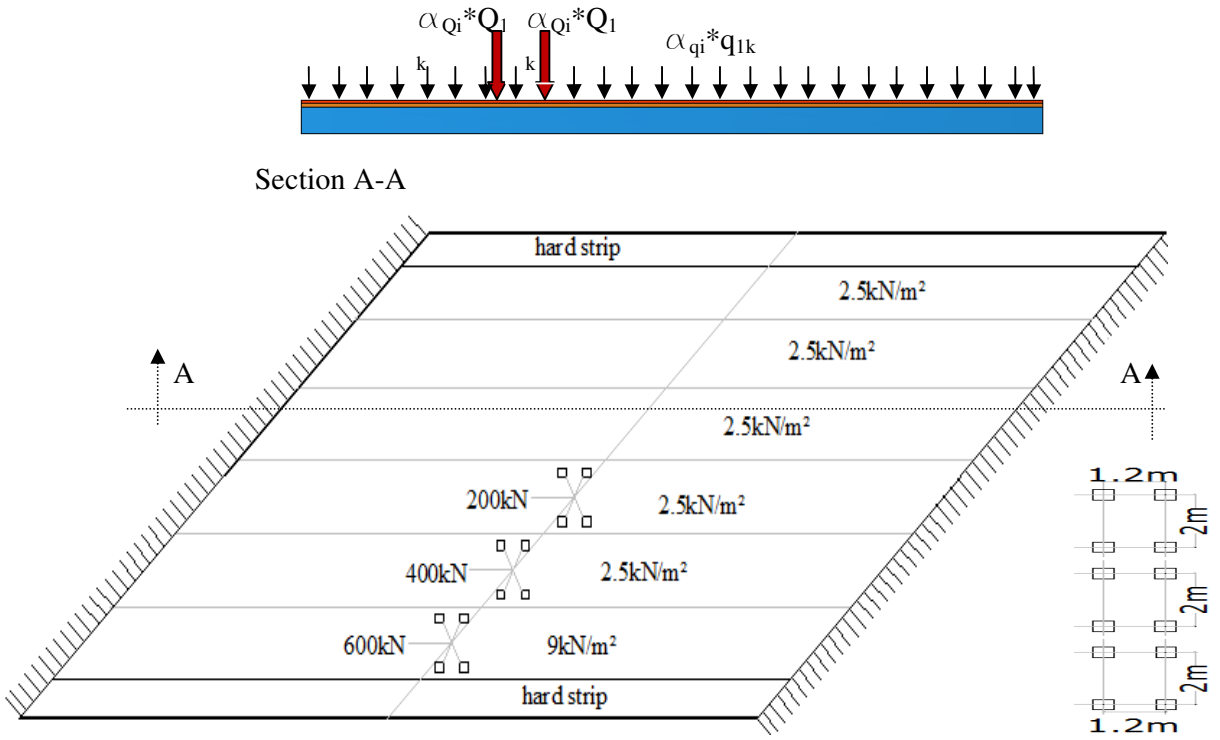

Fig2. 4 variable loads and arrangements from Euro code

As per European code of recommendation,

Lane 1: Axle load, Q_{1k}=300kN: and UDL, q_{1k}=9.0kN/m^2

Lane 2: Axle load, Q_{2k}=200kN: and UDL, q_{2k}=2.5kN/m^2

Lane 3: Axle load, Q_{3k}=100kN: and UDL, q_{3k}=2.5kN/m^2

Lane 4 and5 and remaining area: UDL, q_{4k}=2.5kN/m^2

The above load cases were multiplied by modification factors to get the characteristic design loads. From the national annex of the Netherlands,

αQ_i = 1.00 (modification factor for tandem systems [TS])

αq_{1i} = 1.15 (modification factor for uniformly distributed 1st notional lane load [UDL])

αq_i = 1.40 (modification factor for uniformly distributed remaining lanes loads [UDL])

αq_r = 1.00 (modification factor for uniformly distributed remaining area load [UDL])

Hence, the characteristic design loads after the application of the modification factors were:

Lane 1: Q_{1k}=300kN: q_{1k}=10.35kN/m^2

Lane 2: Q_{2k}=200kN: q_{2k}=3.5kN/m^2

Lane 3: Q_{3k}=100kN: q_{3k}=3.5kN/m^2

Lane 4 and 5: $q_{4k\&5k}$=3.5kN/m^2

Remaining area: q_k=2.5kN/m^2

2.2.4 Variable Load arrangements in the transverse direction

Torsion moments are the focus of this thesis work. However, change in torsion stiffness of the girders and deck due to cracking substantially affects the longitudinal and transverse bending moments. To deal with this effect of torsion stiffness, the longitudinal bending moments and transverse moments in the bridge were critically assessed with their respective unfavourable load positions. Load position in skew bridges for maximum longitudinal bending moments and transverse moments were taken from practice (Spanbeton). However, load positions that create maximum twisting moments have been studded in depth.

Load case 5**,**

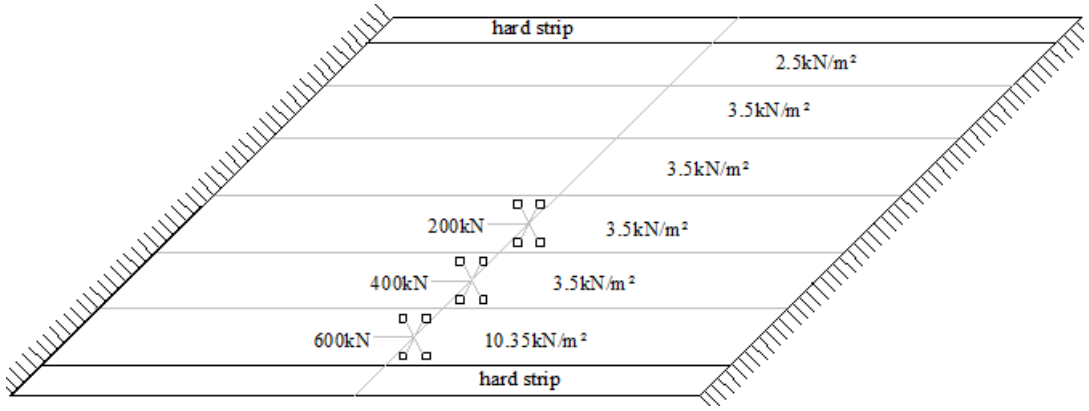

Fig2. 5, variable load arrangement for maximum longitudinal bending moment

Load case 6,

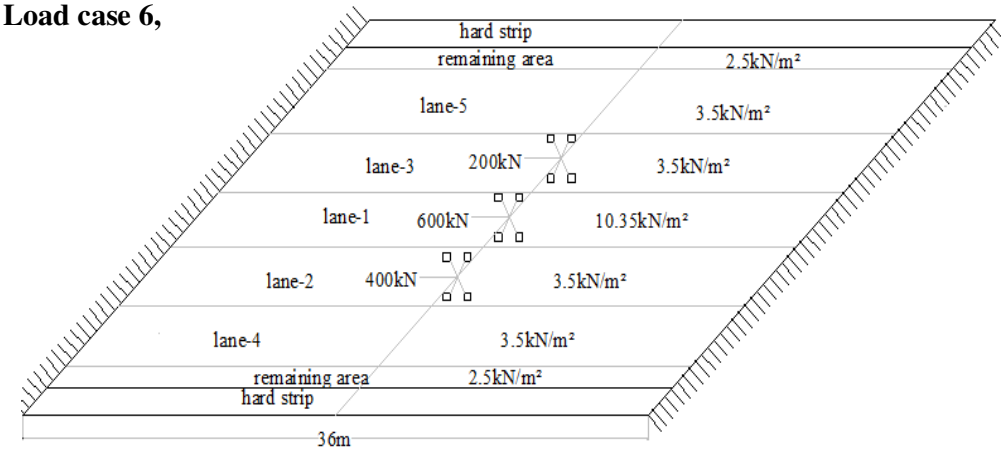

Fig2. 6, variable load arrangement for maximum positive transverse moment

Load case 7,

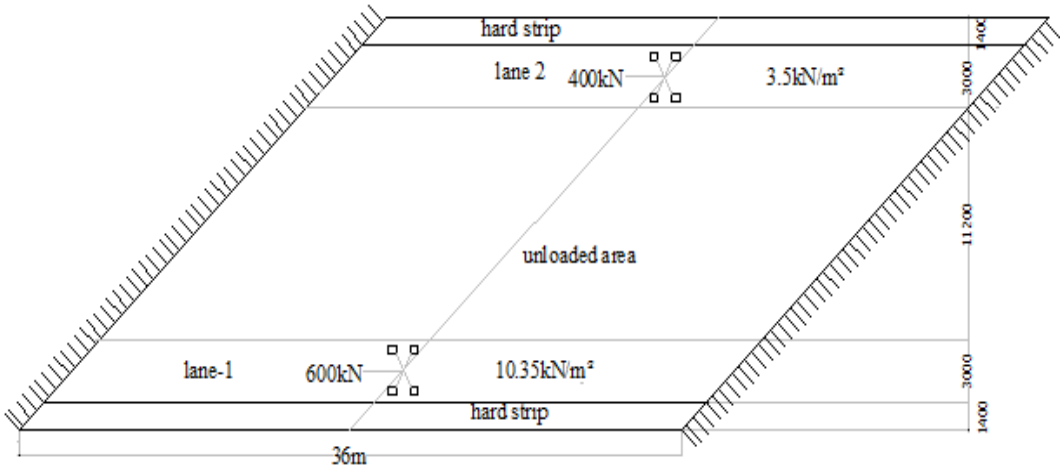

Fig2. 7, variable load arrangement for maximum negative transverse moment

For torsion stiff bridges like solid slab decks the load tends to take the shortest path towards the support of the bridge and axle loads distribute equally in longitudinal and transverse directions. In bridges supported by longitudinal girders, axle load distribution is strongly dependant on the stiffness of the deck and the lateral stiffness of the girders. Due to his fact, the arrangement of axle loads that create maximum torsion moments in the girders is variable with the depth of the deck slab and the shape of the precast girders. Three axle load positions have been tasted in this part of the study and another critical load arrangement for this kind of girders would be sought in the next chapter.

Axle loads create maximum shear stress on the bridge when they placed near to the support. However, due to 'short span shear enhancement' near the support there is a remarkable increase in shear strength.[(13)] For that reason, the recommended position of the first axle loads from Euro-code is 2d distance from face of support. When a concentrated load is placed at a location less than 2d distance from face of support, the shear contribution of this concentrated load should be multiplied by a factor $\beta=a/2d$. Where a- is the distance from face of support to the position of the concentrated load considered and should be greater than 0.5d. Hence, to make this β factor 1, the axle loads for maximum shear force near the support were placed at 2d distance from face of support.

Load case 8,

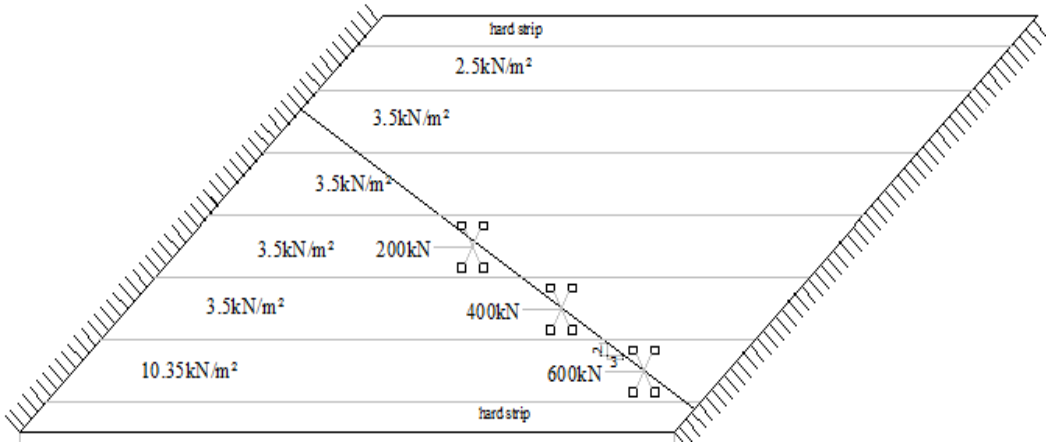

Fig2. 8, variable load arrangement for maximum torsion moment near the obtuse corner (From Spanbeton)

Load case 9,

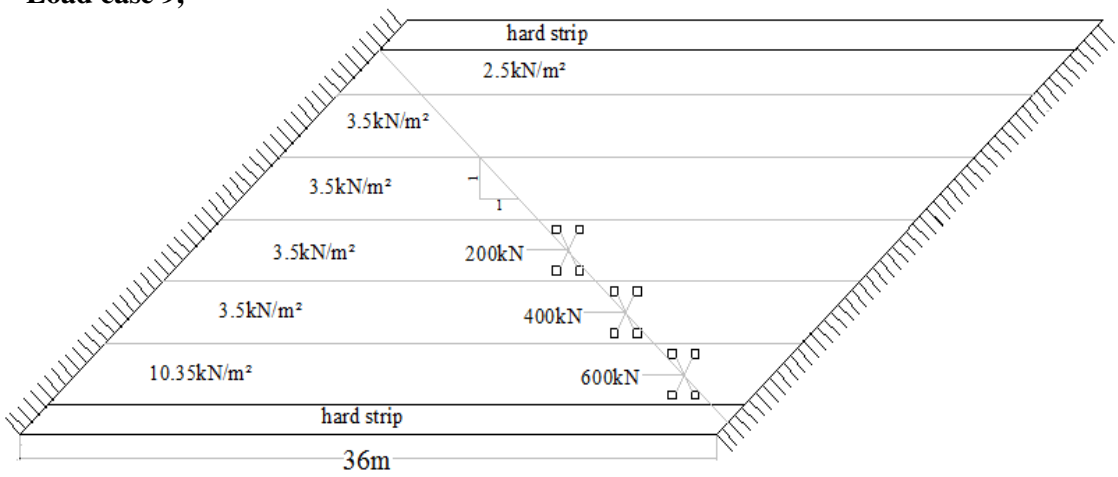

Fig2. 9, Variable load arrangement for torsion near obtuse corner of the bridge, [45^0]
Load case 10,

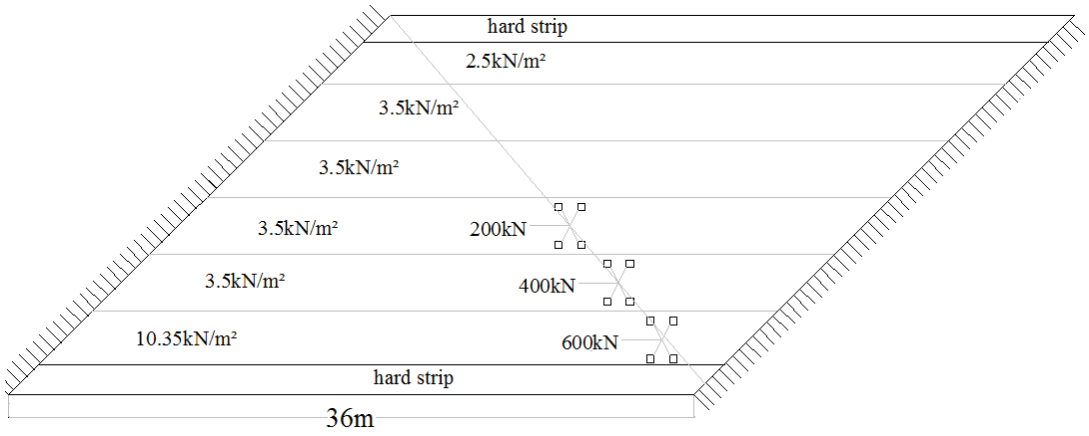

Fig2. 10, variable load arrangement for torsion directly towards the obtuse corners of the bridge

2.3 Load combinations

During construction, the girders would generally act independently and must be capable of carrying their self weight, and weight of the slab and any construction loads present. After deck concrete hardens, the precast presteressed girders and the cast in-situ deck will act compositely to take the traffic load and the permanent loads, such as asphalt layer and edge element loads. The load distribution in the composite system is as per their respective stiffness's. Due to this construction sequence, self weight of the deck and girders were not considered in the finite element model. The effect of these load cases was added to the finite element model results for design with simple hand calculations.

The following load combinations were considered in the model

Comb1 (maximum bending moment in the longitudinal direction)

$=Lc_3+Lc_4+Lc_5$

Comb2 (maximum positive bending moment in the transverse direction)

$= Lc_3+Lc_4+ Lc_6$

Comb3 (maximum negative bending moment in the transverse direction)

$= Lc_3+Lc_4 +Lc_7$

Comb4 (Torsion near obtuse corner)

$= Lc_3+Lc_4+Lc_8$

Comb5 (Torsion near obtuse corner), alternative combinations

$= Lc_3+Lc_4+Lc_9$

Comb6 (Torsion near obtuse corner), alternative combinations

$= Lc_3+Lc_4+Lc_{10}$

In the ultimate limit state, load factor of 1.35 from Euro-code of recommendations for all load cases (live and permanent) has been used.

2.4 Assumptions

- The system is linear elastic and the response under Composite loadings is geometrically linear, superposition is valid.
- The effect of creep and shrinkage is neglected.
- Effect of pretesting in the load distribution is not considered and assumed to be negligible.
- Bridge parapets usually have edge stiffening effect in the bridge. In this study this stiffening effect was neglected and only the weights of these elements were calculated and applied on the model.

CHAPTER 3, ORTHOTROPIC PLATE MODEL

Morice and little have applied orthotropic plate theory to concrete bridge systems, using the approach first suggested by Guyon, neglected torsion and extended by Mossonet to include torsion. This approach has the advantage that a single set of distribution coefficients for two extreme cases of no torsion beams and a full torsion slab enable the distribution behavior of any type of bridge to be found. This is also called the method of distribution coefficient. Its range of applications is limited. It is only applicable to slab, slab-beam types of construction having prismatic cross sections. The spans being simply supported with line supports and right spans only. In practice this analytical tool is of much wider use than what these limitations first suggest. Its results can generally be accepted for skews of up to 20^{o} and a serious of discrete supports can be accepted as representing line supports, provided there is no significant overhand beyond the outer bearings. [(14)]

In high skew bridges, this method of Guyon and Mossonet gives erroneous results. It overestimates the longitudinal moments and underrates torsion in the obtuse corner of the bridge. Recently, orthotropic plate theory has been reformed in a manner which lends itself computerized calculation to model acceptably high skew viaducts. The basis of orthotropic plate method is the study of an equivalent elastic system obtained by transforming the stiffness of a number of beams into a uniformly distributed system of the same overall stiffness.

In orthotropic plate model, bridge deck is assumed to be plate structure stiffened by longitudinal girders. The figure 3.1 shows the bridge under consideration in this case study. This beam and slab type bridge is transformed in to an equivalent slab system. The stiffnesses of the girders are calculated by hand and distributed within center-to-center distance between them and changed the whole system into an idealized system of the same stiffness to the original one.

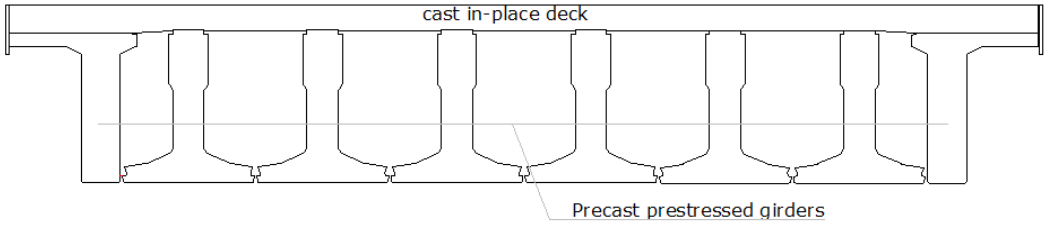

Fig 3. 1, Actual cast in-situ deck on precast prestressed girders

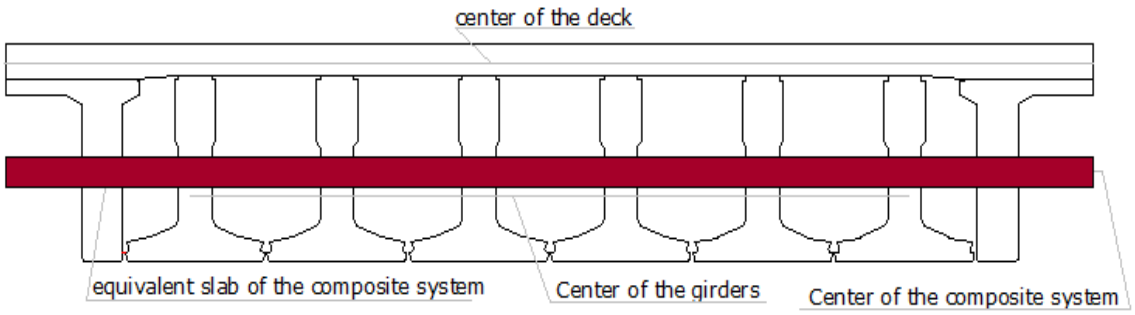

Fig 3. 2, Idealized simple substitution of the real composite system in to equivalent plate of different stiffness in both directions

The general differential equation for an orthotropic slab subjected to a distributed vertical area load q(x, y) is:

$$D_{xx}\frac{\partial^4 w}{\partial x^4}+(D_{xy}+D_{yx}+D_v)*\frac{\partial^4 w}{\partial x^2\partial y^2}+D_{yy}\frac{\partial^4 w}{\partial y^4}=q(x,y)\ldots[15]$$

Where, D_{xx}, D_{yy}, D_{xy} and D_{yx} are the longitudinal and transverse flexural rigidities, as well as the longitudinal and transverse torsional rigidities per unit width or per unit length. To compute the flexural and torsional rigidities, the elastic center of the composite section must be computed in both directions as follows:

$$Z_x=\frac{\sum_{i=1}^{2}E_i*A_{xxi}*Z_i}{\sum_{i=1}^{2}E_i*A_{xxi}}\ldots\ldots Z_y=\frac{\sum_{i=1}^{2}E_i*A_{yyi}*Z_i}{\sum_{i=1}^{2}E_i*A_{yyi}}$$

In the longitudinal direction, a composite action between the cast in place concrete deck and the precast presteressed girders is considered. The transverse stiffness's of the girders are rather small and neglected in this analysis. Hence, the load in the transverse direction is assumed to be carried by the in-situ reinforced concrete deck only. The flexural rigidities in the longitudinal and transverse directions are:

$$D_{xx}=\sum_{i=1}^{2}\frac{E_i}{1-\upsilon_i^2}(i_{xx}+A_{xxi}(Z_x-Z_i)^2)\ldots\ldots D_{yy}=\sum_{i=1}^{2}\frac{E_i}{1-\upsilon_i^2}(i_{yy}+A_{yyi}(Z_y-Z_i)^2)$$

The torsional rigidities are:

$$D_{xy}=\sum_{i=1}^{2}G_i*i_{xy}\ldots\ldots D_{yx}=\sum_{i=1}^{2}G_i*i_{yx}$$

D_v is the coupling stiffness which is equal to v*D_{yy} for $D_{yy} < D_{xx}$. If poison's ratio was assumed to be zero, bending in the longitudinal direction, bending in the transverse direction and torsion are uncoupled phenomenon.

The general constitutive equation for orthotropic plate is then:

$$\begin{aligned} m_x &= D_{xx} * k_{xx} \\ m_y &= D_{yy} * k_{yy} \\ m_{xy} &= D_{xy} * k_{xy} \\ m_{yx} &= D_{yx} * k_{yx} \end{aligned} \quad \ldots\ldots [(16)]$$

In plate analysis, single torsion stiffness is required and the torsion moment m_{xy} and m_{yx} are equal. Due to this fact, the average torsion stiffness should be calculated.

$$\overline{m_{xy}} = \frac{(m_{xy} + m_{yx})}{2} \ldots\ldots \overline{D_{xy}} = \frac{(D_{xy} + D_{yx})}{2}$$

The shear forces in the longitudinal and transverse directions are also expressed interims of shear force deformation stiffness as follows

$$V_x = D_{\gamma x} * \gamma_x \ldots\ldots V_y = D_{\gamma y} * \gamma_y$$

The general constitutive equation in matrix form for orthotropic plate is:

$$\begin{Bmatrix} m_{xx} \\ m_{yy} \\ \overline{m_{xy}} \\ v_x \\ v_y \end{Bmatrix} = \begin{Bmatrix} D_{xx} & D_v & 0 & 0 & 0 \\ D_v & D_{yy} & 0 & 0 & 0 \\ 0 & 0 & \overline{D_{xy}}/2 & 0 & 0 \\ 0 & 0 & 0 & D_{\gamma x} & 0 \\ 0 & 0 & 0 & 0 & D_{\gamma y} \end{Bmatrix} \begin{Bmatrix} k_{xx} \\ k_{yy} \\ \rho_{xy} \\ \gamma_x \\ \gamma_y \end{Bmatrix}$$

3.1 Finite element model formulation

Orthotropic plate finite element model is created using a SCIA Engineer general purpose commercial finite element package. SCIA Engineer is a software system for a static and dynamic analysis of structures and their design to standards. It is grounded on the displacement-based finite element technique. It can be used to calculate and design structures consisting of 1D members (modeled by linear finite elements) and planar parts such as walls, plates, and curved slabs (modeled by 2D finite elements).

4 nodded plate bending elements with three degree of freedom (one displacement, u_z and two rotations, Φ_x and Φ_y) at each node have been created. A Mindlin plate element which accounts Shear force deformation has been used.

3.1.1 Boundary conditions

Flexible Elastomeric bearing of the following features were provided under each girder.

- block length parallel to the girders a=300mm
- block width perpendicular to the girders b=400mm
- thickness one layer of rubber t_i=8mm
- number of layers n=5
- block coating thickness t_c= 4mm

The vertical spring stiffness of the bearing as per Euro code of recommendation was calculated as follows.

$$\frac{1}{k_z} = \frac{n*t_i}{A_i} * \left[\frac{1}{5*G*s_i^2} + \frac{1}{E_b} \right] \quad \text{------ [22]}$$

Where: $A_i = a_i * b_i = (300 - 2*4)*(400 - 2*4) = 114464 mm^2$

a_i= effective length= $a_i = a - 2*t_c$

b_i= effective width = $b_i = b - 2*t_c$

G=0.9N/mm^2

E_b =Bulk modules =2000N/mm^2

l_p=force free parameter= $l_p = 2*(a_i + b_i) = 2*(292 + 392) = 1368 mm$

S_i=form factor= $S_i = \frac{A_i}{l_p * t_i} = \frac{114464}{1368*8} = 10.459$

$$\frac{1}{k_z} = \frac{5*8}{114464} * \left[\frac{1}{5*0.9*10.4591^2} + \frac{1}{2000} \right] = 8.8462*10^{-7}$$

$$k_z = \frac{1}{8.8462*10^{-7}} = 1130 kN/mm = 1130 mN/m$$

Intermediate nodes were created on the plate model exactly at the location of the bearings relative to the ends of the girders. These nodes have been given displacement and rotation constraints. Minimum possible restraints were provided keeping in mind that the system will be statically stable in all directions. The bridge is free to translate in the global X and Y directions and spring stiffness of K_z is provided in the global Z direction to allow limited displacement.

3.2 Orthotropic plate Model without end diaphragm beams

Diaphragms are intended to tie beams together to facilitate construction and maintenance, transfer lateral loads and improve traffic load distributions. Therefore, this element may be one of the important structural elements for live load distributions and bridge load capacities. However, in the calculation of load distribution and capacity verification, researches and many codes of recommendations exclude the presence of diaphragms in the model. As the result, in the orthotropic plate model it is a common practice to abandon the part of the end diaphragms. As a component of this case study, the load distribution of the skew bridge under consideration was tested without considering the end diaphragm beams in ultimate and serviceability limit states.

To distribute the stiffness of the girders transversely and for internal force hand calculation due to self weight of the viaduct, the bridge is divided in to three plates shown in the Fig.3.3 below. These plates have different stiffness in the longitudinal direction due to spacing between girders and cross sectional dimensions of the girders. The transverse stiffness's of the prestressed elements were neglected and the thickness of the deck is constant over the whole bridge. Hence, all these plates have the same stiffness in the transverse direction.

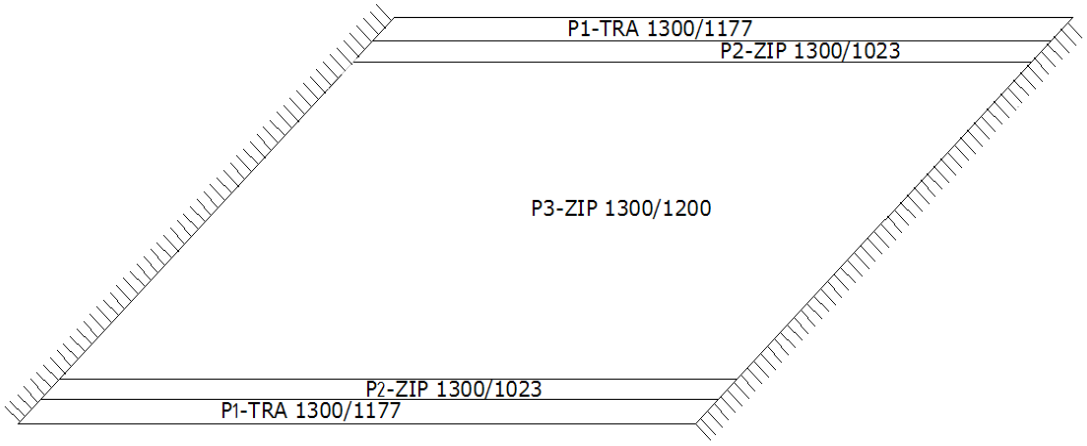

Fig 3. 3, Plates considered for analysis

The cross sections and properties of all the above orthotropic plates were shown in the subsequent figures.

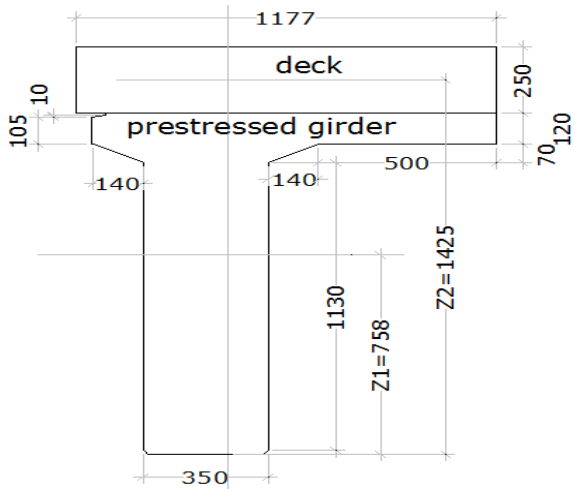

Plate- 1(TRA1300/11177)

Name	TRA beam only	
Type	General cross-section	
Item material	C53/65	
Fabrication	general	
Buckling y-y, z-z	b	c
FEM analysis	✓	
Picture		
A [m²]	5,5850e-01	
A y, z [m²]	1,0386e-01	3,1934e-01
I y, z [m⁴]	9,2801e-02	2,5574e-02
I w [m⁶], t [m⁴]	0,0000e+00	1,6647e-02
Wel y, z [m³]	1,2246e-01	3,3902e-02
Wpl y, z [m³]	2,0340e-01	9,0324e-02
d y, z [mm]	-148	287
c YLCS, ZLCS [mm]	236	758
alpha [deg]	0,00	
AL [m²/m]	4,7584e+00	

Properties of Spandrel beam

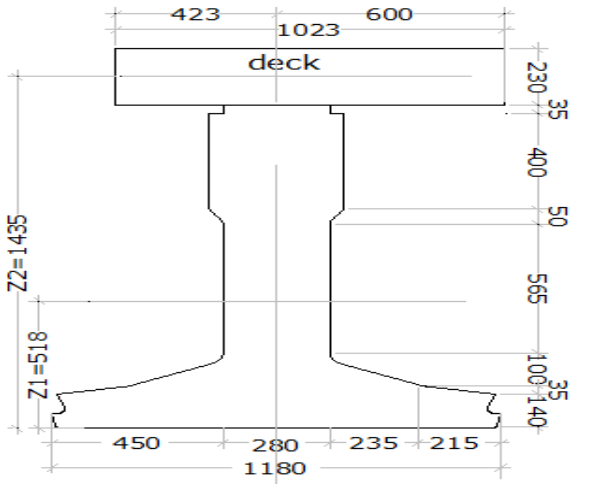

Plate -2 (ZIP 1300/1023)

Name	ZIP beam only	
Type	General cross-section	
Item material	C53/65	
Fabrication	general	
Buckling y-y, z-z	c	c
FEM analysis	✓	
Picture		
A [m²]	5,6946e-01	
A y, z [m²]	3,0008e-01	2,9332e-01
I y, z [m⁴]	1,0175e-01	2,4180e-02
I w [m⁶], t [m⁴]	0,0000e+00	1,4572e-02
Wel y, z [m³]	1,2613e-01	4,0983e-02
Wpl y, z [m³]	2,1263e-01	8,6343e-02
d y, z [mm]	0	-274
c YLCS, ZLCS [mm]	0	518
alpha [deg]	0,00	
AL [m²/m]	4,8638e+00	

property of Inverted T beam

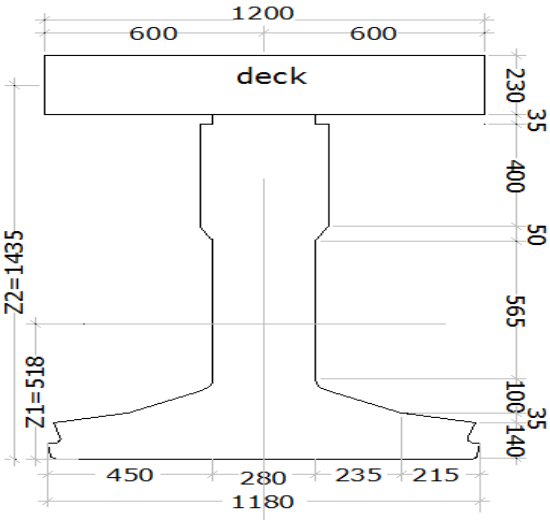

Plate-3 (ZIP 1300/1200)

Name	ZIP beam only	
Type	General cross-section	
Item material	C53/65	
Fabrication	general	
Buckling y-y, z-z	c	c
FEM analysis	✓	
Picture		
A [m²]	5,6946e-01	
A y, z [m²]	3,0008e-01	2,9332e-01
I y, z [m⁴]	1,0175e-01	2,4180e-02
I w [m⁶], t [m⁴]	0,0000e+00	1,4572e-02
Wel y, z [m³]	1,2613e-01	4,0983e-02
Wpl y, z [m³]	2,1263e-01	8,6343e-02
d y, z [mm]	0	-274
c YLCS, ZLCS [mm]	0	518
alpha [deg]	0,00	
AL [m²/m]	4,8638e+00	

property of Inverted T-beam

Fig3. 4, cross sections and properties of the three plates

3.2.1 Stiffness parameter calculations

The elastic center of deck girder composite system is calculated as follows:

$$Z_x = \frac{\sum_{i=1}^{2} E_i * A_{xxi} * Z_i}{\sum_{i=1}^{2} E_i * A_{xxi}} \ldots\ldots Z_y = \frac{\sum_{i=1}^{2} E_i * A_{yyi} * Z_i}{\sum_{i=1}^{2} E_i * A_{yyi}}$$

The stiffness parameters about the center of the composite system

$$D_{xx} = \sum_{i=1}^{2} \frac{E_i}{1-\upsilon^2_i}(i_{xx} + A_{xxi}(Z_x - Z_i)^2) = D_{11}$$

$$D_{11} = \frac{E_{girder}}{1-v^2}(i_{xx(girder)} + \frac{A_{girder}}{b}(Z_x - Z_1)^2) + \frac{E_{deck}}{1-v^2}(i_{xxdeck} + h(Z_x - Z_2)^2$$

$$D_{yy} = \sum_{i=1}^{2} \frac{E_i}{1-\upsilon^2_i}(i_{yy} + A_{yyi}(Z_y - Z_i)^2) = D_{22}$$

$$D_{yy} = D_{22} = \frac{1}{12} * \frac{E_{deck} * h^3}{1-v^2}$$

Coupling stiffness $D_v = v * D_{yy}$

The torsional moment of inertia of a cross-section with thickness h and unit width is equal to $h^3/3$. Half of it is caused by the horizontal stress in the cross-section and the other half is results from the vertical stresses. In continues plates only the horizontal stresses occur and therefore the torsional moment of inertia becomes $h^3/6$. [(15)]

$$D_{xy} = \frac{G_{girder} * I_{tgirder}}{b} + \frac{G_{deck} * h^3{}_{tdeck}}{6}$$

$$D_{yx} = \frac{G_{deck} * h^3}{6}$$

$$D_{33} = \frac{\overline{D_{xy}}}{2} = \frac{(D_{xy} + D_{yx})}{4}$$

$$D_{44} = D_{\gamma x} = (G_{girder} * A_{zgirder} + G_{deck} * A_{zdeck}) / b$$

A_z is the cross-sectional area A divided by the shape factor η, which accounts the warped shape and the inhomogeneous distribution of the shear stress over the cross-section. [(16)]

$$D_{55} = D_{\gamma y} = \frac{G_{deck} * h}{\eta}$$ η=6/5=1.2, for rectangular section.

3.2.2 Model without end diaphragm beams in the serviceability limit state

Initially, both cast in-situ deck and precast prestressed girders have been assumed to be uncracked in SLS condition. However, the stress in the transverse direction of the reinforced concrete deck was found to be far higher than the tensile strength of the deck concrete. As the result, the deck has taken as cracked in the transverse direction. In the longitudinal direction, the tensile stress is resisted by the precast presteressed girders and the deck slab is always in compression. Hence, uncracked stiffness should be used. Nevertheless, the result of this simplified model would be compared with a 3D brick element model using ATENA 3D in the subsequent chapter. In ATENA 3D it was not possible to use different modulus of elasticity in the longitudinal and transverse directions for linear elastic analysis. For this reason, in this particular case study half of the uncracked young's modulus in both directions has been assumed in the deck to take into account cracking. Presteressed and high quality concrete for the girders has been assumed to be uncracked.

All the above stiffness parameters have been computed using simple spreadsheet program and tabulated as follows. [ANNEX A]

Without considering end diaphragm beam					
ZIP 1300/1200		ZIP1300/1023		TRA1300/1177	
SLS		SLS		SLS	
D_{11}	5921.8	D_{11}	6562.9	D_{11}	4584.4
D_{22}	16.1	D_{22}	16.1	D_{22}	20.6
D_v	2.4	D_v	2.4	D_v	3.1
D_{33}	57.7	D_{33}	65.1	D_{33}	68.0
D_{44}	5383.3	D_{44}	6090.7	D_{44}	5945.0
D_{55}	1291.7	D_{55}	1291.7	D_{55}	1404.0

Table3. 1, stiffness parameters in the service limit state without considering the stiffness of end diaphragm beam

3.2.3 Finite element model results

SCIA Engineer automatically generate quadrilateral shell element before analysis has been carried out. To optimize the mesh refinement, ratio that compares the coarse and fine mesh

results has been considered. The result of the comparison indicates that there is virtually no difference between the two results. Based on the comparison 300x300mm finite element size can produce practically accurate results.

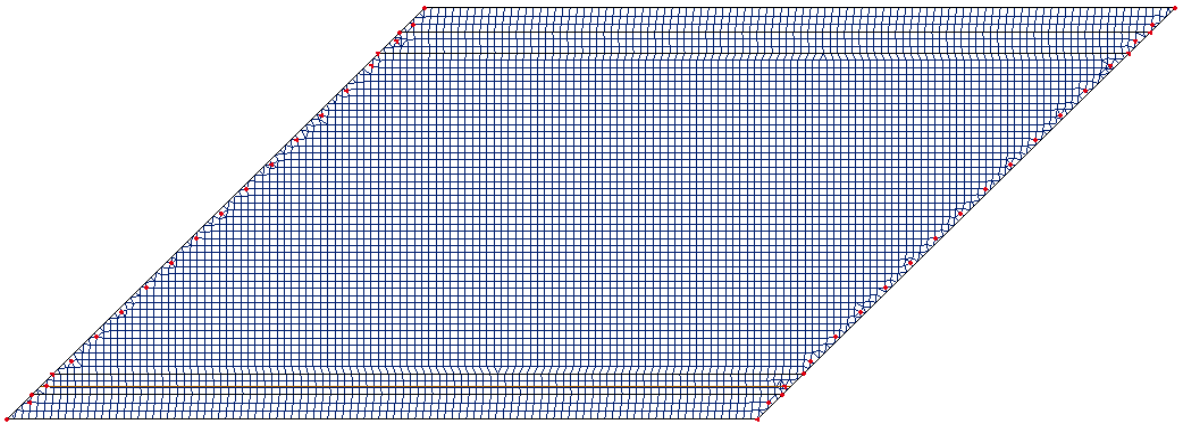

Fig3. 5, finite element mesh generated by Scia engineer

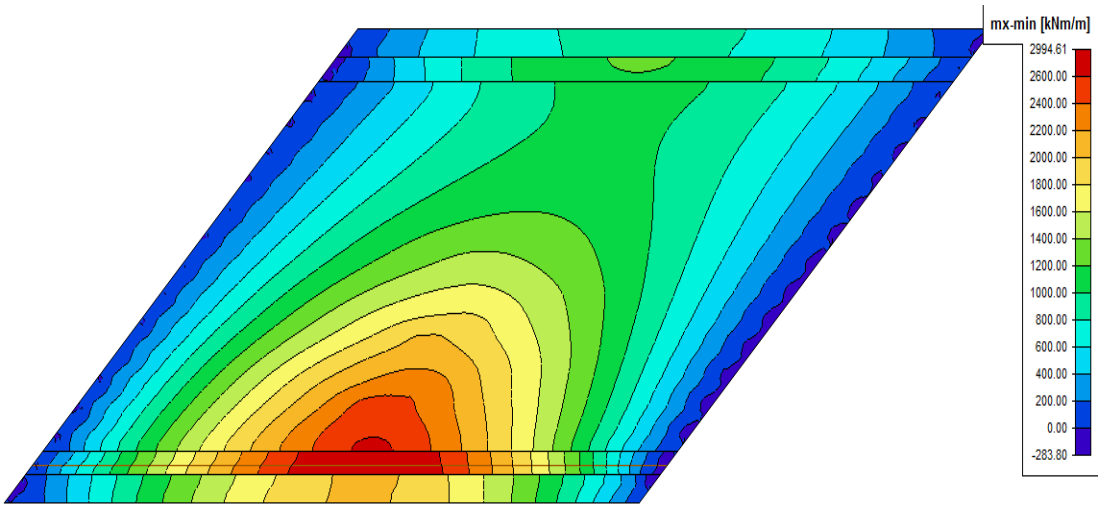

Fig3. 6. Bending moment in the longitudinal direction (excluding self weight)

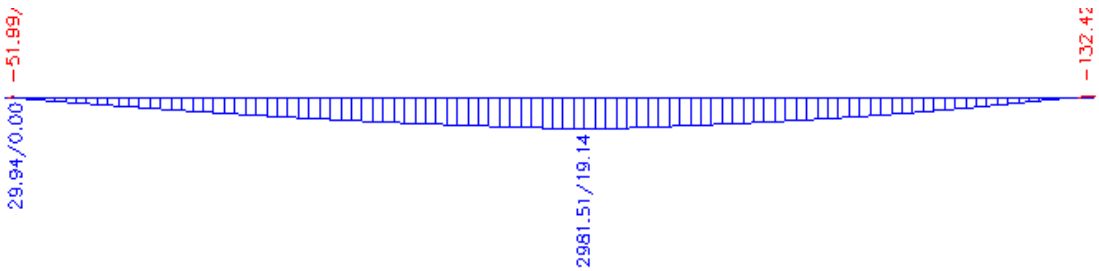

Fig3. 7 Bending moment in the longitudinal direction at the critical girder (excluding self weight)

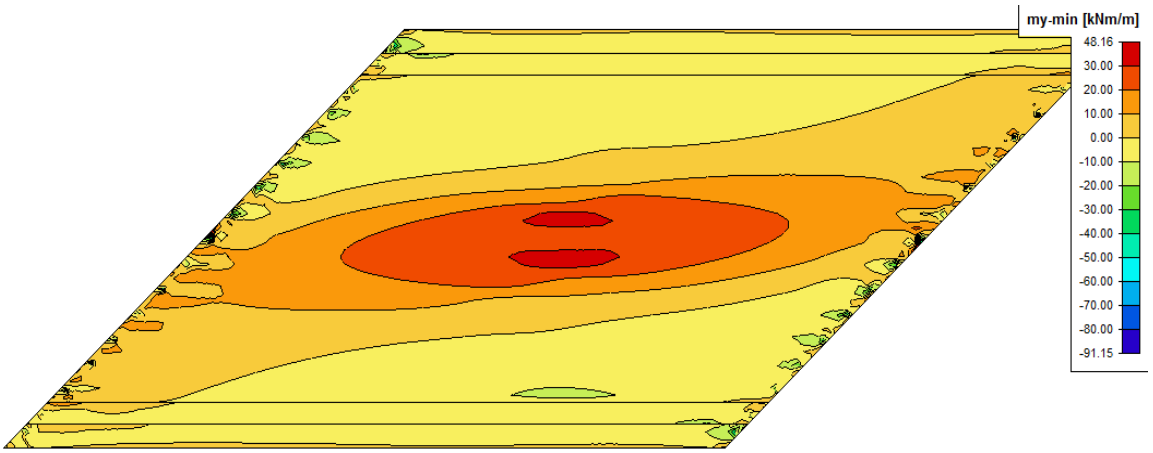

Fig3. 8, Maximum bending moment is the transverse direction (excluding self weight)

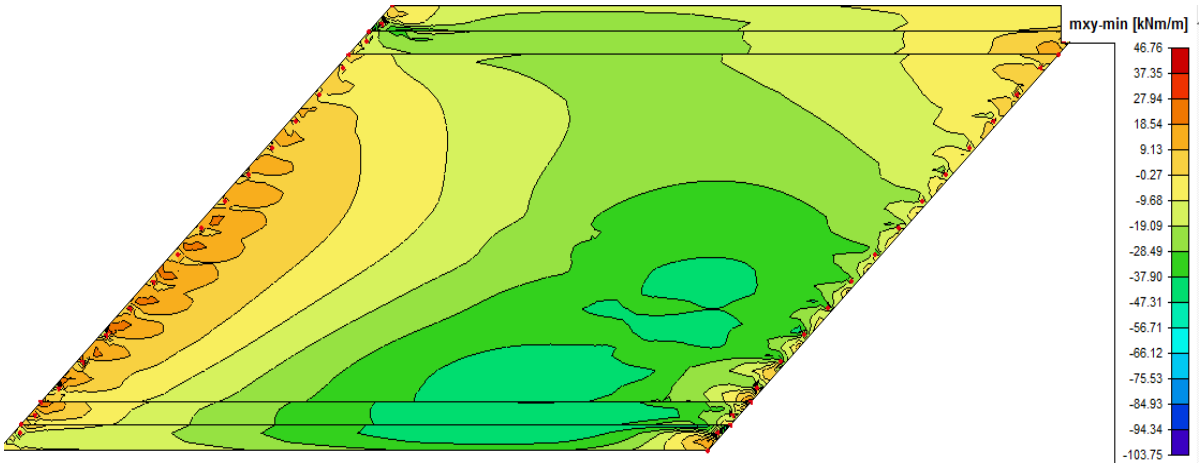

Fig3. 9, Torsion moment in the whole bridge (combination-6)

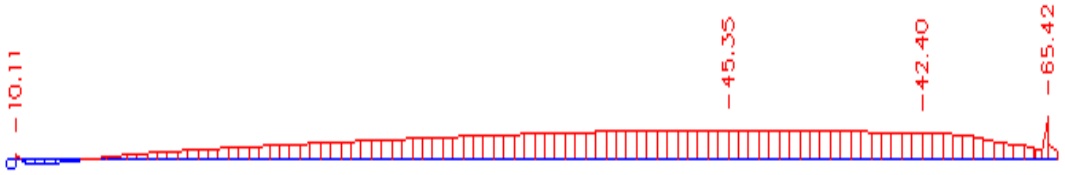

Fig3. 10, Maximum negative torsion moment at the first inverted T-girder (combination 6)

3.2.4 Variable load positions and load combinations for torsion

In the previous chapter of this study, three possible axle load arrangements have been endeavored for torsion moments in the bridge. In this chapter another different arrangements of traffic loads, both axle and UDL have been looked for. In order to determine the worst load combinations for torsion, it is imperative to find the torsion moments produced by each load cases at a specified point. Loads that produce positive and negative torques at one point will be grouped together and superimposed them to get the load combination for positive and negative torsion moments. The design torsion moment is the absolute value of the bigger in magnitude.

3.2.4.1 Critical location of axle loads for maximum twisting moments

Four tracks of the same 600KN tandem axle loads have been placed at positions a, b, c and d as show in the Fig.3.11 below, which is 1.5m left from the center of the bridge on lane 1, 2, 3 and lane 4 respectively.

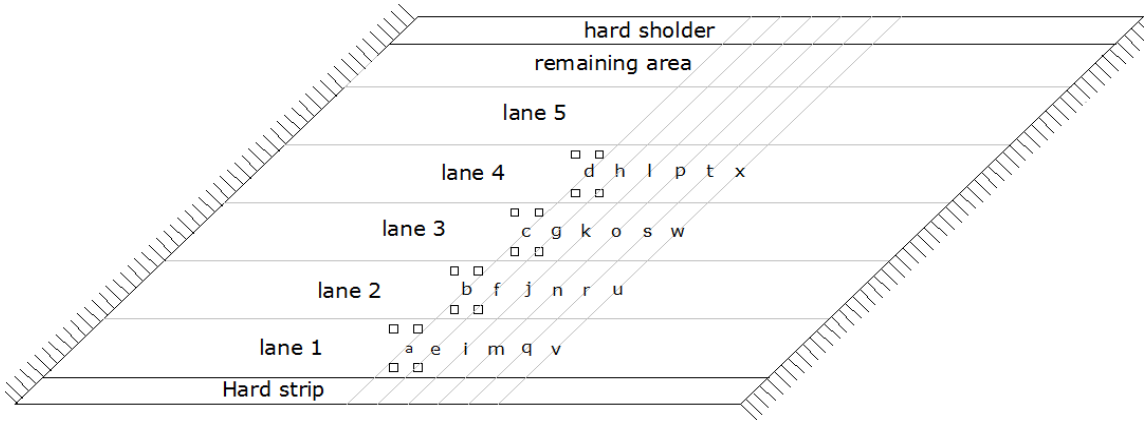

Fig3. 11, Different load positions for axle loads

These tracks have been driven on their respective lanes to the right and twisting moments were recorded at the obtuse corner of the bridge. The calculated torsion moments are exactly d distance from face of support at the first inverted T-girder. Axle load a has been moved to positions e, i, m, q and v step by step as shown in the Fig3.11 above. The longitudinal distance between these stations were 1.5m. Same thing has been done for axle loads b, c and d in their respective lanes. The torsion moments produced by all these load positions were tabulated in the following table.

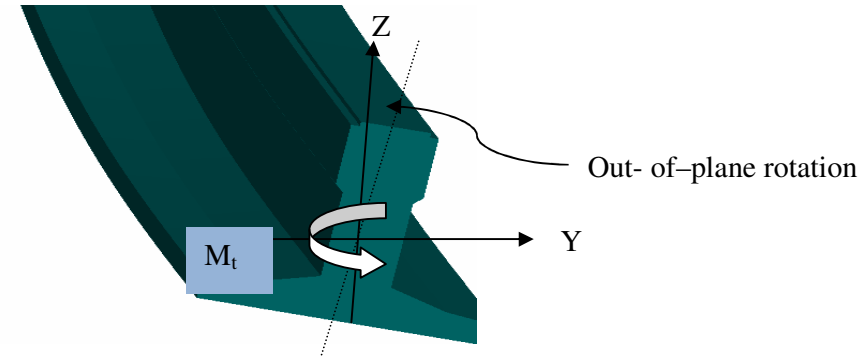

Fig3. 12, Direction of positive torsion moment according to write hand role

Location and Torsion moment for 600kN two Axle load at d distance from face of support at the first Inverted T-girder												
1st lane	Loc.a	-21.2	Loc.e	-21.9	Loc.i	-19.6	Loc.m	-17.7	Loc.q	-15.2	Loc.v	-12.6
2nd lane	Loc.b	12.5	Loc.f	13.4	Loc.j	14.2	Loc.n	14.7	Loc.r	14.8	Loc.u	14.7
3rd lane	Loc.c	10.1	Loc.g	10.2	Loc.k	10.1	Loc.o	9.7	Loc.s	9.2	Loc.w	8.5
4th lane	Loc.d	4.3	Loc.h	4.2	Loc.l	4.1	Loc.p	3.9	Loc.t	3.7	Loc.x	3.4

Table3. 2, Positions 600kN tandem axle load and torsion moment produced by these axle loads at d distance from the face of the bearing

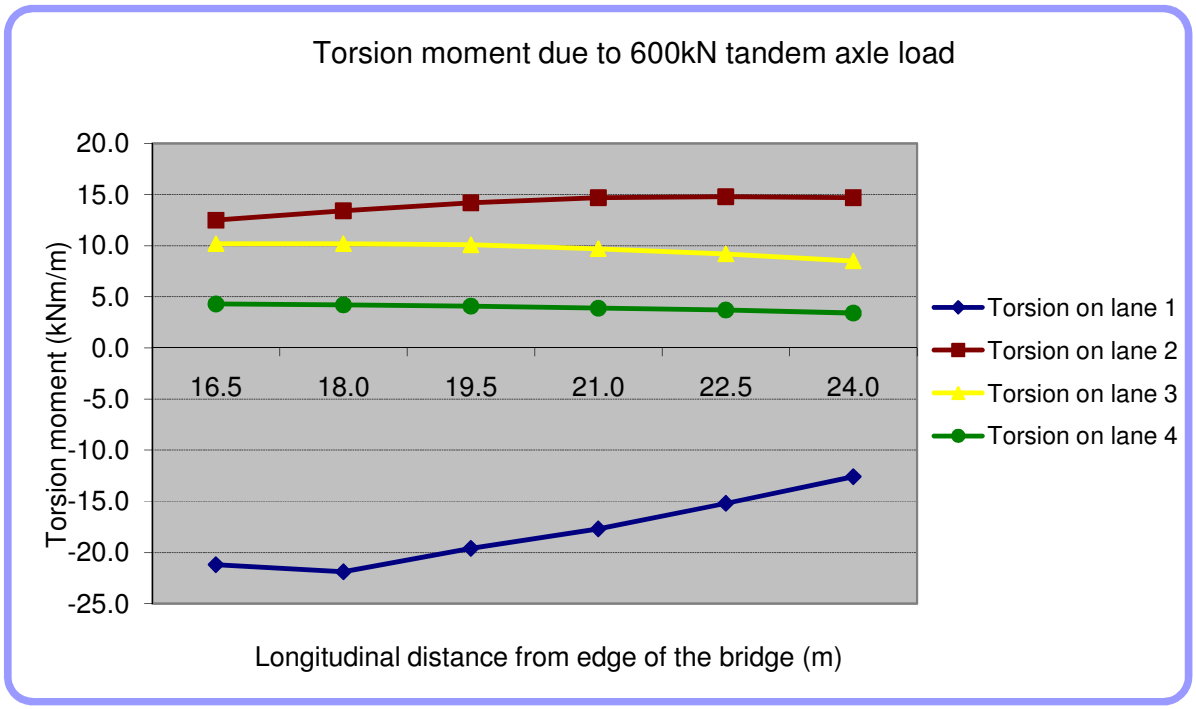

Graph3. 1, Torsion moment at d distance from face of support of the first inverted T- girder due to 600kN tandem axle load

From the above graph, the following things have been observed,

i. When the track moves from lane one to lane two, the torsion moment in the obtuse corner of the bridge changes sign from negative to positive.
ii. The negative twisting moment due to axle load on lane 1 decreases in magnitude when the track drives away from the center of the bridge in both directions.
iii. The maximum torsion moment due to axle load on lane 2 is between location n and r or r and u.
iv. The Maximum torsion moment due to axle load at lane 3 is between location c and g or between location g and k.
v. The maximum torsion due to axle load on lane 4 is in between location d and h or to the left of location d.

Further detail investigation have been carried out to find the exact locations of the axle loads on lane 2, 3 and 4 that creates maximum torque at the benchmark location. The result of the investigation revealed that the critical locations for axle loads on lane 2, 3 and 4 are in between n and r, between c and g, and to the left of d respectively. These locations are exactly at the middle of the bridge in the longitudinal direction.

Load location	torsion moment (kNm/m
Lane 2	14.9
Lane 3	10.2
Lane 4	4.3

Table3. 3, Torsion moment produced by 600kN tandem axle load

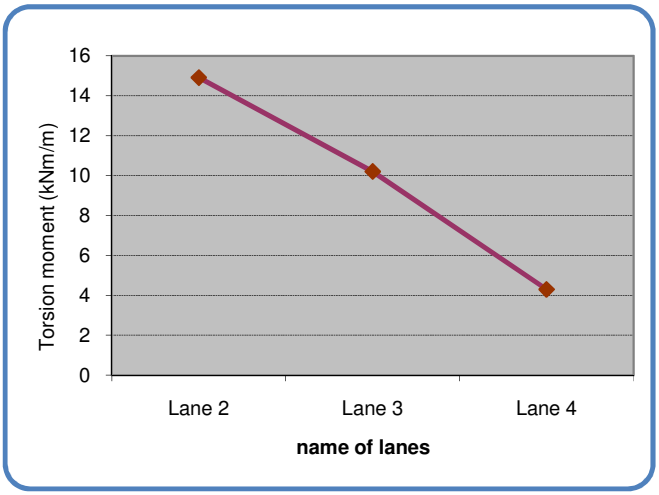

Graph3. 2, Variation of torsion moment with load locations

Hence, placing the first design axle load at the first lane of the bridge and leaving the other lanes unloaded for axle loads would create maximum global negative torsion moments in the obtuse corner of the bridge. On the other hand, leaving unloaded for the first lane and placing the axle loads on lane 2, 3 and 4 shown in the Fig3.13 would create maximum global positive torsion moments in the bridge.

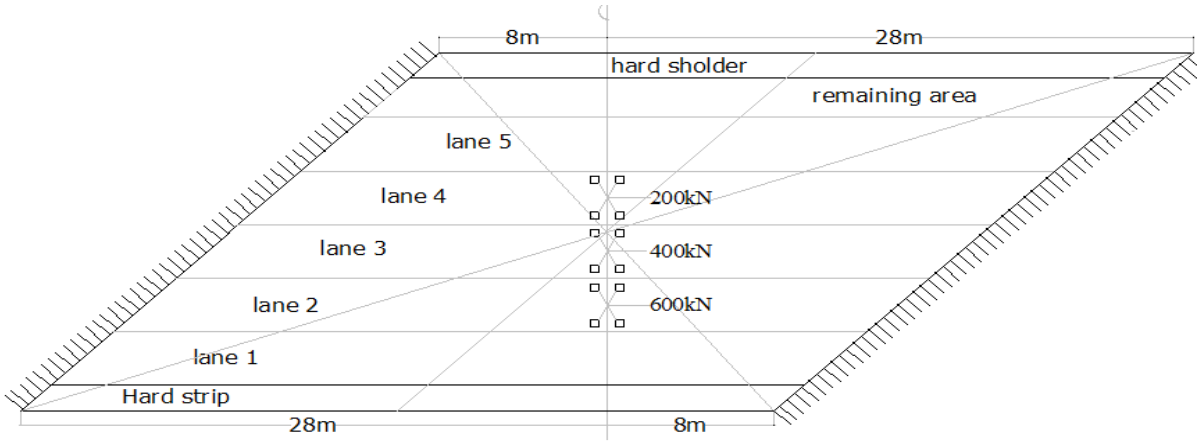

Fig3. 13, Axle load arrangement for maximum positive torsion moment

3.2.4.2 Critical location of lane load for maximum torsion moments

The torsion moments due to lane loads placed at the first lane is negative and the maximum value is just at the obtuse corner. This twisting moment changes sign when the lane load moves to the transverse direction of the bridge. The variation of the twisting moment at a particular benchmark with the location of distributed lane load is determined by moving the load step by step to the transverse direction of the bridge. In this study a 3m wide10.35kN/m^2 uniformly distributed load rolls to the transverse direction by 1m interval has been considered. A total of 13load positions have been assessed as shown in the Fig3.14 and twisting moments at d distance from face of support of the first inverted T-girder was traced. The following figure shows the load arrangements.

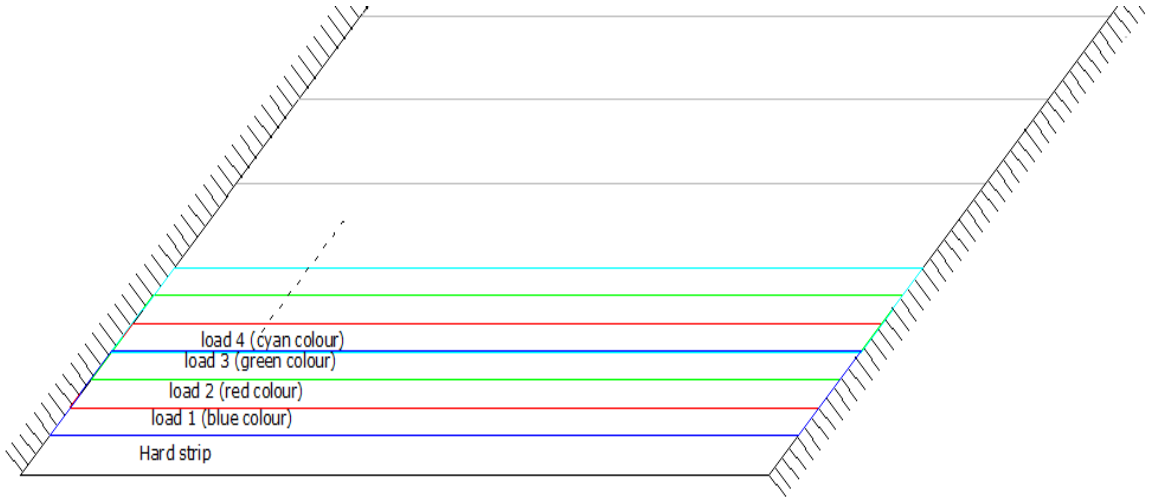

Fig3. 14, Lane load positions considered

The values of the twisting moments produced by all the above load cases has been tabulated and plotted in the subsequent figures.

Location and Maximum Torsion moment for 10.35kN/m^2 Lane load at d distance face of support for the first ZIP Girder									
Loc. 1	-17.8	Loc. 4	16.2	Loc. 7	12.0	Loc. 10	4.9	Loc. 13	1.4
Loc. 2	1.8	Loc. 5	16.4	Loc. 8	9.3	Loc. 11	3.4		
Loc. 3	12.1	Loc. 6	14.6	Loc. 9	6.9	Loc. 12	2.2		

Table3. 4, Torsion moments as the result of 3m wide 10.35kN/m^2 uniformly distributed load

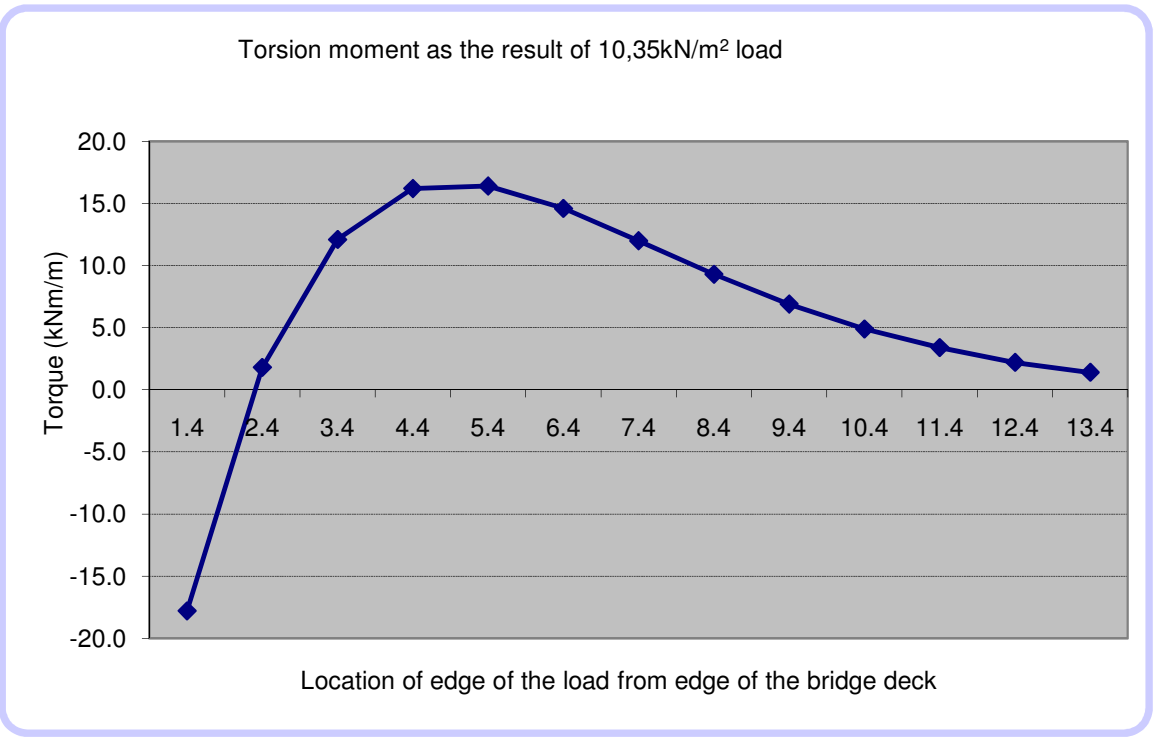

Graph 3. 3, Torsion moments versus location of UDL in the transverse direction from the bridge edge

Load case 1 is placed fully in the first notional lane. Load case 2 and 3 are partly on lane 1 and partly on lane 2. Load case 4 is fully on notional lane 2. From the graph above, negative twisting moments is produced when the lane load is placed fully on the first notional lane (load case 1). However, it changes its sign when this load moves 1m to the transverse direction (load case 2). Maximum positive torsion moment is produced on load case 4, which means when the lane load is placed exactly on the second notional lane. Governing negative twisting moment due to lane loads is created when the first notional lane is loaded and leaving

unloaded for the remaining lanes. And the total maximum positive torque produced by loading all lanes except the first national lane as shown in the following figure.

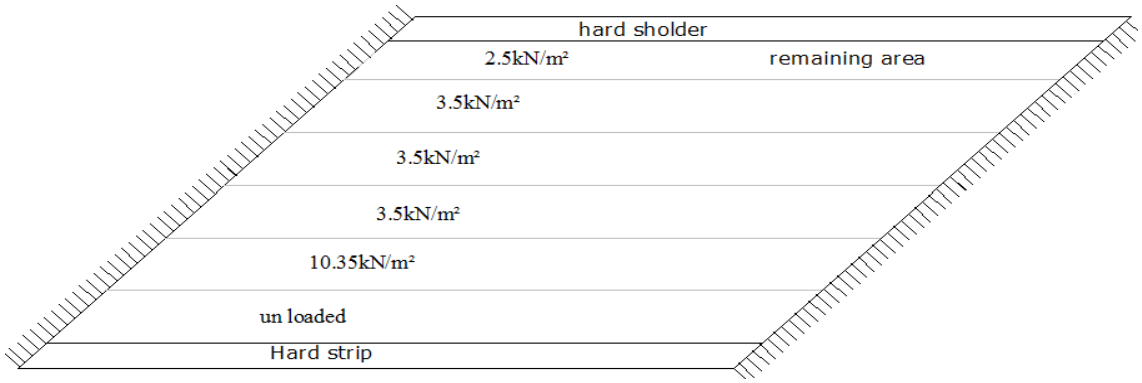

Fig3. 15, Lane load arrangement for maximum positive torsion moment

3.2.4.3 Live Load combinations for Torsion

Load cases having the same sign torsion moments have been superimposed to find the worst scenario. The following two figures show, the variable (traffic) load cases and arrangements for maximum negative and positive torsion moments.

Load case 11,

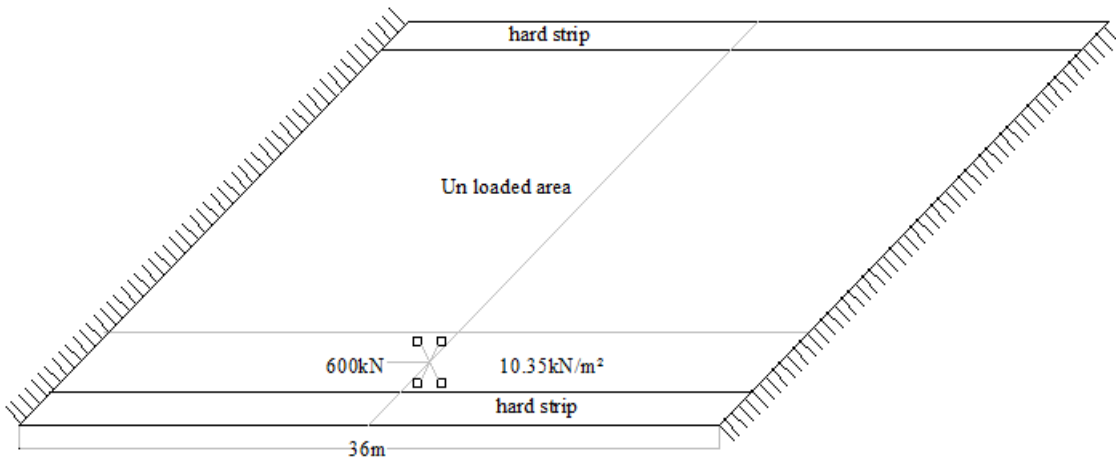

Fig3. 16, Variable load arrangement for maximum negative torsion moment

Load case 12,

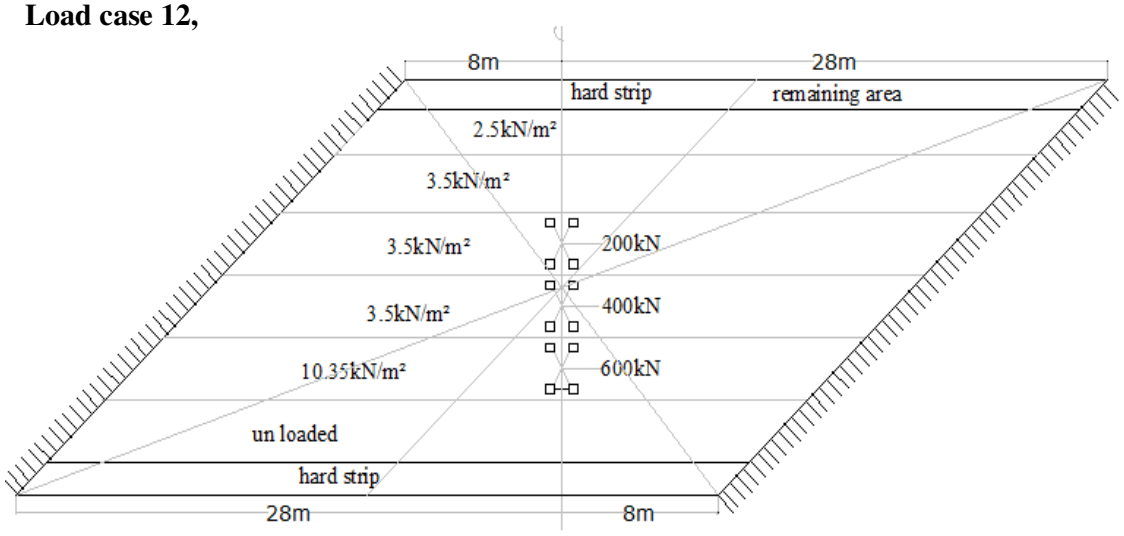

Fig3. 17, Variable load arrangement for maximum positive design torsion

In conclusion the following load combinations were considered as an additional combination with the previous 3 cases explained in chapter two.

Comb7: $L_{c3}+L_{c4}+L_{c11}$, (maximum negative torsion moment)

Comb 8: $L_{c3}+L_{c4}+L_{c12}$ (maximum positive torsion moment)

The design torsion moment is the maximum in magnitude of the above two combinations. In this study, combination 7, which is the negative torsion moment, has been found to be governing. The maximum twisting moment in the serviceability limit state without stiffness of the end diaphragm beams from combination 7 is shown in the following figure. This twisting moment is clearly higher than the torsion moment shown in Fig.3.10 on page 32

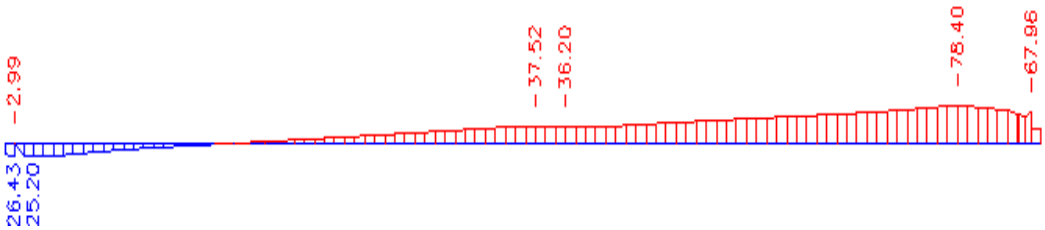

Fig3. 18, Torsion moment at the first inverted-T girder (combination 7)

3.2.5 Model without end diaphragm beams in the Ultimate limit state

In the ultimate limit state concrete for both deck and girder were assumed to be severely cracked in flexure and shear. The torsion stiffness is particularly fascinating in the ULS. Prior to cracking, a torsional moments coming to the structural elements is resisted by internal shear stresses. Shear stresses lead to diagonal principal tensile and compressive stresses. When the diagonal principal tension exceeds the tensile strength of the concrete, diagonal cracking occurs. It has been observed in experiments on beams subject to torsion that once crack initiates, it spirals around the perimeter of the member. Simultaneously, the beam torsional stiffness drops significantly [(17)]. For this reason, in this case study as per ROBK6 (Netherlands bridge design recommendations) art.12.3 only 40% of the full torsion stiffness for both the deck and girders is used in the ULS. Full and half flexural stiffness were assumed for the prestressed girders and cast in-situ deck slab respectively. Using these assumptions, the stiffness parameters had been calculated and tabulated in the following table. [ANNEX A]

Without considering end diaphragm beam, ULS					
ZIP 1300/1200		ZIP1300/1023		TRA1300/1177	
D_{11}	5921.8	D_{11}	6562.9	D_{11}	4584.4
D_{22}	16.1	D_{22}	16.1	D_{22}	20.6
D_{v}	2.4	D_{v}	2.4	D_{v}	3.1
D_{33}	25.8	D_{33}	29.3	D_{33}	30.7
D_{44}	5383.3	D_{44}	6090.7	D_{44}	5945.0
D_{55}	1291.7	D_{55}	1291.7	D_{55}	1404.0

Table 3. 5, Stiffness parameters in the ultimate limit state, without end diaphragm

3.2.5.1 Finite element model results

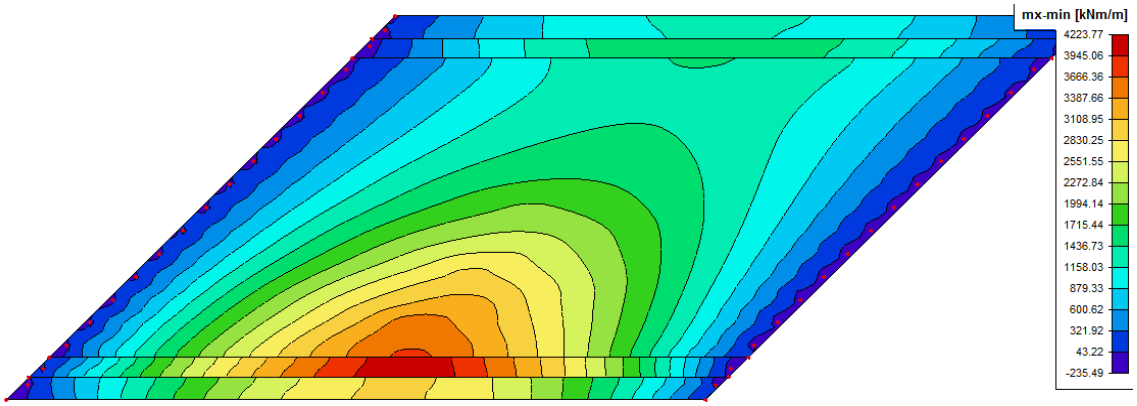

Fig3. 19, Bending moment in the longitudinal direction in the ULS (excluding self weight)

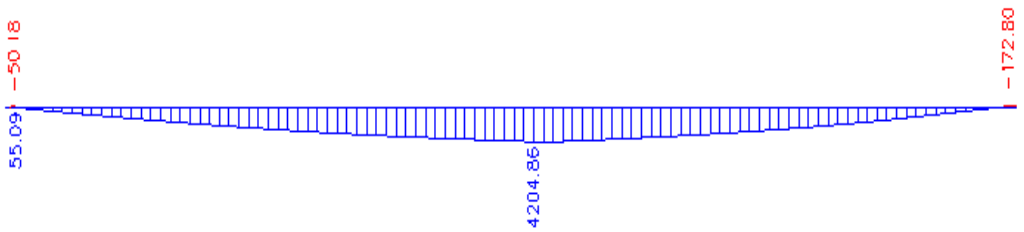

Fig3. 20, Bending moment in the longitudinal direction at the critical girder in the ULS (excluding self weight) critical combination

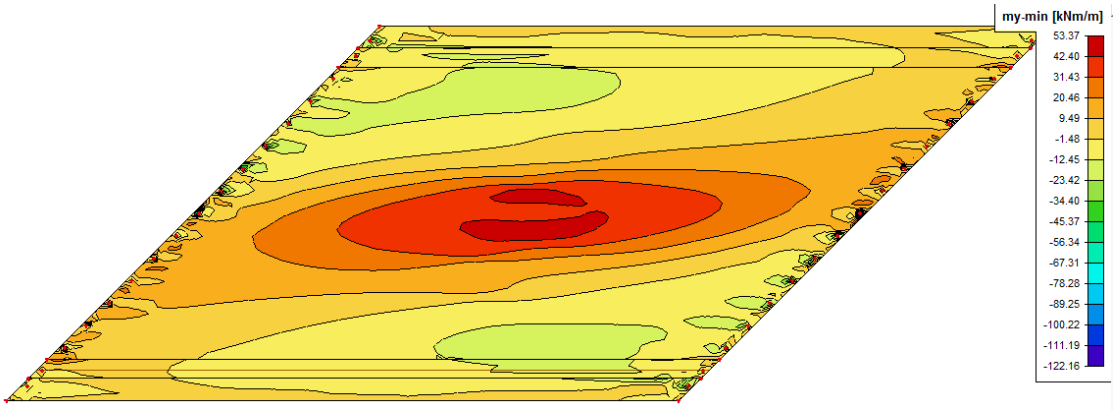

Fig3. 21, Maximum bending moment in the transverse direction (excluding self weight), critical combinations

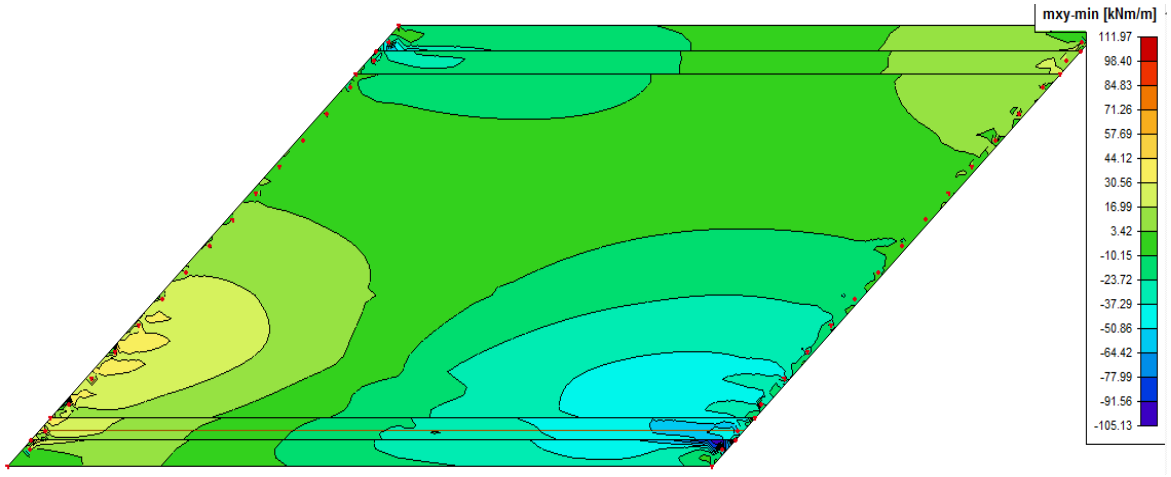

Fig3. 22, Torsion moment in the whole bridge, critical combinations

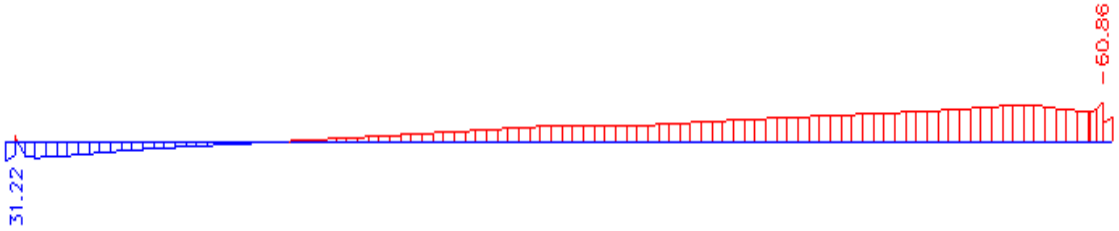

Fig3. 23, Torsion moment at the first inverted T-girder in the ULS, due to variable load

3.2.6 Model without end diaphragms and no torsion stiffness for girders in the ULS

The torsion moments coming to the girders are strongly dependant on the torsion stiffness of the cross section. If large torsion stiffness is used in the analysis then the twisting moments will be large as well and much torsion reinforcement should be provided. On the contrary, when small torsion stiffness is assumed in the analysis, the torsion moments absorbed by the section would be small and little torsion reinforcement will be required. In this case the load will find an alternative path.

For bridges with inverted T-girders, the torsional inertia is an order of magnitude less than the bending inertia. For less angle of skewness the analysis of such bridges can be simplified by ignoring the torsion stiffness of the girders. The torsion moment here is not the result of equilibrium. Consequently, in the ultimate limit state, torsion reinforcement might be left out altogether. However, the resulting load distribution is less effective and this gives rise to slightly increased bending moments. The correspondingly increased design strength in bending is considered adequate to carry the torques which would be associated with a full torsion model [(1)]. In this part of orthotropic plate model, the increase in bending in the girders and transverse moments in the deck slab as the result of ignoring the torsion contributions of the girders have been thoroughly assessed.

Without torsion stiffness for the Girders in ULS					
ZIP1300/1200		ZIP1300/1023		TRA1300/1177	
D_{11}	5921.8	D_{11}	6562.9	D_{11}	4584.4
D_{22}	16.1	D_{22}	16.1	D_{22}	20.6
D_{v}	2.4	D_{v}	2.4	D_{v}	3.1
D_{33}	5.5	D_{33}	5.5	D_{33}	7.0
D_{44}	5383.3	D_{44}	6090.7	D_{44}	5945.0
D_{55}	1291.7	D_{55}	1291.7	D_{55}	1404.0

Table3. 6, Stiffness parameters with zero torsion stiffness for girders and without end diaphragm in ULS [ANNEX A]

3.2.6.1 Finite element model output

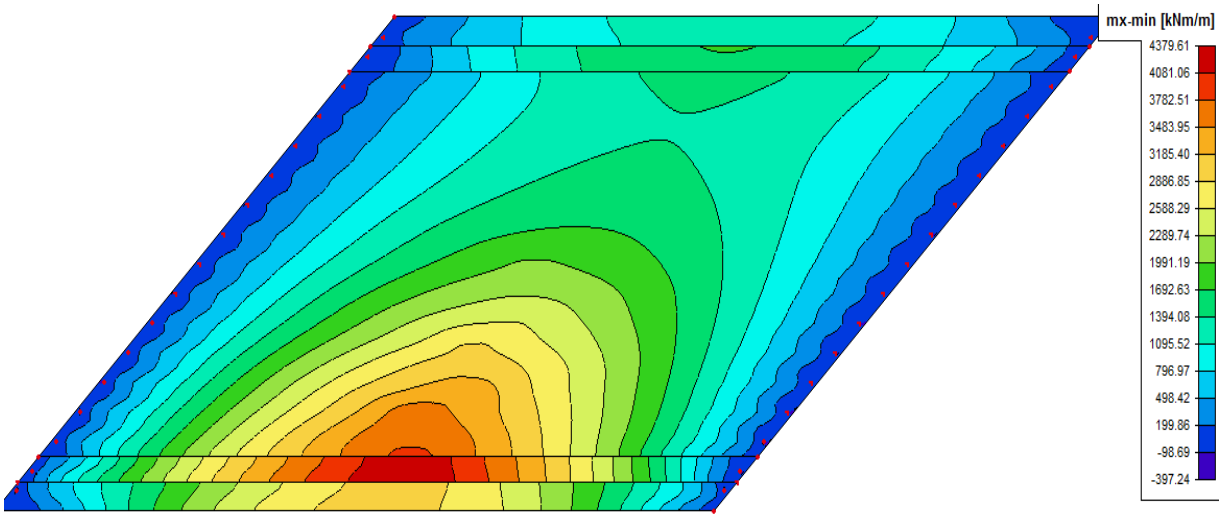

Fig3. 24, Longitudinal bending moment for the whole ridge (excluding self weight)

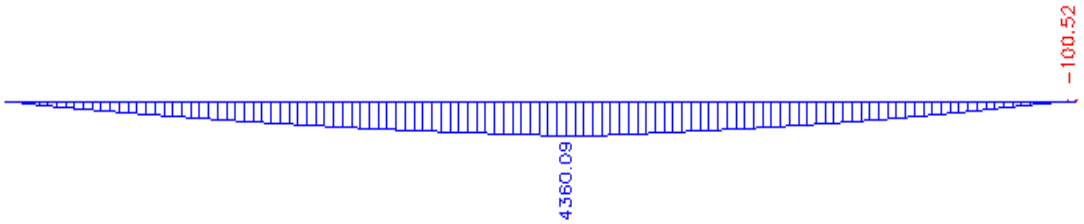

Fig3. 25, Longitudinal bending moment at the first Inverted T-girder (excluding self weight)

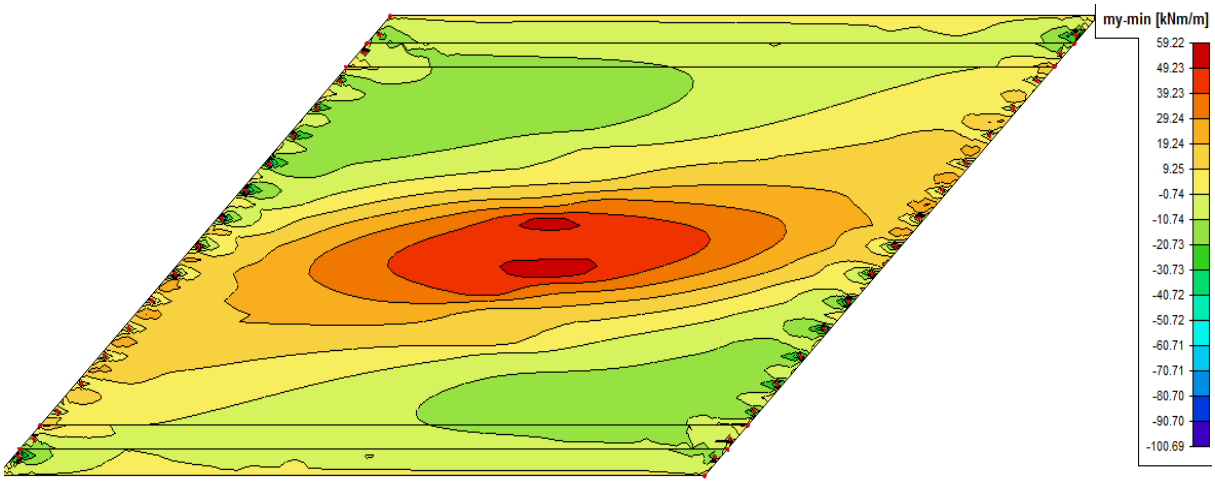

Fig3. 26, Bending moment in the transverse direction (excluding self weight of the bridge)

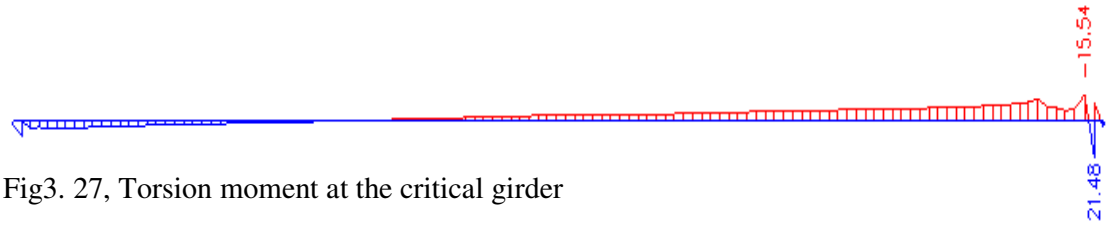

Fig3. 27, Torsion moment at the critical girder

3.2.7 Comparison of the above two ultimate limit state models

Two ULS systems without end diaphragm beams have been illustrated in the above sections. In the first system, 40% of full torsion stiffness for both the girders and deck was assigned; and in the second model, the torsion stiffness for the girders was totally overlooked. In the first model, the maximum torsion moment (m_{xy}) at the highly loaded girder was 61kNm. This torque decreased to 13.0kNm in the second model. This decrease in torque was accompanied by a slightly higher longitudinal and transverse bending moments in the girders and deck. The maximum longitudinal moment due to permanent and traffic load in the first model was found to be 4302kNm at the first inverted T-girder. This longitudinal bending moment increases to 4460kNm in the torsionless system. In addition to this the transverse bending moment in the deck increases from 51kNm/m to 58kNm/m. It is evident that the maximum bending moments from the 40% torsion model is about 4% lower than the bending moments from the torsionless model. The relatively small difference between these two results illustrate how this types of bridges have poor load distribution characteristics and are not very sensitive to the torsion inertia of the girders. Therefore, an equilibrium system could be secured by providing sufficient bending reinforcement or prestresssing cables in the ultimate limit states without torsion reinforcement at all. When torsion arises from compatibility only, Euro-code requires the member to be designed to avoid excessive cracking. In practice; this means that stirrups and longitudinal reinforcements should satisfy the detailing rules.

3.3 Orthotropic plate model with end diaphragm beam

A diaphragm is a transverse stiffener, which is placed between girders in order to maintain section geometry and to help load distribution. Cast-in-place concrete diaphragms are commonly used in prestressed concrete girder bridges. These transverse beams used in presteressed girder bridges on skewed bents cause difficulties in detailing and construction. As the skew angle increases and the girder spacing decreases, the connection and the construction become more difficult. Even the effectiveness of the diaphragms is questionable at these high skews.

In this part of this study the advantage of considering end diaphragm beams in the analysis have been examined. In the serviceability limit state, relatively high stiffness has been considered. However, in the ULS the cast in place reinforced concrete diaphragms would be severely cracked and the stiffness would be reduced at large. This reduction in stiffness has

also considered in the model. Finally, the load flows in the ultimate limit state with zero torsion stiffness for the girders have been scrutinized.

3.3.1 Model with end diaphragm beams in the Service limit state condition

Originally both cast in-situ deck and end diaphragms have been assumed to be uncracked and uncracked young's modulus were assumed. However, the stresses at the bottom fiber of the deck and diaphragms have been found to be much higher than the tensile strength of the cast in place concrete and half of its young's modulus was finally used.

To decrease the calculation complexity the contribution of the longitudinal girders in the end plate has been ignored. The end plates were considered to be a continuous cast in-situ concrete element same width as the width of the end diaphragm beams as shown in the following figure.

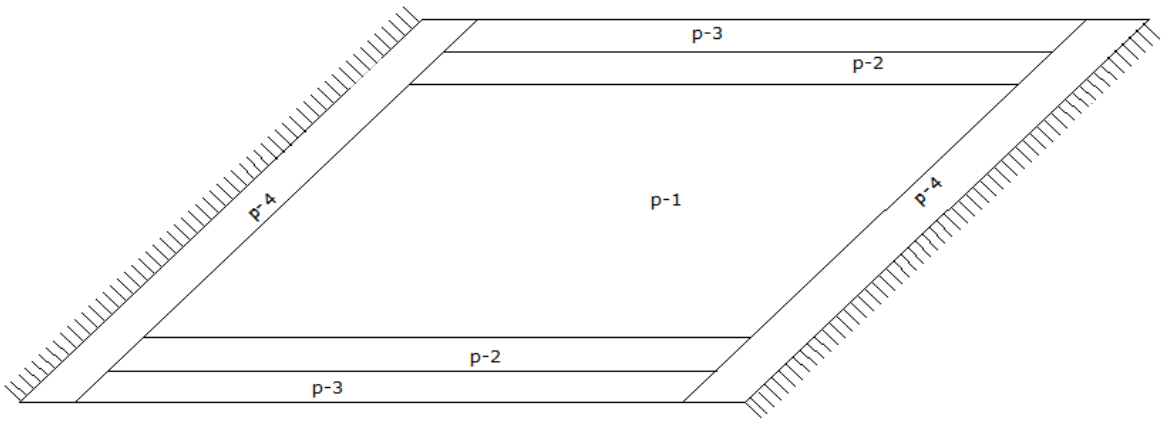

Fig3. 28, name of four plates considered for the model

Plates 1, 2 and 3 have been defined in the above without end diaphragm models. Their property is exactly the same. The end plates are assumed as an isotropic plate. The stiffness parameters are the same in all directions. Simple spreadsheet program were developed to make repeated calculations and the stiffness parameters for all the above four plates were tabulated in the following table. [ANNEX A]

Considering the stiffness of the end diaphragm beam in SLS							
(P-1)ZIP1300/1200		(p-2)ZIP1300/1023		(P-3)TRA1300/1177		(P-4)End plates	
D_{11}	5921.8	D_{11}	6562.9	D_{11}	4584.4	D_{11}	3704.2
D_{22}	16.1	D_{22}	16.1	D_{22}	20.6	D_{22}	3704.2
D_v	2.4	D_v	2.4	D_v	3.1	D_v	555.6
D_{33}	57.7	D_{33}	66.4	D_{33}	68.0	D_{33}	1574.3
D_{44}	5383.3	D_{44}	6090.7	D_{44}	5945.0	D_{44}	7918.5
D_{55}	1291.7	D_{55}	1291.7	D_{55}	1404.0	D_{55}	7918.5

Table3. 7, Stiffness parameters in SLS with end diaphragm beam

3.3.2 Result of the finite element model

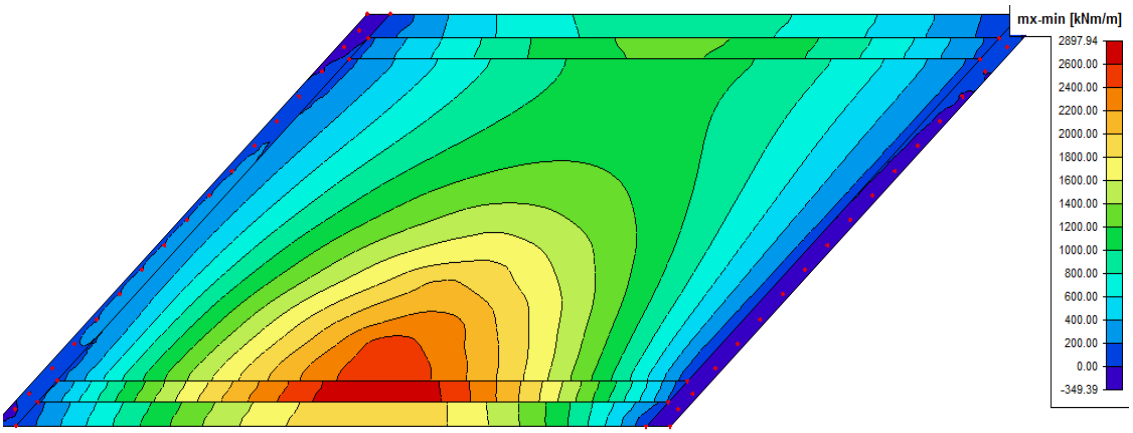

Fig3. 29, Longitudinal bending moment in the whole bridge (excluding dead load)

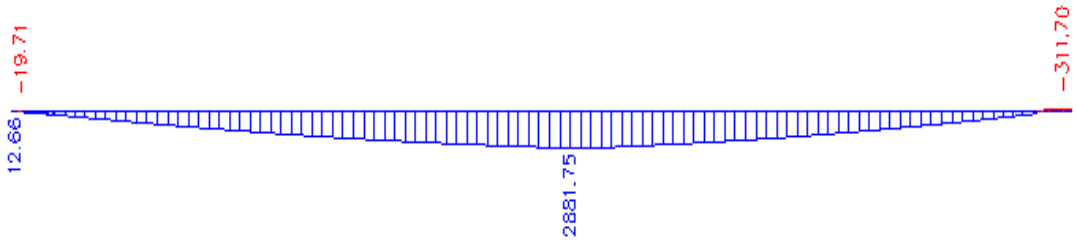

Fig3. 30, Bending moment at the first inverted T-girder in the longitudinal direction (live load and permanent load)

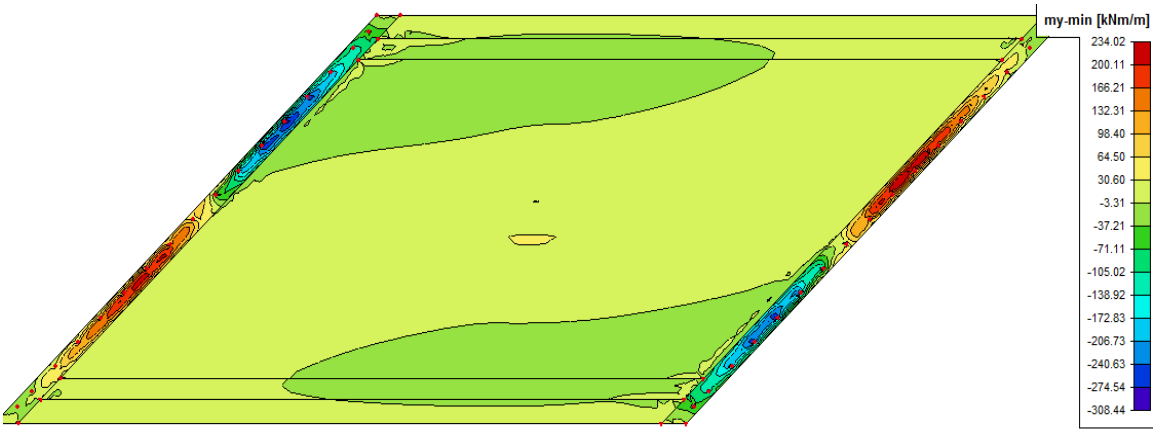

Fig3. 31, Bending moment in the transverse direction (excluding self weight of the bridge)

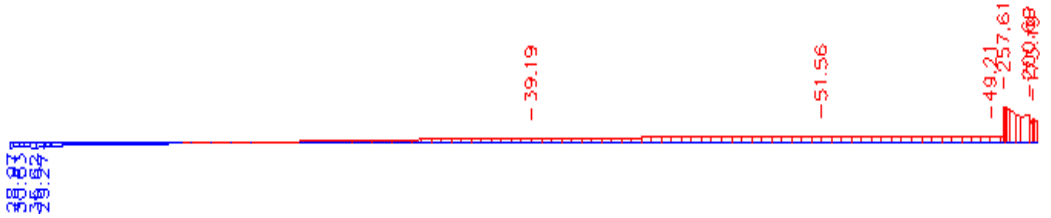

Fig3. 32, Torque at the first inverted T-girders (critical combination)

3.3.3 Model with end diaphragm in the Ultimate limit state

In the ultimate limit state, cast in-situ concrete deck and transverse beams would be cracked severely. To take this cracking into account, the flexural stiffness parameters have been calculated with half of the young's modulus for deck and end diaphragm beams. In addition to this, only 40% of torsion stiffness has been used for all structural elements.

Considering the stiffness of the end diaphragm beam in ULS							
(P-1)ZIP1300/1200		(P-2) ZIP1300/1023		(P-3) TRA1300/1177		(P-4) End plates	
D_{11}	5921.8	D_{11}	6562.9	D_{11}	4584.4	D_{11}	3704.2
D_{22}	16.1	D_{22}	16.1	D_{22}	20.6	D_{22}	3704.2
D_v	2.4	D_v	2.4	D_v	3.1	D_v	555.6
D_{33}	25.8	D_{33}	30.0	D_{33}	30.7	D_{33}	865.3
D_{44}	5383.3	D_{44}	6090.7	D_{44}	5945.0	D_{44}	7918.5
D_{55}	1291.7	D_{55}	1291.7	D_{55}	1404.0	D_{55}	7918.5

Table3. 8, Stiffness parameters in the ULS, considering the stiffness of the end diaphragm beams

3.3.3.1 Result of finite element model

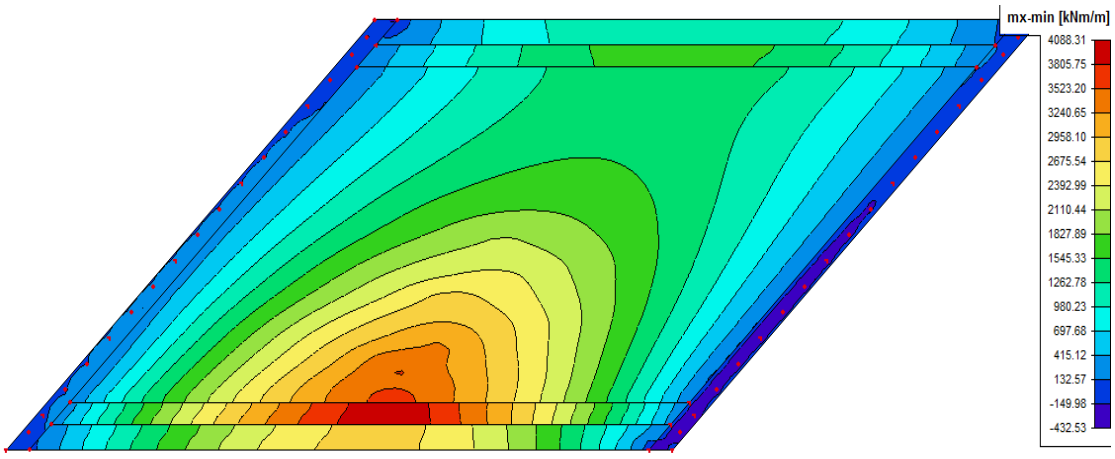

Fig3. 33, Bending moment in the longitudinal direction

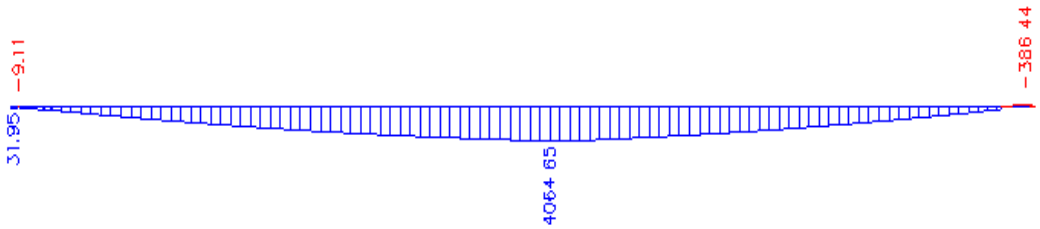

Fig3. 34, Bending moment at the critical girder in the longitudinal direction

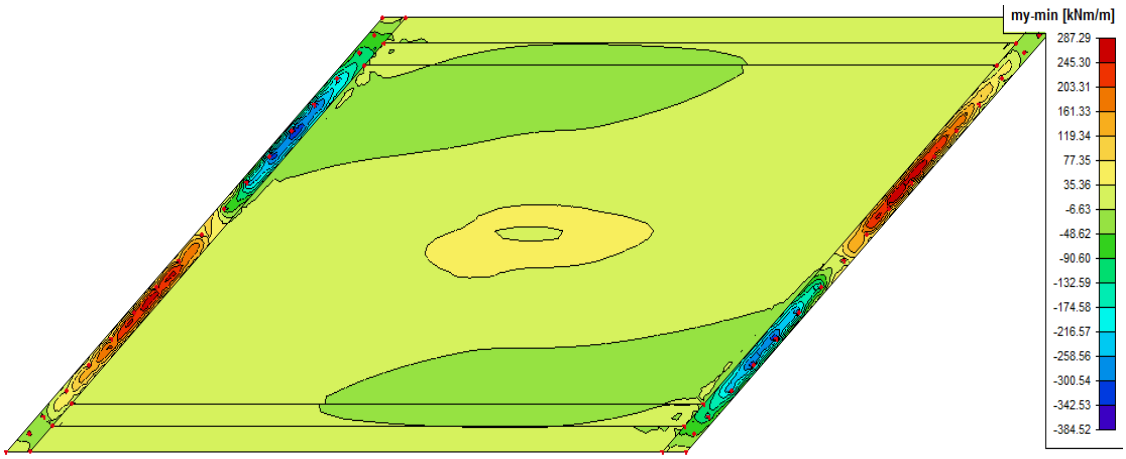

Fig3. 35, Bending moment in the transverse direction

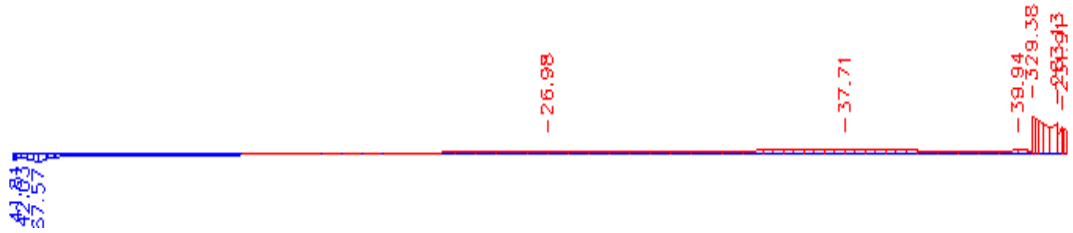

Fig3. 36, Torsion moment at the critical girder

3.3.4 Model with end diaphragms and without torsion stiffness for the girders in ULS

In 3.2.7 part of this thesis work, it has been apparent that the load distribution is insensitive with torsion stiffness of the girders. The increase in longitudinal bending moment due to zero torsion stiffness in the girders was insignificant. In this part of the study, the effect of considering the stiffness of end diaphragms in the load distribution of torsionless design has been investigated. Half of the young's modulus for the deck and end diaphragms has been assumed to take cracking into consideration in the flexural stiffness calculation. Moreover, 40% of the torsion inertia was assumed for the deck and transverse beams. Cracks in Prestressed girders have been assumed to be limited and full stiffness was considered for bending. On the contrary, the torsion inertia of these girders was totally overlooked. Using the above assumptions, the stiffness parameters have been calculated and tabulated in the following table. [ANNEX A]

Considering the stiffness of the end diaphragm beam and without torsion stiffness for the Girders in ULS							
(P-1)ZIP1300/1200		(P-2) ZIP1300/1023		(P-3) TRA1300/1177		(P-4) End plates	
D_{11}	5921.8	D_{11}	6562.9	D_{11}	4584.4	D_{11}	3704.2
D_{22}	16.1	D_{22}	16.1	D_{22}	20.6	D_{22}	3704.2
D_v	2.4	D_v	2.4	D_v	3.1	D_v	555.6
D_{33}	5.5	D_{33}	5.5	D_{33}	7.0	D_{33}	865.3
D_{44}	5383.3	D_{44}	6090.7	D_{44}	5945.0	D_{44}	7918.5
D_{55}	1291.7	D_{55}	1291.7	D_{55}	1404.0	D_{55}	7918.5

Table3. 9, Stiffness parameter with Zero torsion stiffness for the girders

3.3.4.1 Finite element result

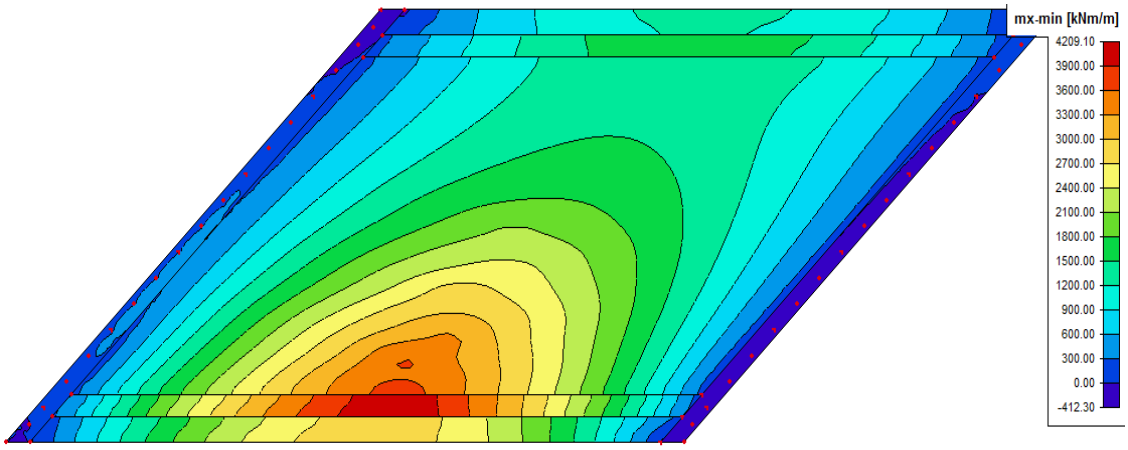

Fig3. 37, Bending moment in the longitudinal direction

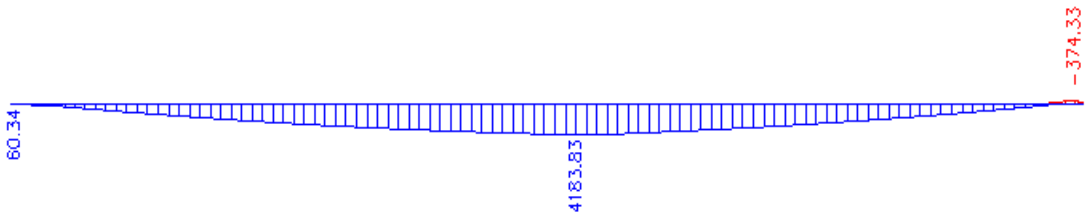

Fig3. 38, Bending moment at the critical girder

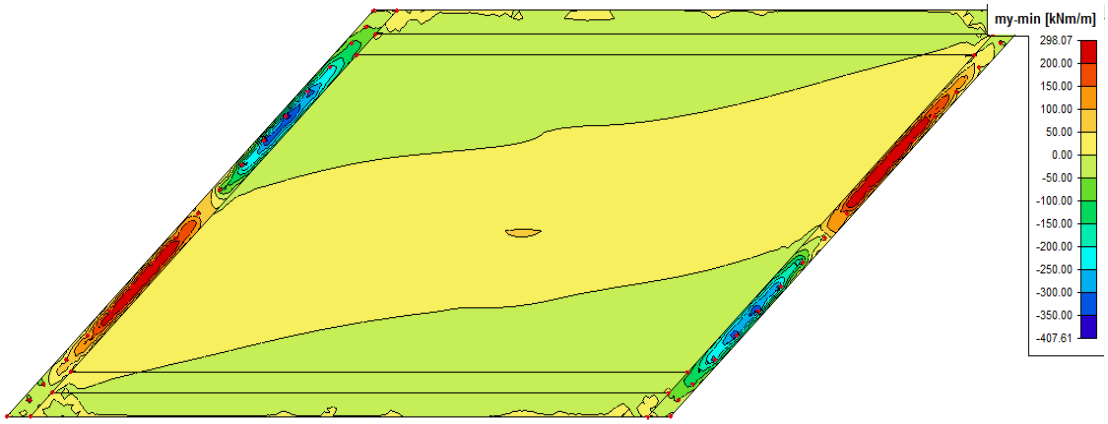

Fig3. 39, Bending in the transverse direction

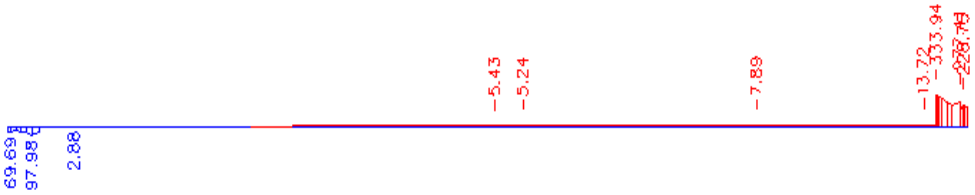

Fig3. 40, Torsion moment at the critical girder in the ULS with zero torsion stiffness for girders

The small torsion moments observed in the heavily loaded girder is due to the torsion stiffness of the deck slab. Reinforced concrete slabs resist torque using longitudinal and transverse bending reinforcements. Two layers of reinforcement are always provided at the top and bottom face of the deck slab for bending. Hence, it is not helpful to make Torsionless design for the deck slab.

3.3.5 Comparison of the two ULS models (considering stiffness of end diaphragm beams)

The torque at the location of the first inverted-T girder has been found to be 41kNm with 40% torsion stiffness model. This torque diminishes to 13.0kNm in the torsionless system. A considerable amount of torsion moments have been observed in both systems at the end diaphragms near the obtuse corner of the bridge. The twisting moments in the end diaphragm beams are fairly similar in the two systems; 323kNm/m in the first system and 292kNm/m in the second system. In the exceedingly loaded girder longitudinal bending moments of 4158KNm at span and -395kNm at support were found in the first model. Yet, the span moment increases to 4280kNm and the support moment decreases in magnitude to -384kNm in the second model.

This model revealed that the increase in longitudinal bending moments in the highly loaded girder as the result of neglecting the torsion inertia of the girders was smaller than 3%.

3.4 Comparison of with and without end diaphragm beams in Orthotropic plate model

The following table summarizes the internal forces for all orthotropic plate models that have been carried out in this chapter of this study.

without considering the stiffness of the end diaphragm beams in the finite element model					
	SLS, full torsion stiffness for girders and 50% for deck	40% of torsion stiffness for deck and girder(ULS)	no torsion stiffness for the girders and 40% for deck(ULS)	Effect of zero torsion stiffness for girders (ULS)	
Torsion moment (kNm)	-78	-62	-15	-47	decrease
Longitudinal Span moment(kNm)	3050	4301	4460	159	increase
Longitudinal support moment(kNm)	-132	-176	-102	-74	decrease
Transverse moment (KNm)	43	53	59	6	increase

Considering the stiffness of end diaphragm beams in the finite element model					
Torsion moment (kNm)	-52	-41	-14	-27	decrease
Longitudinal Span moment(kNm)	2948	4158	4280	122	increase
Longitudinal support moment(kNm)	-319	-395	-383	12	decrease
Transverse moment (KNm/m)	38	50	55	5	increase
Torsion in the end diaphragm beam	233	300	302	2	increase

Table3. 10, Summary of all the orthotropic plate models

In the above table, the longitudinal bending moments and torsion moments are the maximum values in the first inverted T-girder with their respective critical load combinations.

In the orthotropic plate model, when we consider the stiffness of the end diaphragm beams, a small decrease in torsion and span longitudinal bending moments at the critical girders have been observed. The decrease in torsion moments and longitudinal moments were accompanied by a substantial torque at the end diaphragm beams and negative moments at the support of the bridge near the obtuse corner.

In conclusion, placement of torsion reinforcement in the end diaphragm beams is intricate and securing homogeneity at the interface between the precast girders and the cast in situ diaphragm is also unrealistic. Hence, these decreases in torsion moments and longitudinal moments in the girders seem unjustifiable.

CHAPTER 4, CENTRIC BEAM ELEMENTS FOR THE GIRDERS AND PLATE BENDING ELEMENTS FOR THE DECK

4.1 Finite element model description

In chapter 3 of this study, the application of orthotropic plate modeling techniques for the skew bridge under consideration has been investigated in depth. In this chapter, another simplified modeling method is tested. The deck slab has been modelled by using quadrilateral plate bending elements. The precast presteressed girders and end diaphragms have been idealized using beam elements. The centroid of each of the girders and diaphragms coincided with the centroid of the concrete slab as shown in Fig 4.1. Three degree of freedom, one translation (U_z) and two rotations (Φ_x and Φ_y) at each node were provided.

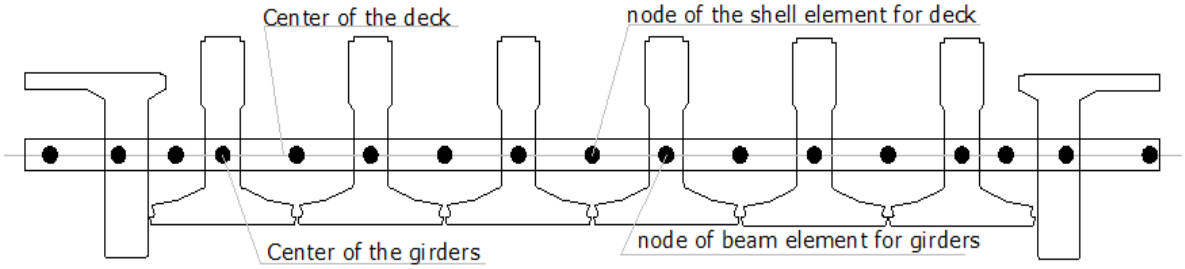

Fig 4. 1, Model of centric beam element for the girders and plate elements for the deck

SCIA Engineer commercial finite element software package is adopted for this model. This model is the most economical and simplified modeling technique in SCIA Engineer. All the important section properties of each structural element are automatically calculated by the software. This makes the model less time consuming. However, it fails to consider the eccentric distance between the center of the deck and center of the girders. As the result, it underestimates the flexural strength of the composite system in the major axis. Moreover, the levels of the centroid of internal and edge member sections are at different levels for this type of bridges. In spite of this fact, this model disregards the transverse variation of these neutral axes and the program automatically created one common neutral axis for the whole bridge as shown in the following figure.

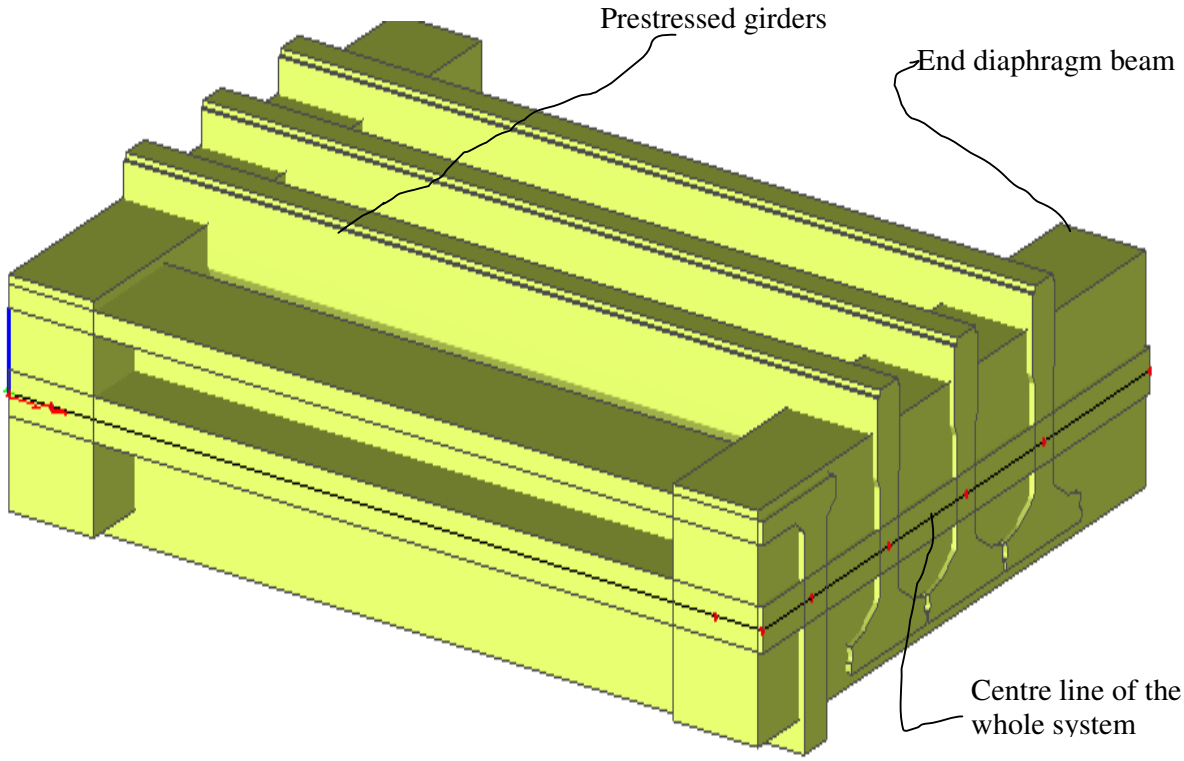

Fig 4. 2, 3D view SCIA engineer model

Support constraints used in this finite element model have been chosen to closely resemble to those of the real bridge deck bearings. Flexible elastomeric bearings are provided under each girder in the construction of the viaduct. To simulate these bearings elastic springs with vertical spring stiffness calculated in orthotropic plate model part of this work were provided at the location of each bearing.

4.1.1 Load cases and combinations

In chapter 2, different load cases and combinations for critical longitudinal bending, transverse moments and torsion have been considered. In addition, another different load arrangements and combinations were investigated for torsion in chapter three. All those load cases and combinations were accounted in this model as well.

4.1.2 Effective width

In the calculations of the internal forces and moments of the composite system, part of the deck which is considered effective in carrying the load as part of the girder should be defined in the model. The internal girders spacing in the subject bridge is 1.2m which is relatively small. As the result, it is reasonable to assume that all the center to center distance between

girders is effective. Fig 4.3 shows the effective width provided for each individual presteressed girder.

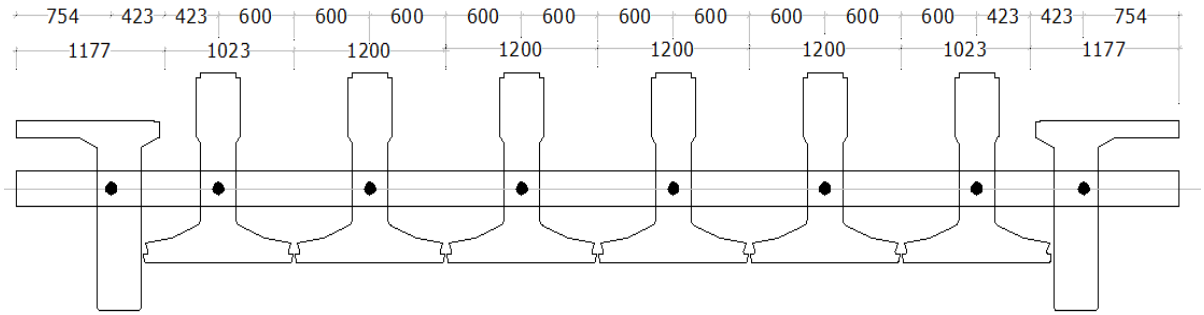

Fig 4. 3, Effective with assigned for each girder

Internal forces and bending moments in this width of the slab are then added to the internal forces calculated in the girders itself. The internal forces and moments in the slab are transformed into the local coordinate system of the girders before integration.

4.2 Model in the serviceability limit state

Like orthotropic plate model done in the previous chapter, full stiffness for all structural elements has been assumed at the beginning of the analysis. The tensile stresses in the deck and support transverse beams were compared with the tensile capacity of the in-situ concrete and the comparison reveals that the tensile stress is much higher than the tensile strength. Hence, the reinforced concrete deck slab is fully effective in compression for longitudinal sagging moments but behaves as a cracked section for transverse bending. Despite this, the result of this model would be compared to the result of ATENA 3D model in chapter 8 of this work. To do the comparison, the material property of this model should be exactly same as the ATENA model. In ATENA 3D orthotropic plate deck definition is impossible. And hence, in this model, half of the young's modulus for the in-situ concrete has been assumed in both directions to make isotropic and take into account cracking. In the same reasoning cracked stiffness is assumed in the end diaphragm beams as well. The longitudinal girders are presteressed and are made up of high quality concrete and uncracked stiffness was assigned.

4.2.1 Finite element model result

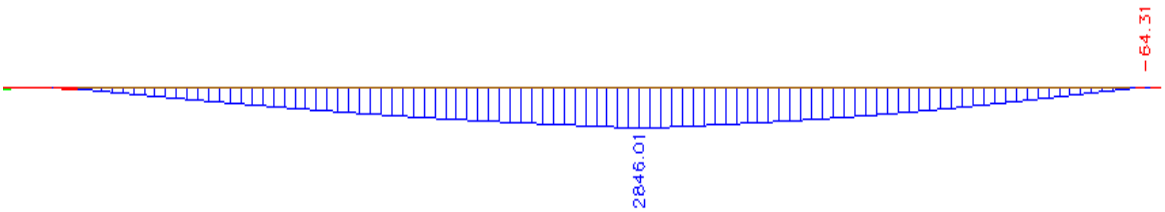

Fig4. 4, Bending moment at the first ZIP beam

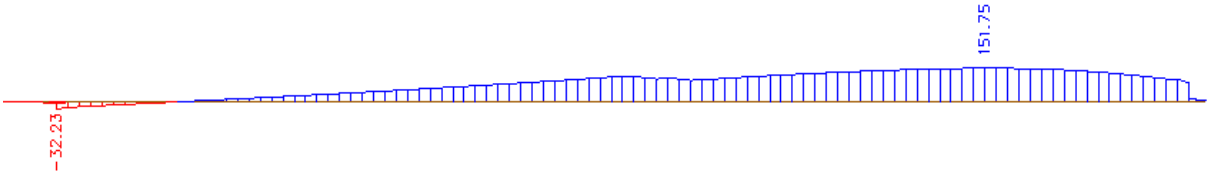

Fig4. 5, Twisting moment at the first ZIP girder

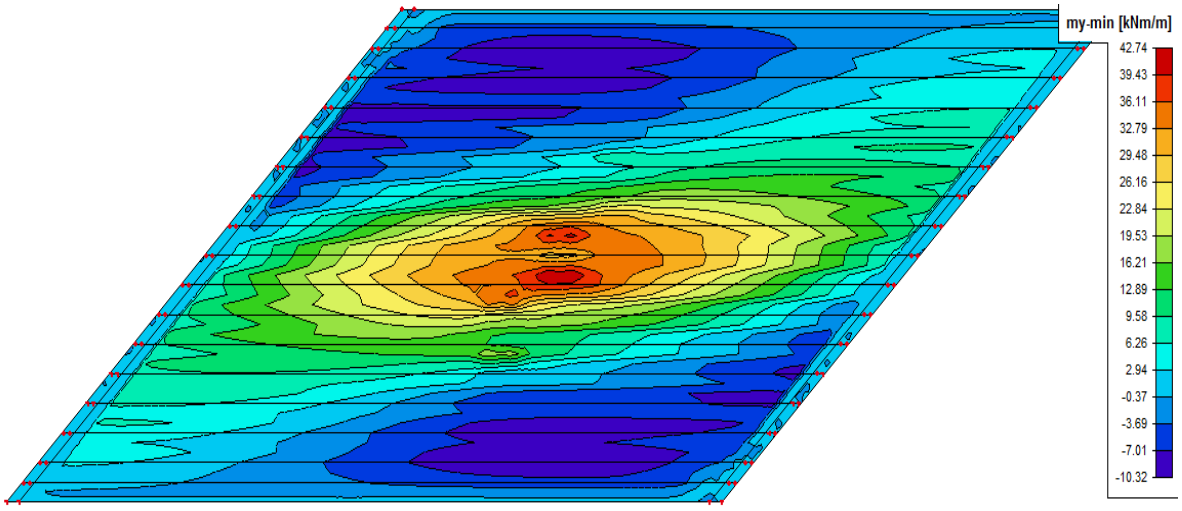

Fig4. 6, Bending moment in the transverse direction

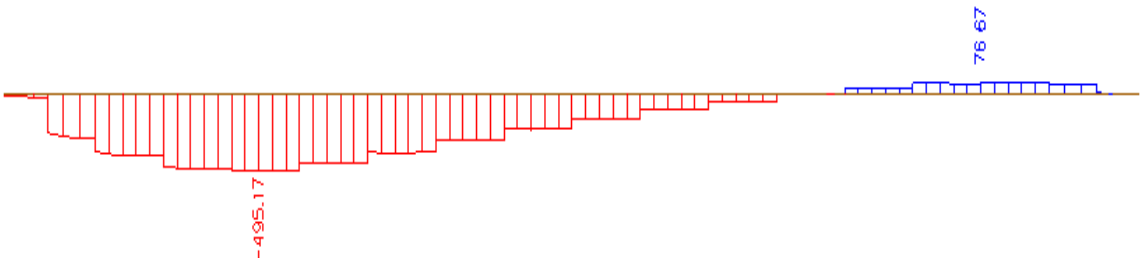

Fig4. 7, Torsion in the end diaphragm beams

4.3 Model in the Ultimate limit state

In the ultimate limit state, all structural elements including the presteressed girders would be thoroughly cracked both in shear and flexure. As per ROBK 6 (Netherlands bridge design recommendations) only 40% of the torsion stiffness has been assumed for all structural elements. In flexure full stiffness was assumed for presteressed girders and half stiffness for the deck and transverse beams.

4.3.1 Finite element model result

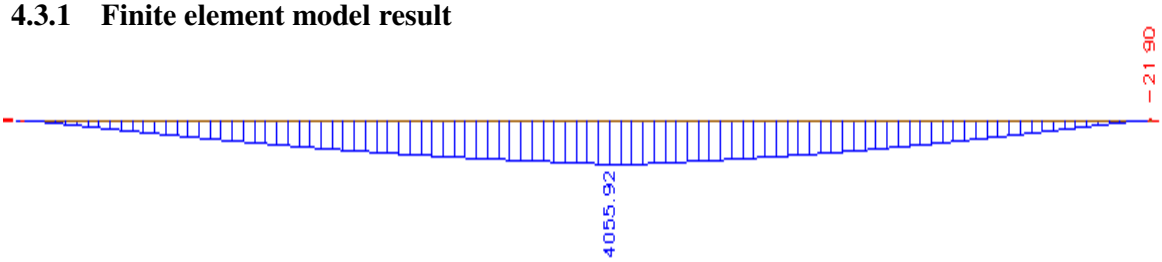

Fig4. 8, Bending moment diagram for first ZIP beam

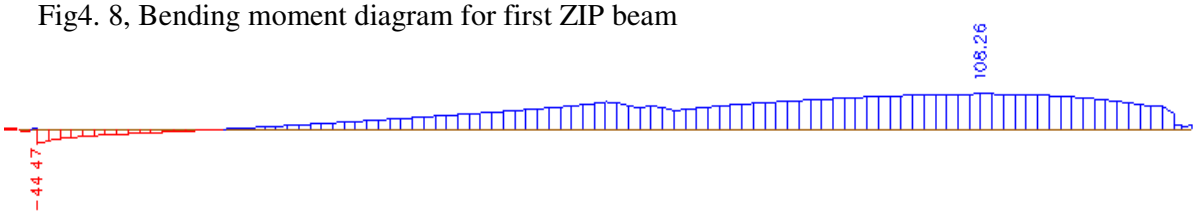

Fig4. 9, Torsion moment diagram for first ZIP beam

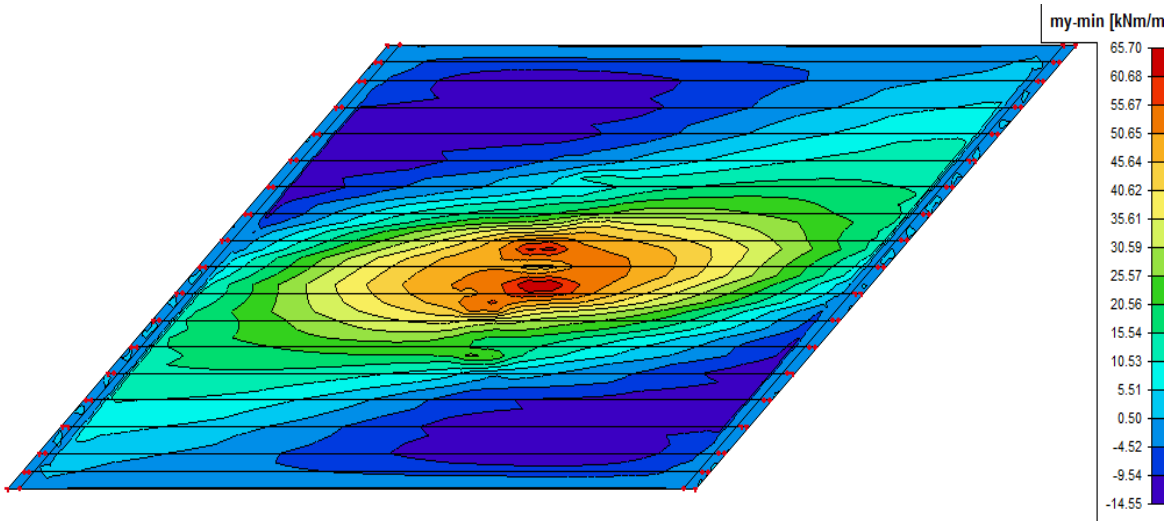

Fig4. 10, Bending moment on the deck in the transverse direction

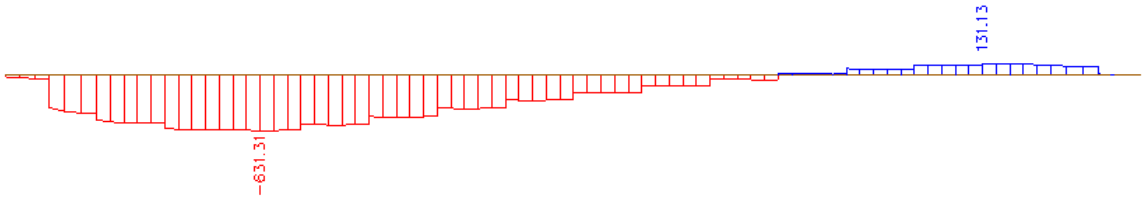

Fig4. 11, Torsion moment at the right diaphragm

4.4 Comparison of orthotropic plate model and Centric beam element model

Serviceability Limit State with end diaphragm beams		
	Orthotropic plate	Isotropic plate for deck and Centric beam element for girders and diaphragms
Torsion moment at first inverted T girder (kNm)	52	152
Longitudinal Span moment (kNm)	2948	2846
Longitudinal support moment (kNm)	-319	-64
Transverse moment (KNm)	38	43
Torsion moment at the end diaphragm beam (kNm)	252	495
Ultimate Limit State with end diaphragm beams		
	Orthotropic plate	Isotropic plate for deck and Centric beam element for girders and diaphragm
Torsion moment at first inverted T girder (kNm)	41	108
Longitudinal Span moment (kNm)	4158	4056
Longitudinal support moment(kNm)	-395	-21
Transverse moment (KNm)	50	66
Maximum torsion moment at the end diaphragm beam (kNm)	322	631

Table4. 1, Comparison of results (SLS and ULS)

From the above table, one could observe that, as compared to orthotropic plate model the longitudinal bending decreases and the torsion and transverse moments increases in the centric beam element model. This is due the fact that, the second model underrates the bending stiffness of the composite system keeping the other stiffness parameters unaffected. As mentioned earlier half of the young's modulus was considered in both directions for the deck in the finite element model to make isotropic. But in reality the deck is fully effective to resist sagging moment in compression in the longitudinal direction. Due to this fact in the real bridge the flexural stiffness of the composite system underestimated more than this model did. And the percentage decrease will increase more than this model revealed. The torsion moment in the girders and end diaphragm beams and the transverse moment in the deck on the contrary increased at large than the corresponding orthotropic plate model.

In the comparison, the torsion moments obtained from orthotropic plate model should be multiplied by two to get the design values.

CHAPTER 5, ECCENTRIC BEAM ELEMENTS FOR THE GIRDERS AND SHELL ELEMENTS FOR THE DECK

5.1 Introduction

In chapter 4, centric beam element for the girders and plate bending element for deck model was applied. That type of analysis is referred to as planar (two dimensional) as all of the structural elements are located in one plane. It is only suitable for bridge decks where the neutral axis remains substantially straight across the deck and is coincident with the centroidal axis of the whole bridge. When this is not the case, like the bridge in this case study, some form of three dimensional techniques such as eccentric beam element model is required to achieve an accurate representation of the behavior of the structure. Eccentric beam element model involves the modeling of each part of the bridge deck as a separate element located at the centroid of the portion of bridge deck which it represents. The eccentricity between these different elements is then connected with rigid vertical member. Fig 5.1 shows a space frame element for girders and shell element for the deck model of the subject bridge. In this, the cast in place concrete deck is modelled using quadrilateral shell elements which are located at the center of the deck while the girders are modelled as a beam elements located at their respective centroid. This model is relatively simple to use and has a very good similitude with the actual bridge. Three translational and three rotational, six degree of freedom in total has been provided at each finite element node.

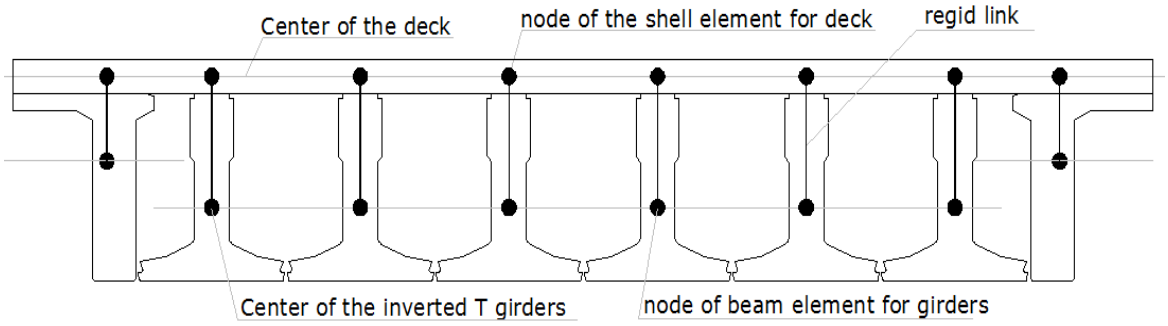

Fig5. 1, Model of eccentric beam element and shell element

The numerical simulation was performed using the general-purpose finite element software package, SCIA Engineer. SCIA has the capability to input an offset distance for nodes of beam elements from the center of the deck. Hence, it was not important to connect the eccentricity between shell elements of the deck and beam elements for the girders using rigid

link. The property of each part of the bridge is determined relative to its own centroid. As the model is three dimensional it will automatically determine the location of the neutral axis.

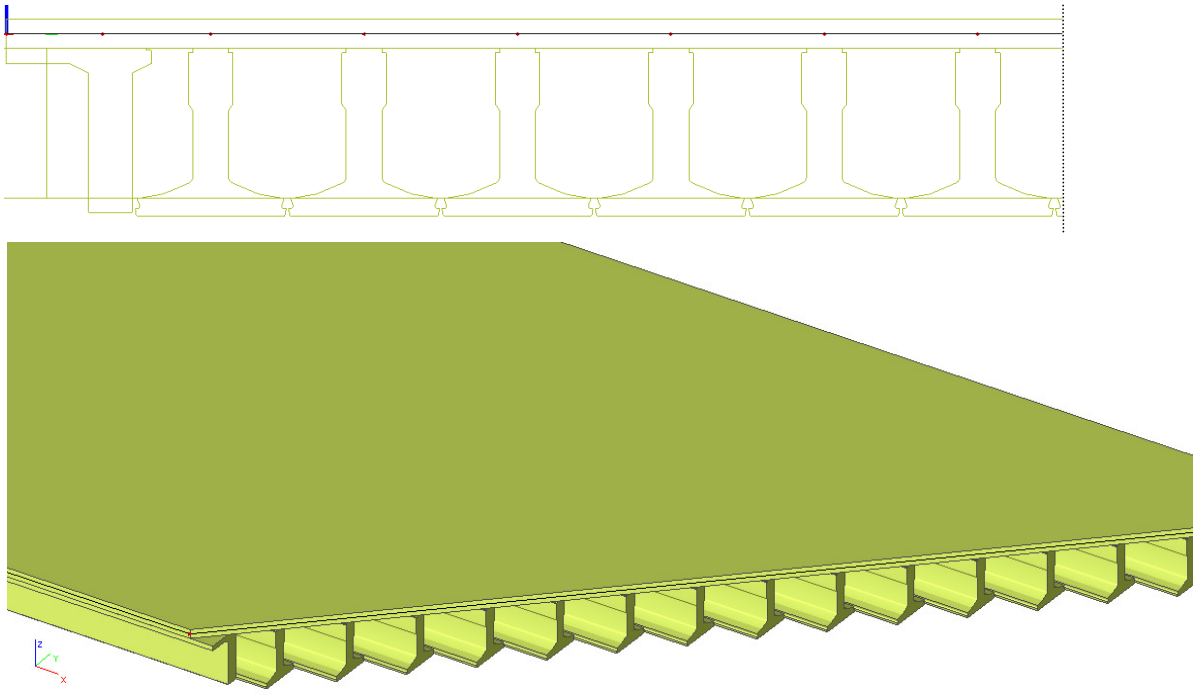

Fig 5. 2, Three-dimensional view SCIA Engineer model without support transverse beam

5.1.1 Effective width

In the calculations of the internal forces and moment for the composite system, part of the deck which is considered effective in carrying the load as part of the girder should be defined in the model. If the longitudinal beams are spaced at more than 1/5 of span, shear lag reduces the effective width of flange and interbeam shear transfer is small. The width of slab considered as flange to each side of the beam should be limited to 1/10 of the span [1]. The girder spacing in this case study is 1.2m which is relatively small. As the result, all the center-to-center distance between girders has been considered effective. Fig 5.2 shows the effective flange width provided for each single girder.

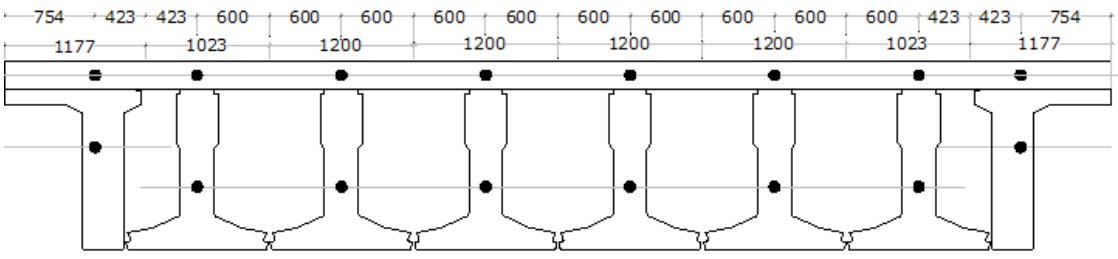

Fig5. 3, Effective width for each girder

The internal forces in the slab are transformed into the local coordinate system of the girders before addition. In the following way SCIA Engineer calculates the total internal forces and moments in the composite system.

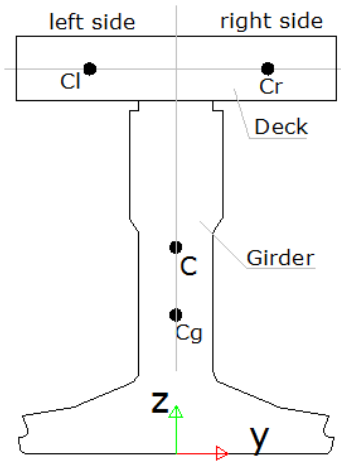

Fig5. 4, Internal force calculation for the composite system

C	The center of gravity of the composite system
C_l	the centre of gravity of the left hand side part of the deck
C_r	the centre of gravity of the right hand side part of the deck
C_g	the centre of gravity of the girder part only

The coordinates of centers of gravities of each part are used to determine lever arms in Y and Z directions from the y-z coordinate system shown in the above figure

Lever Arm $Z_l = C_{lz} - C_z$	Lever Arm $Y_l = C_{ly} - C_y$
Lever Arm $Z_r = C_{rz} - C_z$	Lever Arm $Y_r = C_{ry} - C_y$
Lever Arm $Z_g = C_{gz} - C_z$	Lever Arm $Y_g = C_{gy} - C_y$

The final internal forces in the girder-deck composite system could be calculated from the formulas below:

$$N = N_{girder} + N_{slab,left} + N_{slab,right}$$
$$V_x = V_{x,girder} + V_{x,slab,left} + V_{x,slab,right}$$
$$V_y = V_{y,girder} + V_{y,slab,left} + V_{y,slab,right}$$

$$M_x = M_{x,girder} + M_{x,slab,left} + M_{x,slab,right}$$

$$M_y = M_{y,girder} + M_{y,slab,left} + M_{y,slab,right} - N_{,slab,left} * Z_l - N_{,slab,right} * Z_r + N_{girder} * Z_g$$

$$M_z = M_{z,girder} + M_{z,slab,left} + M_{z,slab,right} + N_{,slab,left} * Y_l - N_{,slab,right} * Z_r + N_{girder} * Y_g$$

[SCIA Engineer manual]

5.1.2 Load cases and load combinations

All the load cases and combinations mentioned in chapter two and three of this study have been checked and the maximum internal forces and moments would be shown in the subsequent sections

5.1.3 Boundary conditions

Boundary conditions were carefully evaluated in order to avoid unwanted constraints to the nodes and, consequently, to the model. The number of constraints required to provide stability to the bridge model was kept to the minimum possible, keeping in sight that actual bridge behavior and performance had to be achieved. Unnecessary constraints would generate secondary stresses, thus altering the stresses distribution in the structural elements. Girder supports were simulated by applying proper boundary conditions to nodes at both ends. Nodes at the exact location of the bearings were created and appropriate displacement and rotation constraints were provided. All girders, except the one at the middle of the bridge, are free to translate in the global X and Y directions and elastic spring stiffness of K_z is provided in the global Z to simulate the elastomeric bearing provided under each girder. Displacements in global X and Y directions were restricted at one support of the middle girder. At the opposite end of this same girder, displacements along Y were constrained and free to translate in the X direction. This was done to avoid unwanted rotation around the z-axis of the entire bridge. All supports at each girder ends are free to rotate in all directions. That means, rotational constraints were not provided at all.

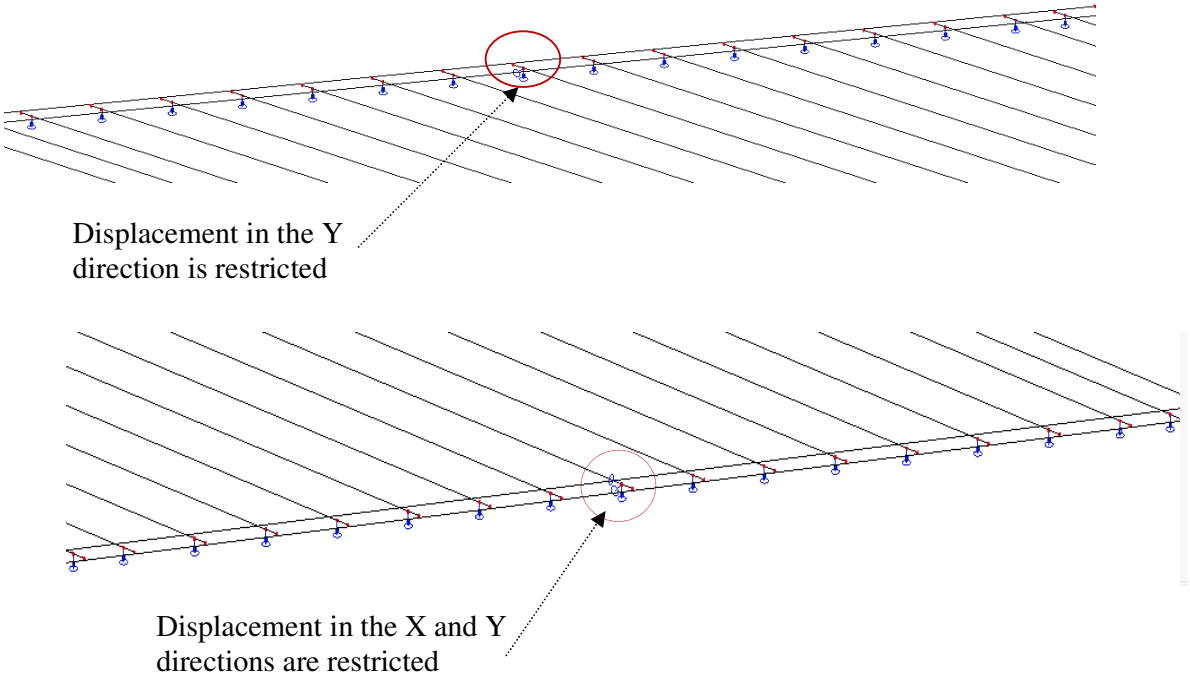

Fig 5. 5, Boundary conditions provided in the model

5.2 Eccentric beam element for girders and shell element for deck model in the SLS

As done in the past two finite element models, cracked stiffness has been considered for the deck and end diaphragm beams in SLS. Isotropic plate with half the young's modulus of the in-situ concrete was used for the deck. Prestressed girders were taken as an uncracked and full stiffness was effective.

5.2.1 Finite element model result

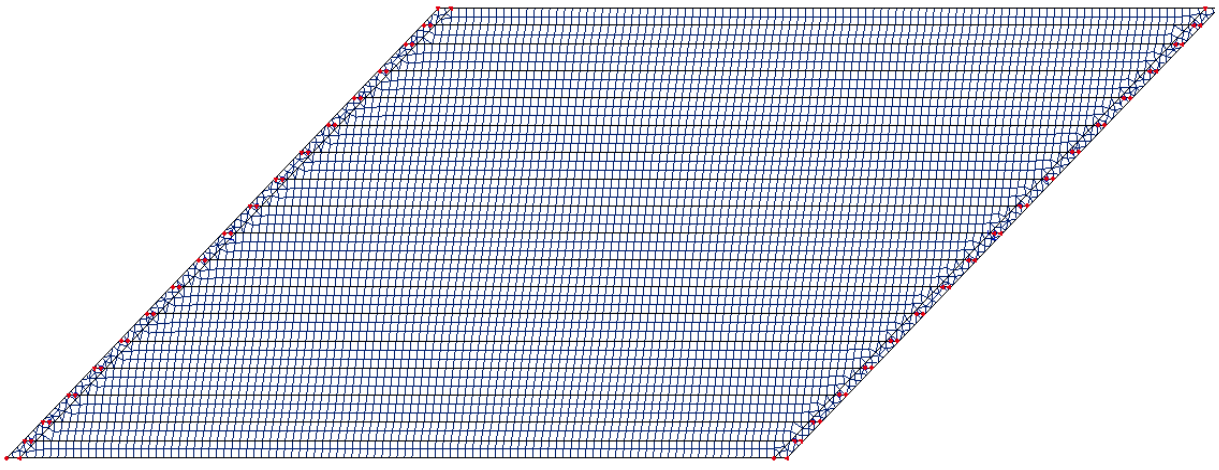

Fig5. 6, Finite element mesh generated by SCIA Engineer

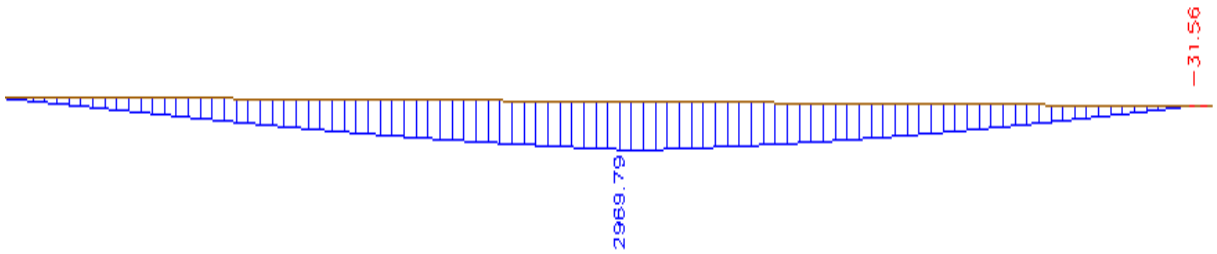

Fig5. 7, Bending moment in the first inverted T-girder in the longitudinal direction (composite system)

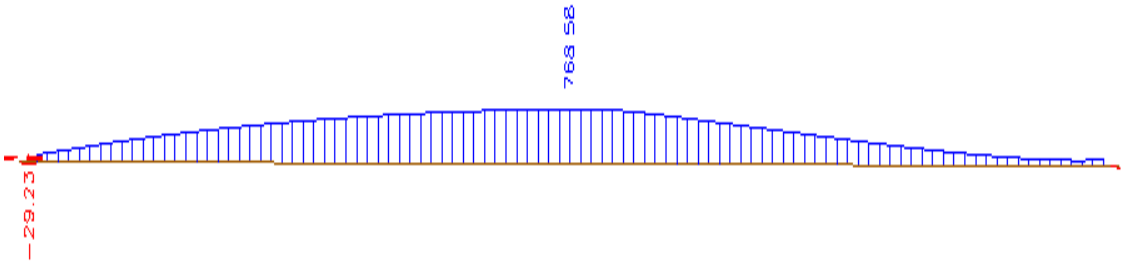

Fig5. 8, Normal force in the first Inverted T girder (composite system)

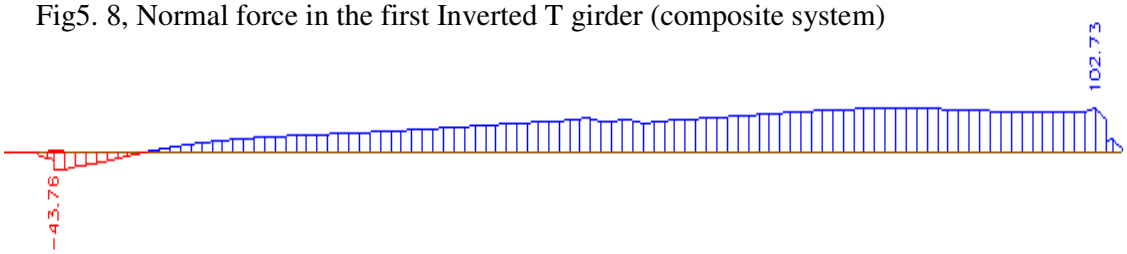

Fig5. 9, Torsion moment in the first inverted T Girder, critical combinations (composite system)

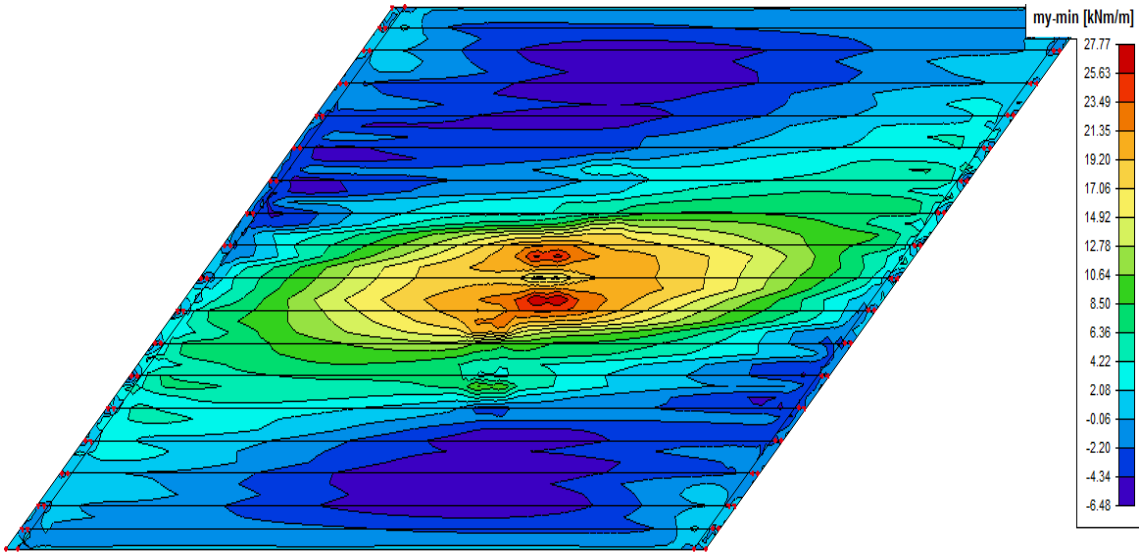

Fig5. 10, Bending moment in the deck slab in the transverse direction

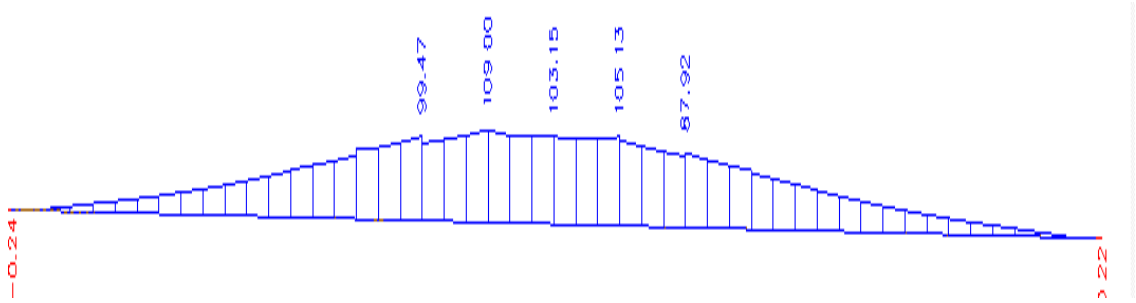

Fig5. 11, Normal force n_y in the transverse direction (kN/m) (section at the middle of the deck)

5.3 Model in the ultimate limit state

Cracked stiffness for all structural elements was assumed for torsion. The torsion constants were reduced by 60% for the girders and end diaphragms in the ULS as per [ROBK6] recommendations. For the deck part, the shear modulus was reduced to decrease the torsion stiffness. For flexure half of the young's modulus for end transverse beams and deck was used. The cracks in the prestressed girders were assumed to be limited and full flexural stiffness was assumed.

5.3.1 Finite element model result

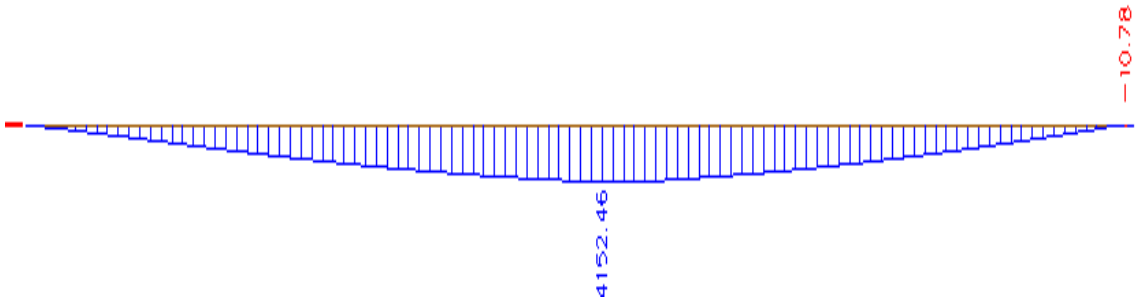

Fig5. 12, Bending moment diagram for first ZIP beam (composite system)

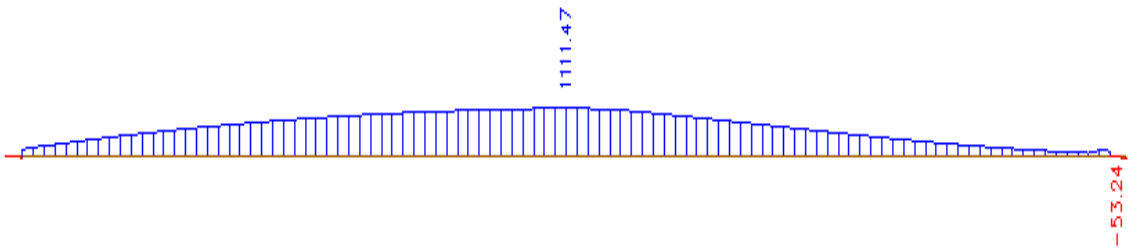

Fig5. 13, Normal force in the first ZIP Girder (Tension) (composite system)

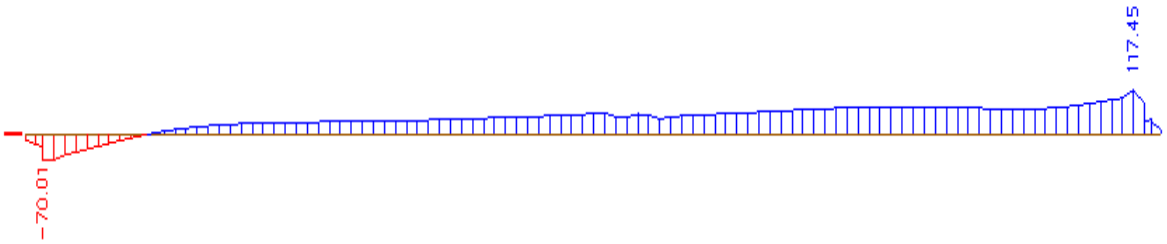

Fig5. 14, Torsion moment diagram for first ZIP beam (composite system)

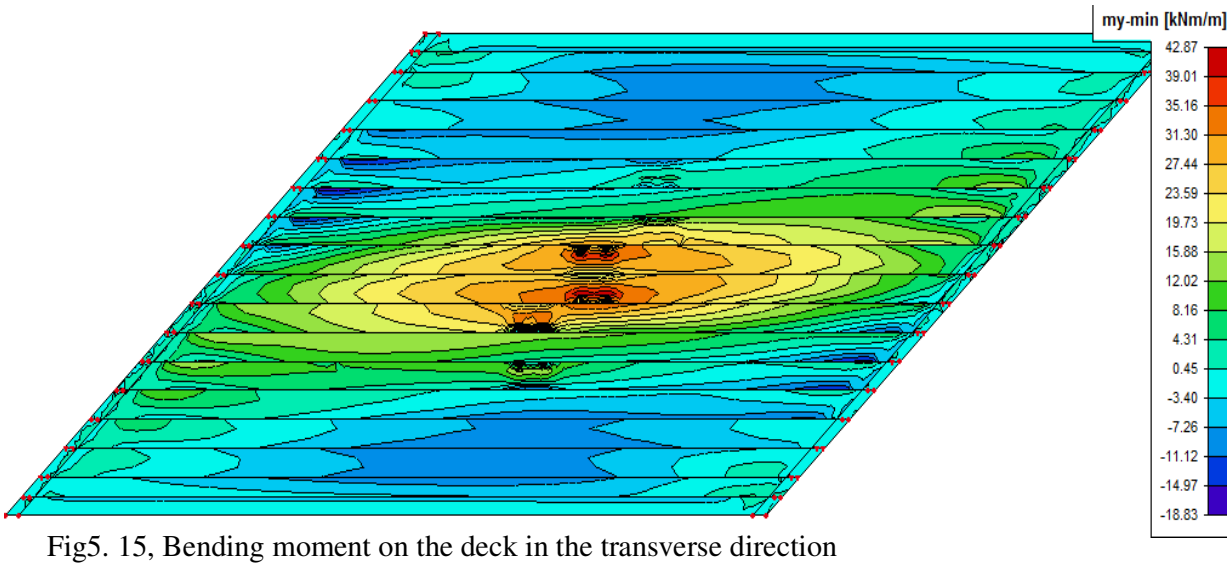

Fig5. 15, Bending moment on the deck in the transverse direction

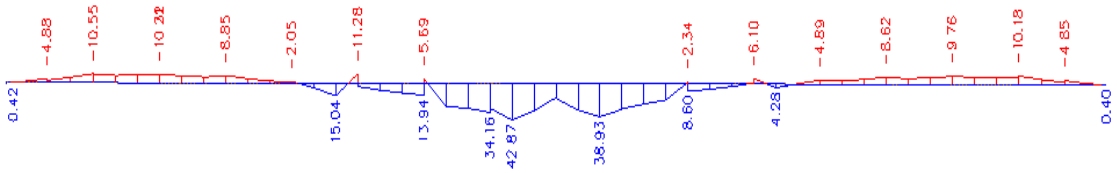

Fig5. 16, Bending moment in the transverse direction at the middle of the deck

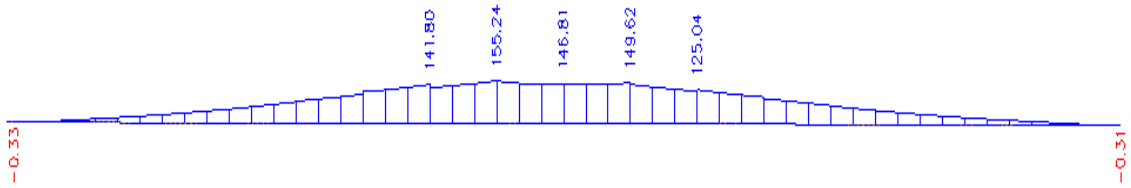

Fig5. 17, Normal force on the deck in the transverse direction at the middle of the deck

5.4 Effect of slab membrane action on beam-and-slab deck behavior

The preceding two planar models can simulate vertical deflections and twisting of the composite system and accompanying transfer of load by vertical shear and transverse bending of the slab. Inspection of the ends of the separate girders in plan or elevation in the eccentric beam element model revealed that if all the beams flex about a neutral axis passing through their centroid, the ends of the slab flanges are displaced relative to each other. In reality this step displacement cannot happen, and the relative moment of the tops of the beam is resisted and reduced by longitudinal shear forces in the connecting slab as shown in the figure below. [1]

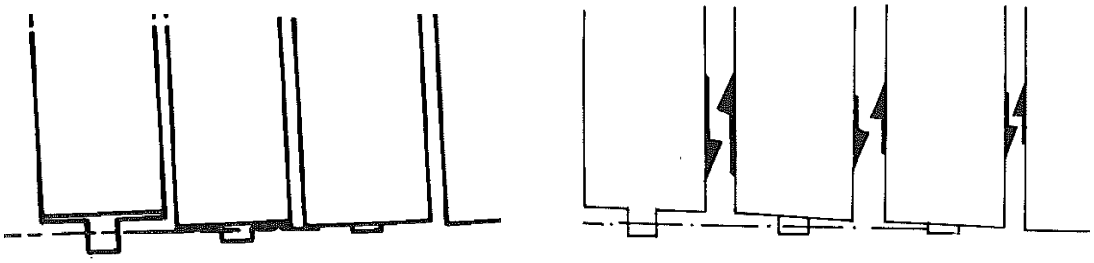

a) relative displacement b) interface shear force

Fig5. 18, relative displacement and interface shear forces in eccentric beam element model

These shear forces are in equilibrium with axial tension in the loaded area and compression forces elsewhere in the girders. Due to this fact, a tension normal force was observed in the highly loaded girders and compression force in the spandrel beam and in the unloaded internal girders. These transfers of shear forces between beams with balancing axial forces cannot be simulated in conventional planar analysis.

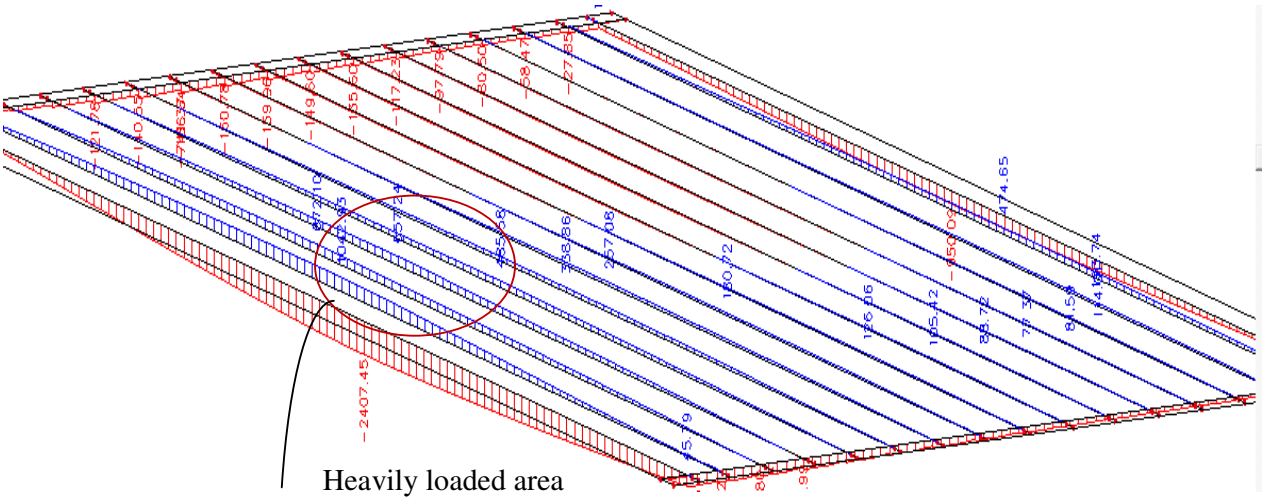

Fig5. 19: Normal force in all girders (load combination-1)

5.5 Comparison of orthotropic plate, Centric beam element and eccentric beam element models

Internal forces and moments in the SLS- end diaphragm beams are considered in all cases			
	Orthotropic plate model	Isotropic plate for deck and Centric beam element for beams	Isotropic plate for deck and Eccentric beam element for beams
Torque near obtuse corner (kNm)	52	152	108
Longitudinal Span moment (kNm)	2997	2846	2970
Longitudinal support moment (kNm)	-322	-64	-32
Normal force(kN)	-	-	769
Deck transverse moment (KNm)	38	43	30
Transverse normal force in the deck n_y (KN/m)	-	-	109
Torsion moment at the end diaphragm beam (kNm) – critical combination	252	495	414
Internal forces and moments in the ULS- end diaphragm beams were included in all cases			
Torque near obtuse corner (kNm)	41	109	113
Longitudinal Span moment(kNm)	4158	4056	4127
Longitudinal support moment(kNm)	-395	-21	-8
Normal force (KN)	-	-	1114
Deck transverse moment (KNm)	50	66	43
Transverse normal force in the deck n_y (KN/m)	-	-	155
Torsion moment at the end diaphragm beam (kNm)-critical combination	322	631	511

Table5. 1, Comparison of the previous three different modeling techniques

Note that: the torsion moment in the orthotropic plate shown in the above table is on one face of the plate and should be multiplied by two to get the design value.

The above table makes known that orthotropic plate and eccentric beam element models have fairly similar longitudinal span bending and torsion moments. However, orthotropic plate produced substantial negative moment at the support of the bridge near the obtuse corner and eccentric beam element model produce tension normal force at the mid span of the heavily loaded girders.

CHAPTER 6, SHELL ELEMENTS FOR BOTH THE DECK AND THE GIRDERS

6.1 Introduction

A better idealization of the real cast in-situ deck on precast presteressed girders is shell elements for the deck, girder and end diaphragm beams. It consists of a number of planes of plate finite elements connected together by rigid members. The deck is idealized by horizontal finite elements located at the centroid of the deck slab while the girders and end transverse beams are idealized using vertical finite elements located along the mid-surface of each member as shown in Fig 6.1. Overlapping deck and girder shell elements by sharing the same node results in modeling errors. Moving the top edge of the girders to the centre of the deck and share same node decreases the center-to-center vertical distance between the deck and the girders (see Fig 6.1 b). This reduces the flexural stiffness of the composite system about the primary bending axis. To avoid overlapping of the deck and girders, the nodes of the deck shell elements and nodes of girder elements should be connected by rigid link or the shell elements of the girders must be placed at an offset distance from the deck shell element node locations. These two actions could help to model the geometry of the bridge more accurately and predict the stiffness of the composite system correctly.

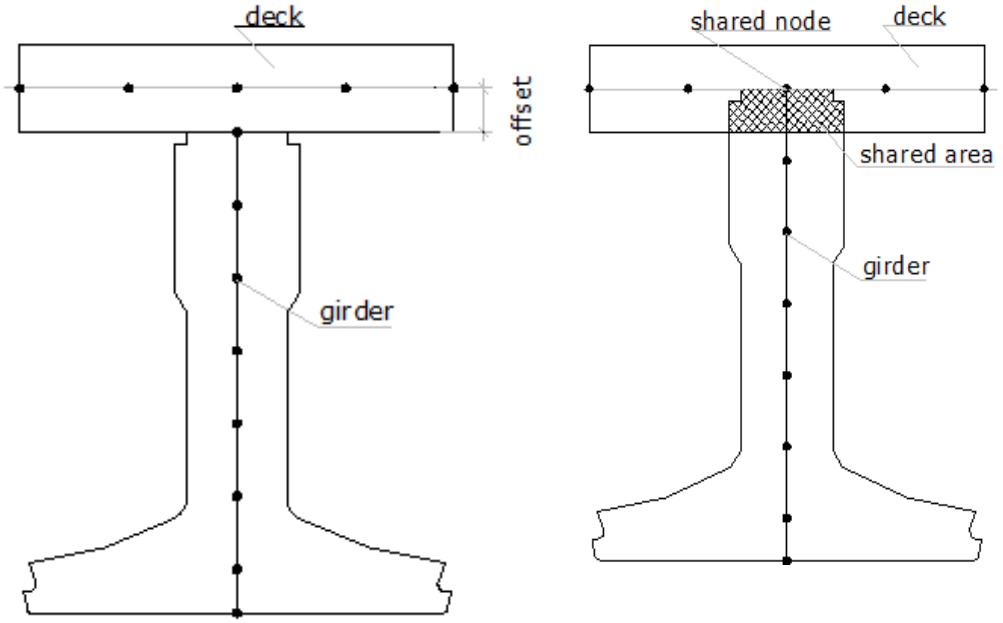

a) accurate model of deck and girder b) inaccurate model of deck and girder

Fig 6. 1, Modeling of the deck and girders with shell elements

For modeling the bridge used in this study, SCIA Engineer finite element program has been taken up. Neither of connecting nodes of the deck and girders with rigid link nor input with offset distance was found to be possible with SCIA Engineer. As a result, an approximate model that shell elements of the deck and shell elements of the girders were sharing the same node was adopted as shown in the following figure. As explained earlier, moving the node of the girders up to the node of the shell elements will make the model by far incorrect. Due to this fact, a better approximation by extending the girders to the centre of the deck was used. Same approximation is adopted to connect the end diaphragm beams with the girders and the deck. This approximation increases the bending and torsion inertias of the girders. An increase in height of the girders would move the centroid of the girders up from its true location. Consequently, the center of the composite system would move a little up and the distance between the centroid of the deck and the centroid of the girders decreases by the same amount. This decrease in center-to-center distance between the deck and the girders offsets part of the increase in flexural stiffness about the major axis caused by extending the girders to the center of the deck. For this reason, the increase in flexural stiffness in the major axis is comparatively minute. However, the torsion stiffness and the transverse flexural stiffness of the composite system increase with the same magnitude with the increase in inertia of the girders. The geometry of the end diaphragm beams are very complex and the approximate connection of the end diaphragms with the girders and the deck increases the torsion and transverse bending stiffness of the bridge at large. The high stiffness of the model near the support of the bridge attracts more transverse bending and torsion moments. Hence, the torsion moments predicted by this model is higher than the other models.

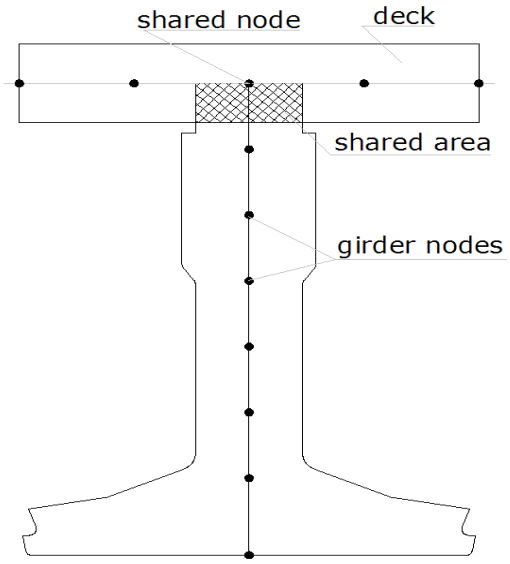

Fig 6. 2, Approximate shell element model

Quadrilateral shell elements with six degree of freedom (three translations and three rotations) at each node were created for all structural elements. To decrease the geometrical modeling errors, the inverted T-girders have been divided in to 7 parts as shown in the Fig 6.3 a. The thicknesses of each shell elements are the width of the respective elements.

Intermediate nodes at the exact location of the bearings under each girder were created and appropriate boundary conditions were provided. The number of constraints required to provide stability to the bridge model was kept to the minimum possible to achieve the actual bridge behavior and performance. The boundary conditions used in this model is exactly the same as the conditions used in the eccentric beam element model in chapter five.

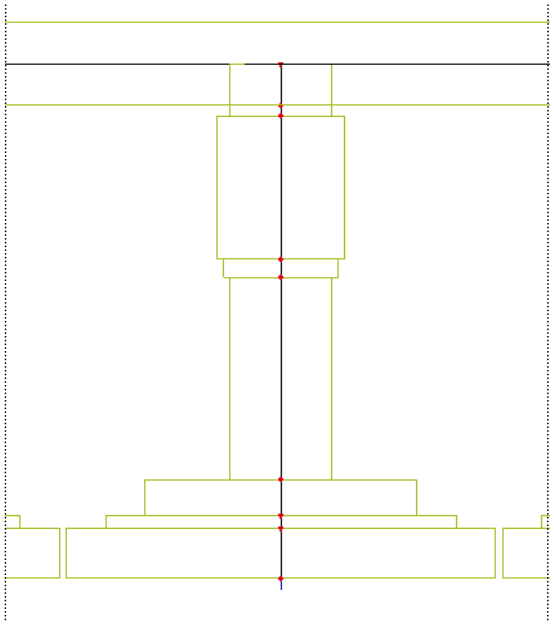

a) Cross-section of one girder

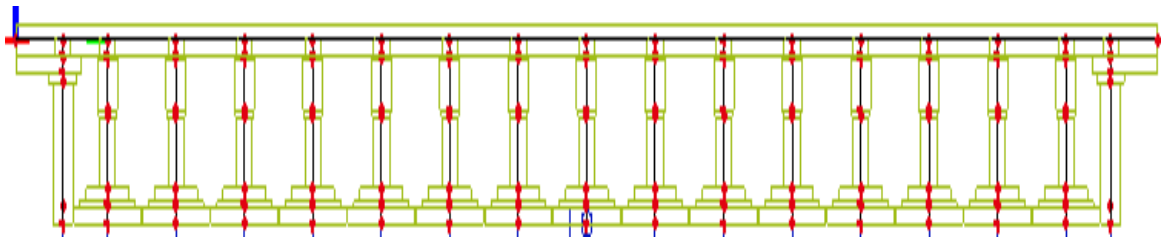

b) Cross-section of the entire bridge

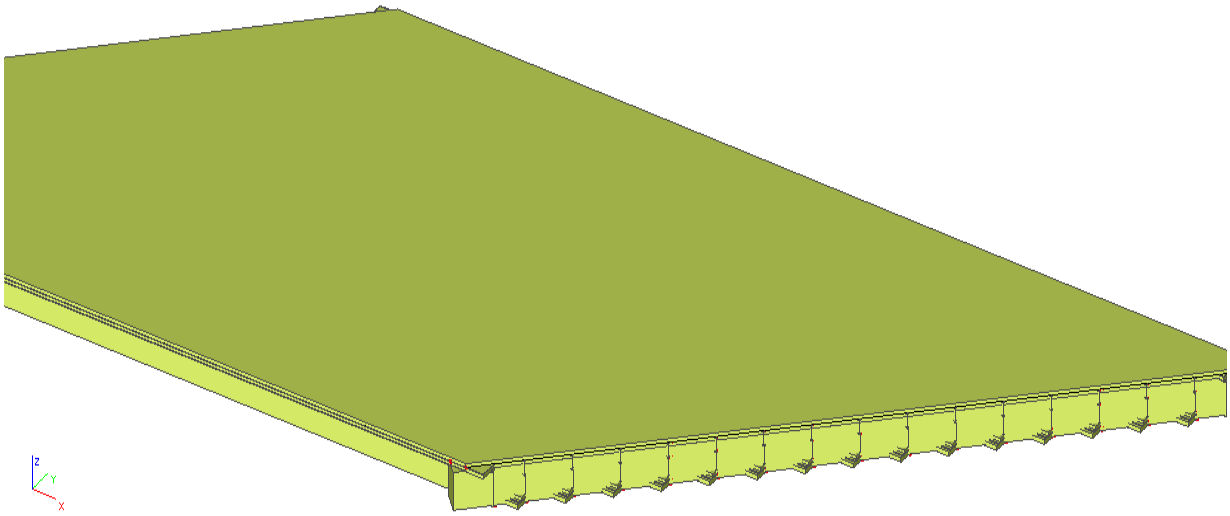

c) 3D view of the whole bridge

Fig6. 3, SCIA Engineer model of the bridge deck

6.2 Shell element model in SLS and ULS

Effect of cracking in the concrete has been considered in the SLS and ULS conditions. In the serviceability limit state, limited cracking in the girders has been assumed and full stiffness in torsion and flexure was assumed. On the contrary the in-place concrete of the deck and end transverse beams were cracked rigorously even in SLS and half of the young's modulus has been adopted. Same property in transverse and longitudinal directions was assigned in the deck.

In the ultimate limit state, cracking is assumed to substantially decrease especially the torsion stiffness of all structural elements and only 40% of full torsion stiffness was applied for all elements. This is possible by decreasing the shear modulus of the material keeping the young's modulus and the poison's ratio unaffected.

6.2.1 Finite element model result-SLS

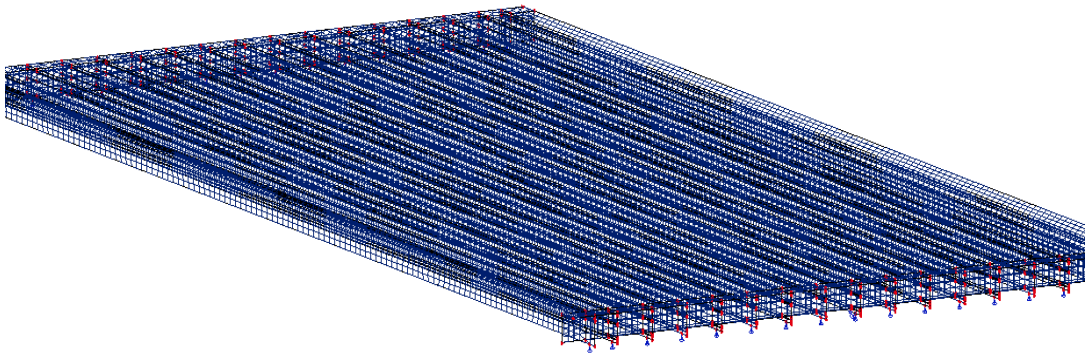

Fig 6. 4, Finite element mesh

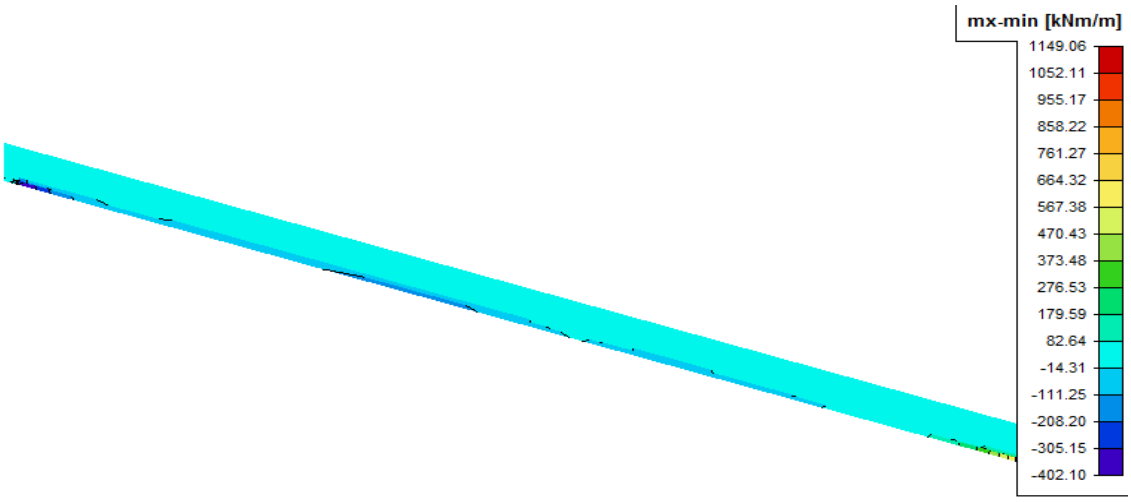

Fig 6. 5, Longitudinal moment (mx) in the first inverted T-girder (excluding self weight)

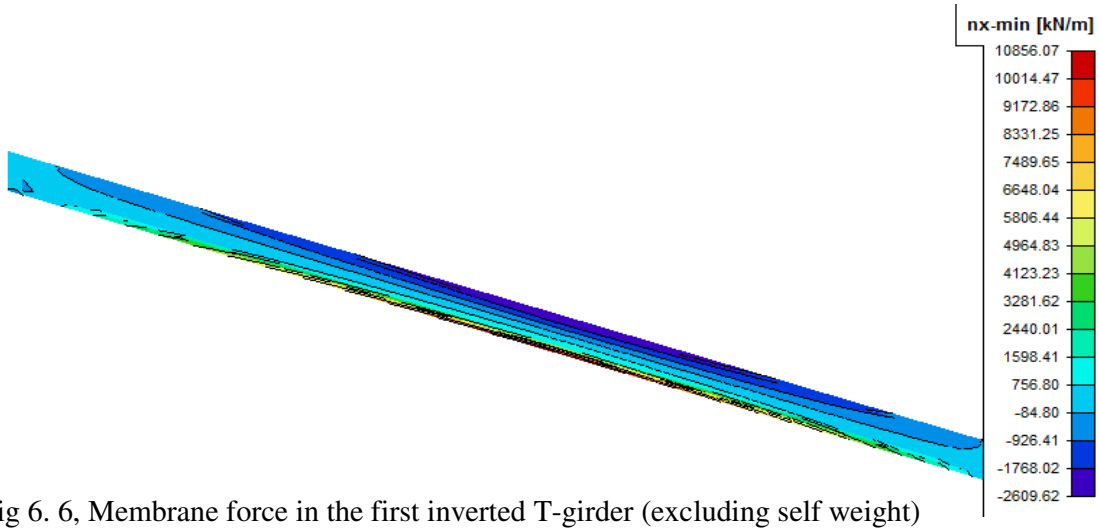

Fig 6. 6, Membrane force in the first inverted T-girder (excluding self weight)

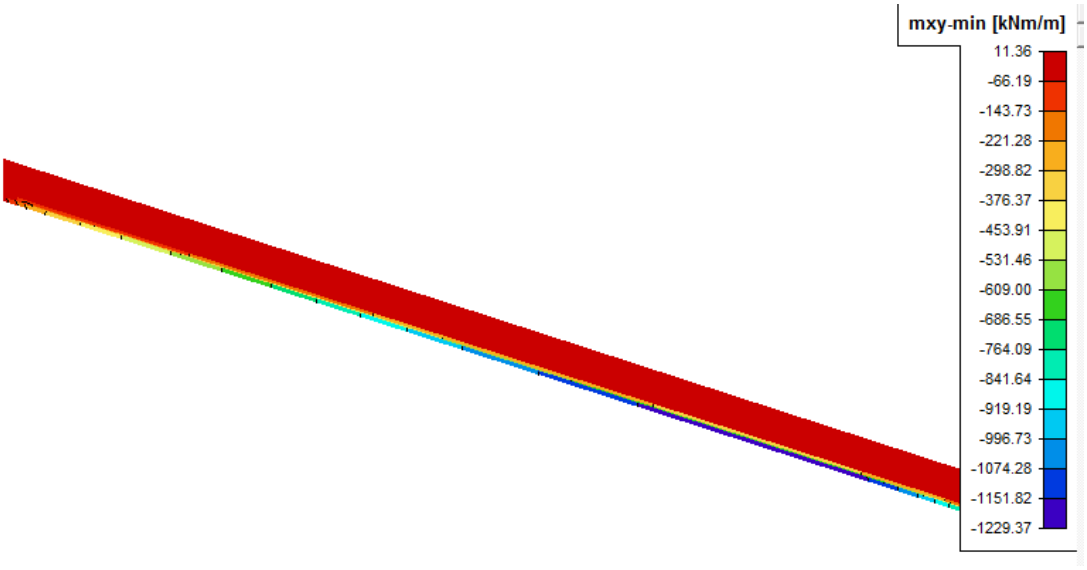

Fig 6. 7, Twisting moment in the first inverted T-girder (kNm/m) (excluding self weight)

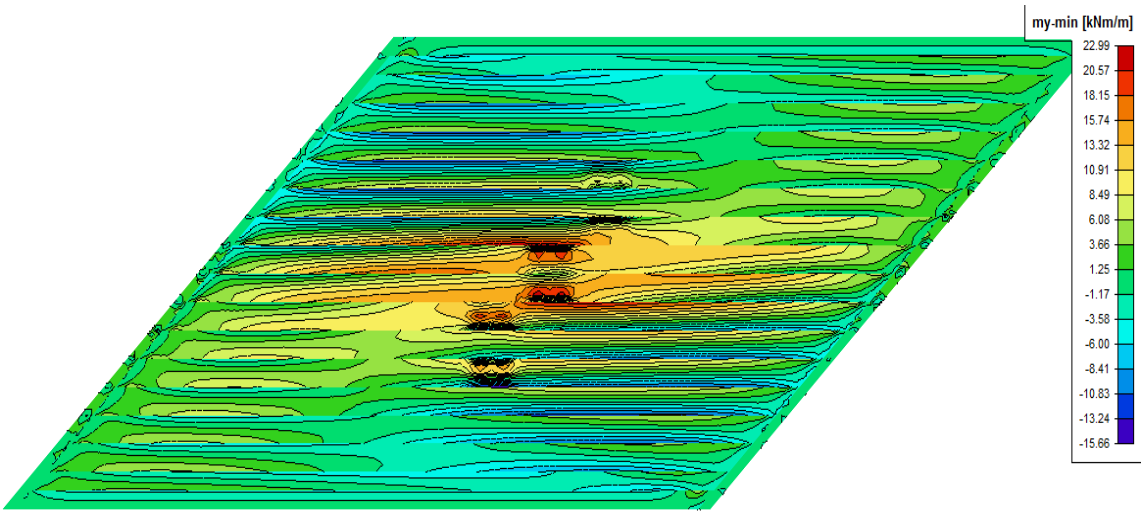

Fig6. 8, transverse bending moment in the deck

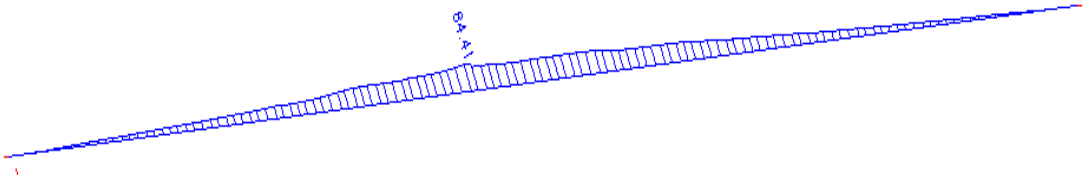

Fig 6. 9, transverse normal force in the deck (kN/m)

6.2.2 Finite element model result-ULS

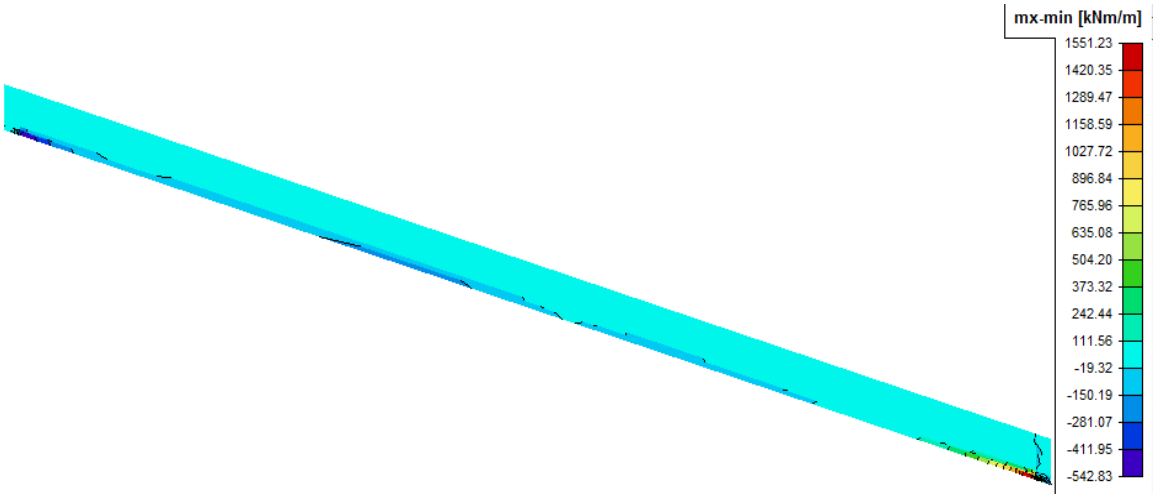

Fig 6. 10, bending in the longitudinal direction (m_x) in the first inverted T-girder (excluding self weight)

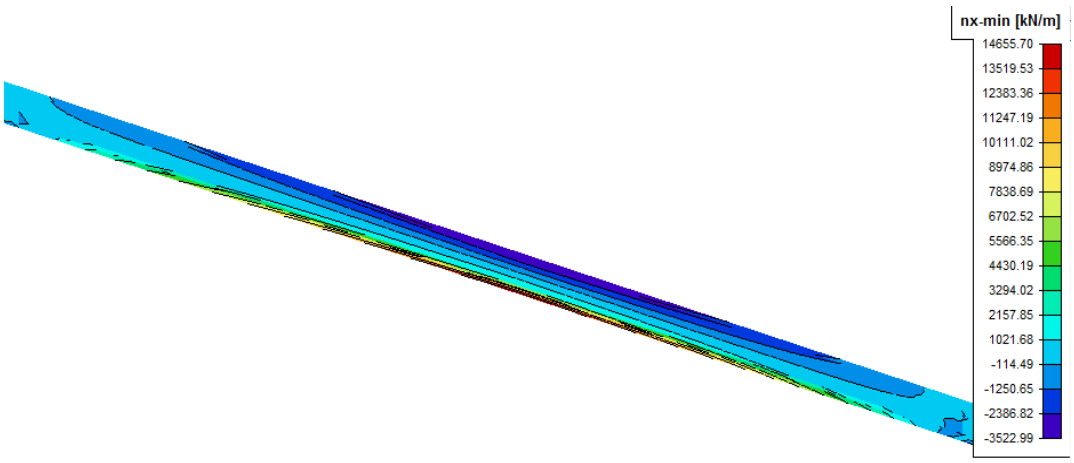

Fig 6. 11, Normal force in the first inverted T-girder (kN/m)

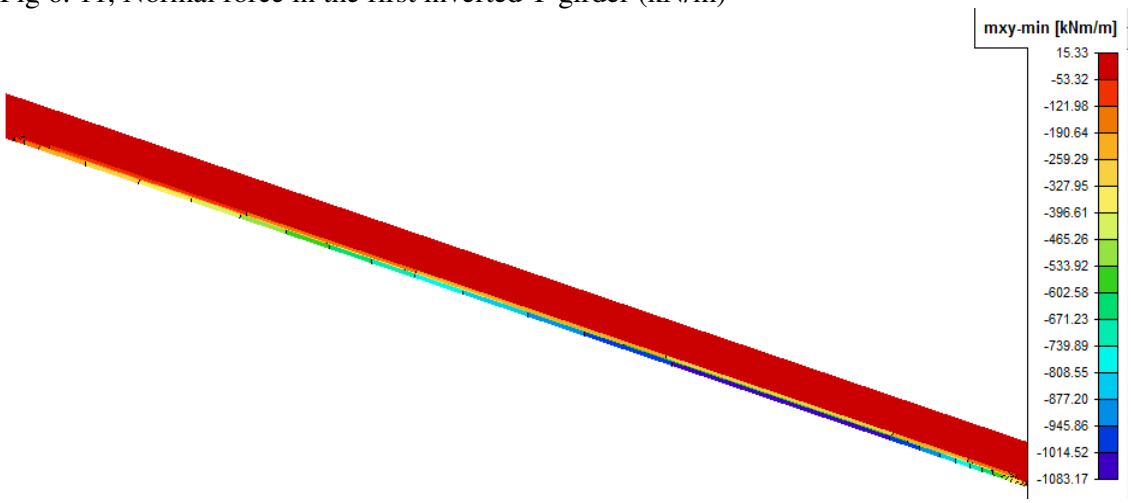

Fig 6. 12, Torsion moment in the first inverted T-girder (kNm/m)

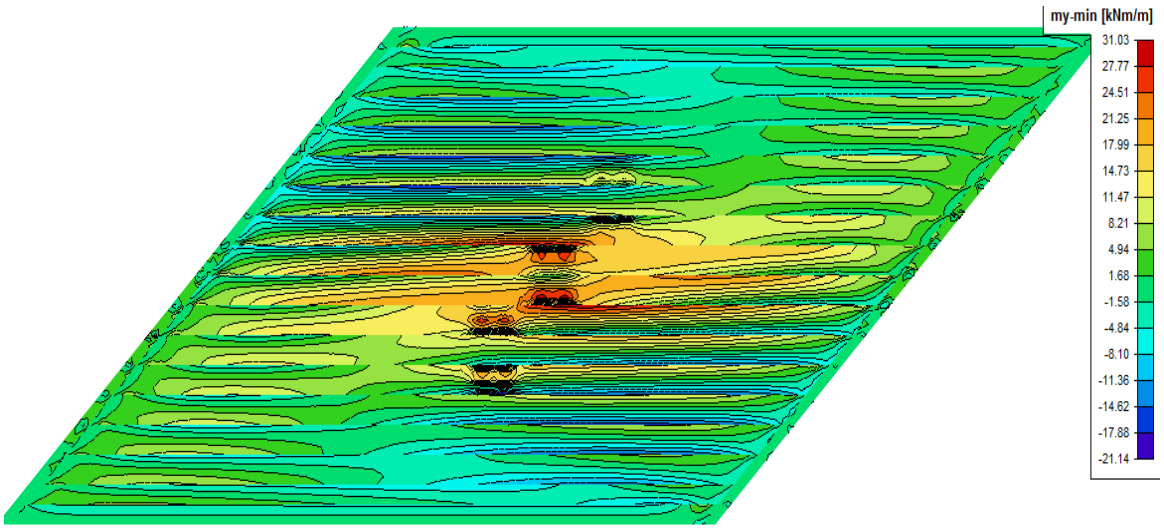

Fig 6. 13, Transverse bending in the deck slab (kNm/m)

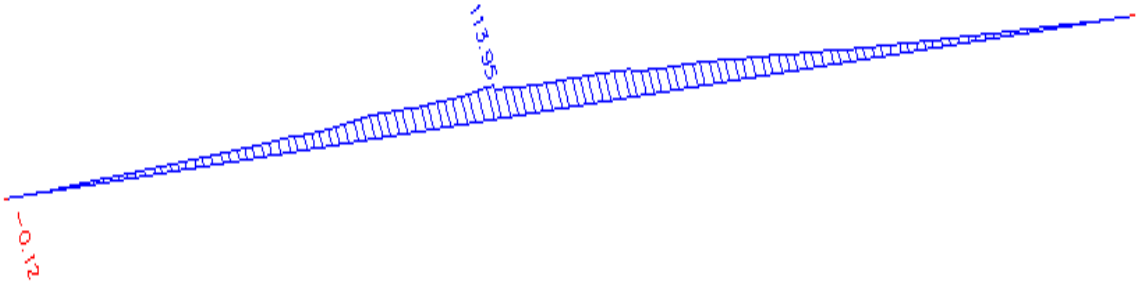

Fig 6. 14, Normal force n_y in the deck in the transverse direction (kN/m)

6.3 Post-processing

In order to compare the results of this model to the previous results, post-processing of this finite element outputs are required. The results of shell element model are moments in kNm/m and membrane forces in kN/m. These moments and membrane forces are integrated over the whole cross section to find the moments and internal forces in the composite system.

As mentioned previously, to decrease geometrical modeling errors, the girders were divided into seven parts. The resultant bending moment in a girder is then the sum of the bending moments in all these seven parts and the moment produced by the axial membrane forces about the center of the composite system. Moments and resultant axial forces in the deck and in the girder have been determined independently about their respective centroid and transformed to the composite centroid to find the composite action. The entire center-to-center distance between girders is used in calculating the internal force of the deck that should be added to the girder itself to find composite moments and internal forces. The results of the deck are transformed to the local axis of the girders before addition.

The bending moment (M_y) about the major axis and the normal force of the composite system is calculated using the following two consecutive formulas.

$$M_y = \sum z * n_{xi} * z_i$$ + The bending contribution in the x direction

$$N = \sum n_{xi} * z_i$$

Where: n_{xi} is the axial membrane force in the x direction

z is measured from the center of the composite system

In shell finite element model twisting moment m_{xy} and m_{yx} are equal. The total torsion moment is the sum of the two values and the torque as the result of shear forces as shown in the following figure.

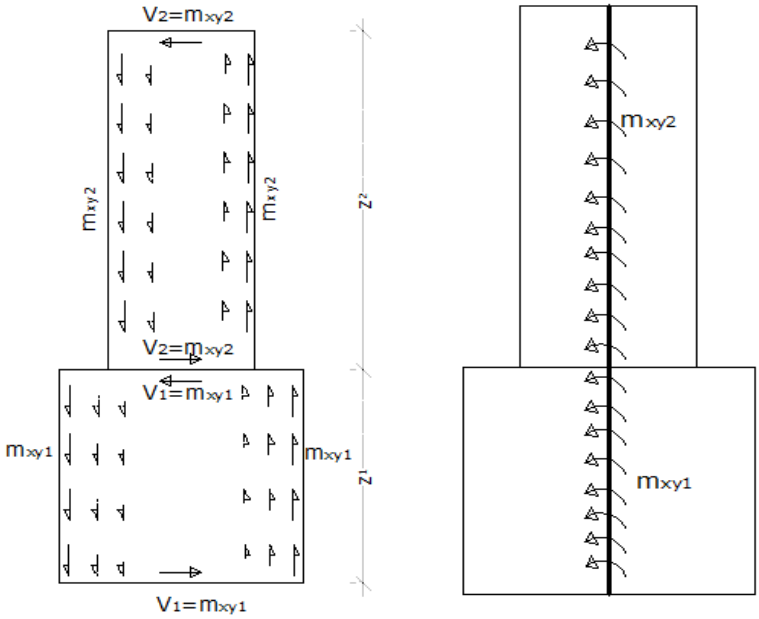

Fig 6. 15, Torsion moment distribution in a particular section

The torsion moment in the above cross section would be calculated in the following way:

$$M_x = 2 * (m_{xy1} * z_1 + m_{xy2} * z_2)$$

The above formula can be generalized for a cross section created out of n elements as follows

$$M_x = 2 * \sum_{i=1}^{n} (m_{xyi} * z_i)$$ - a_i is the height of each individual element.

The integration of the moments and forces has been done with simple spreadsheet program. See [ANNEX C]

6.4 Comparison of the above four SCIA Engineer models

Internal forces and moments in the SLS- end diaphragm beams are considered in all cases				
	Orthotropic plate model	Isotropic plate for deck and Centric beam element for beams	Isotropic plate for deck and Eccentric beam element for beams	Shell element model for deck, end diaphragms and girders
Torque near obtuse corner (kNm)	52	152	108	162
Longitudinal Span moment (kNm)	2997	2846	2970	2537
Longitudinal support moment (kNm)	-322	-64	-32	-50
Normal force(kN)	-	-	769	540
Deck transverse moment (KNm)	38	43	30	23
Transverse normal force in the deck n_y (KN/m)	-	-	109	85
Internal forces and moments in the ULS- end diaphragm beams are considered in all cases				
Torque near obtuse corner (kNm)	41	109	113	169
Longitudinal Span moment(kNm)	4158	4056	4127	3372
Longitudinal support moment(kNm)	-395	-21	-8	-35
Normal force (KN)	-	-	1114	695
Deck transverse moment (KNm)	50	66	43	29
Transverse normal force in the deck n_y (KN/m)	-	-	155	114

Table6. 1, Comparisons of all SCIA Engineer model results

The live load longitudinal bending moments in the shell element model is smaller by about 15% than the other models. This is due to the fact that the transverse flexural stiffnesses of the girders were effective and takes part of the load.

As mentioned at the beginning of this chapter, due to the limitation of the software, an approximate modeling technique extending the girder to the center of the deck was used in the shell element model. With the same reasoning the end diaphragm beams were extended to the center of the deck in the vertical direction and to the center of the girders in the horizontal direction and shared the same node with the deck slab and the girders. This approximation

increases the transverse and torsion stiffness of the whole bridge especially near the support. For this reason, torsion moments produced by this model is much higher than the other models.

6.5 Comparison of the above four SCIA Engineer models with design values

In orthotropic plate model, the twisting moment m_{xy} and m_{yx} are equal. The design torque is the sum of the two or $2*m_{xy.}$ Hence, in the following table, the torsion moment in the orthotropic plate column is multiplied by two.

Design Internal forces and moments in the ULS- end diaphragm beams were included in all cases				
	Orthotropic plate model	Isotropic plate for deck and Centric beam element for beams	Isotropic plate for deck and Eccentric beam element for beams	Shell element model for deck, end diaphragms and girders
Torque near obtuse corner (kNm)	82	109	113	169
Longitudinal Span moment(kNm)	4158	4056	4172	3372
Normal force (KN)	-	-	1114	695
Deck transverse moment (KNm)	50	66	43	30
Transverse normal force in the deck n_y (KN/m)	-	-	155	114

Table6. 2, comparisons of all SCIA Engineer models with design values

From the above table, the design torsion moments produced by the first three models were approximately similar. However, shell element model overestimates the torsion moments near the obtuse corner.

Additional longitudinal and transverse bending reinforcements or prestressing cables are required to take the torsion moments. These additional bending reinforcements could be calculated using Euro-code of recommendations.

CHAPTER 7, 3D MODEL WITH VOLUME ELEMENTS

The analysis methods presented in the previous four chapters are simplified models to simulate a cast in-situ deck on precast prestressed girders composite skew bridge. In order to check the behavior of the structure in detail, an advanced calculation method is required. Therefore, a 3D finite element model using volume elements was created using ATENA 3D commercial finite element package. The efficiencies of the preceding simplified models to capture the three-dimensional response of the skew bridge have been tested using this model as a reference.

ATENA 3D is generally used for non linear finite element analysis of structures. It is especially designed to simulate real behavior of concrete and reinforced concrete structures including concrete cracking, crushing and reinforcement yielding. Geometrical and physical non linear elastic analysis is also possible in ATENA 3D. In this case study, 3D linear elastic analysis has been carried out using standard brick elements. Even though tetrahedral elements are relatively easy to model and cost effective when compared to hexahedral (brick) elements, hexahedral elements are shown to yield accurate results for linear and nonlinear analysis and used in this case. To decrease the computational time first order linear interpolation elements were employed.

In the ultimate limit state concrete structures are thought to be cracked severely. As a result the carrying capacity of the concrete section would be dropped. The decrease in torsion stiffness due to cracking is outweighing the other stiffness parameters. For this reason, only 40% of full torsion stiffness of the section has been considered in the earlier four simplified models [ROBK 6]. Reduction in torsion stiffness is possible either by reducing the torsion moment of inertia of the section or by reducing the shear modulus of the material. Reduction in torsion moment of inertia is not possible for shell and volume finite elements. Consequently, the only remaining possibility is to reduce shear modulus of the material and create an artificial material property. However, in ATENA 3D it was not possible to change the shear modulus keeping the modulus of elasticity and poison's ratio unchanged. Therefore, linear elastic analysis with limited torsion stiffness was not possible and hence, only SLS with full torsion stiffness has been investigated in this part of this work.

7.1 Model description

The geometrical model of ATENA represents dimensions, material properties and loading. The ATENA model consists of an assembly of macro elements (solids) connected by contacts. Each macro element is an independent object defined by joints, lines and surfaces. The geometry of the bridge at hand is constructed out of 475 macro elements of standard type. 8 nodded brick elements were employed for the girders, deck and end diaphragm beams and tetrahedral elements were used for other non structural elements. Three displacement (in the global x, y and z directions) degrees of freedom at each node have been provided for all elements. In ATENA 3D, brick elements are only possible for 6 faced polygons. As a result all structural elements have been divided into parts having 6 boundary surfaces each. For other macro-elements that do not fulfill this requirement tetrahedral shape mesh would be automatically generated.

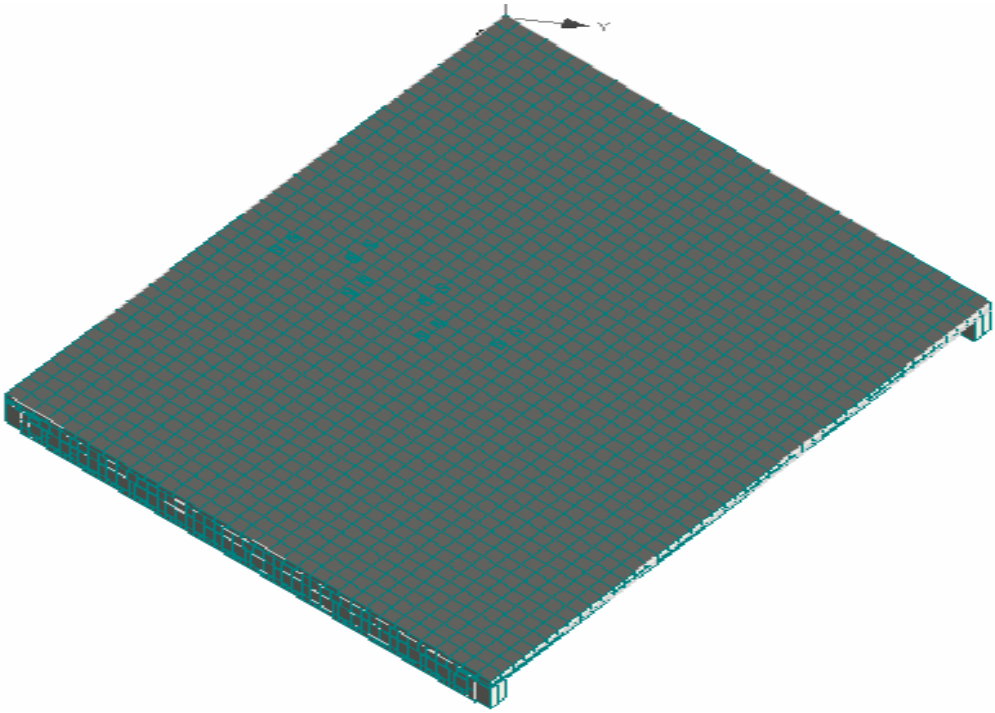

Fig 7. 1, 3D view of ATENA Model

To reduce geometrical modeling errors, the precast prestressed girders were constructed out of 9 macro elements in the thickness direction as shown in the figure below.

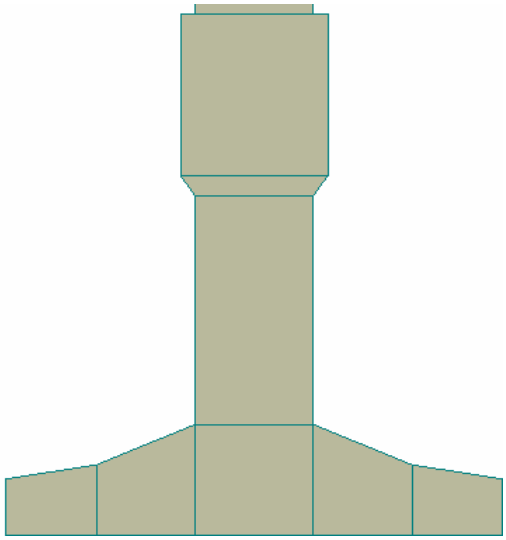

Fig 7. 2, Model of the precast prestressed girders

Transverse end diaphragm beams are modelled by blocks of concrete filling the space between the girders as shown in the figure 7.3. Each of these blocks has been divided in two 6 parts to generate a brick finite element mesh. Contact planes are automatically generated in ATENA 3D on border planes between macro elements. The contact between the cast in-situ concrete of the end diaphragm beams and the precast girders was assumed to be fully rigid.

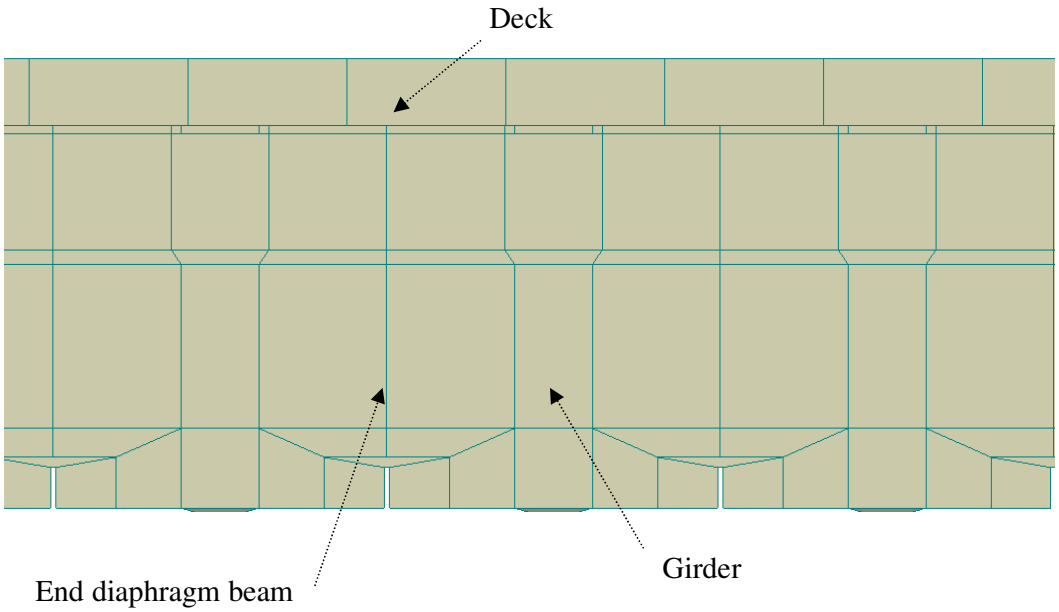

Fig 7. 3, Model of the end diaphragm beams

To simulate the elastomeric bearings provided under each girder, 5 nodded pyramidal shaped plate macro elements were created under each girder at the exact location of the bearings. The number of restraints required at these 5-nodded macro elements to provide stability to the bridge model was kept to the minimum possible. To allow limited displacement in the vertical direction, spring having stiffness K_z is attached to the global Z direction at these pyramidal shaped macro elements. All girders, except the one at the middle of the bridge, are free to translate in the global X and Y directions. Displacement restraints in global X and Y directions were provided at one support of the middle girder. At the opposite end of this same girder, displacements along Y were constrained and free to translate in the X direction. This has been done to limit the rotation of the entire bridge about the global Z direction.

7.2 Load cases and combinations

7.2.1 Load cases

To compare the results of this model to the previous approaches, the load cases and arrangements of the variable (traffic) loads should be exactly similar to the last four finite element models. To decrease computational time only three variable load arrangements and combinations were considered in this model. The following load arrangements were taken up for maximum longitudinal bending, maximum twisting moments at the obtuse corner and maximum transverse moments in the deck respectively. ATENA supports the application of loads or boundary conditions only at geometrical entities. It is not possible to apply the prescribed axle loads at the top of concrete deck. Therefore it has been necessary to create a 400mmx400mm sized rectangular macro element to apply the axle loads on top of the concrete deck.

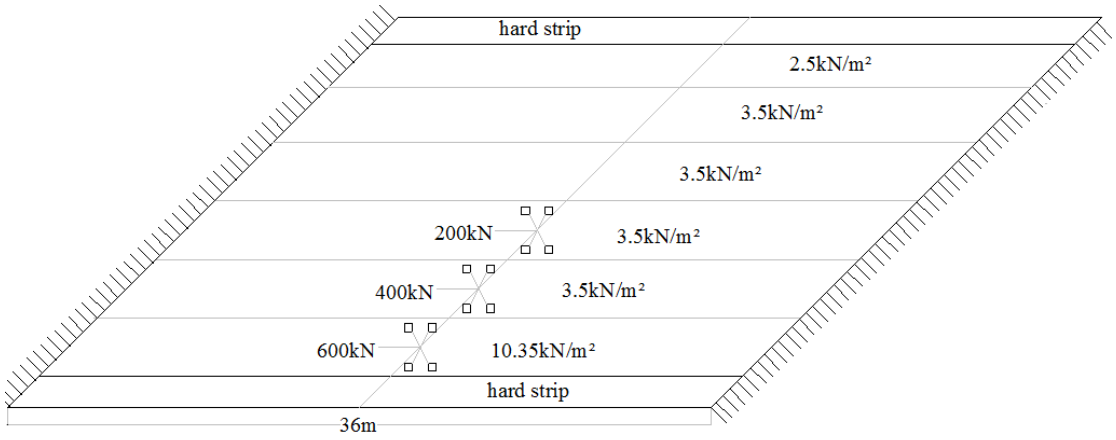

Fig 7. 4, Load case 1(Load arrangement for maximum longitudinal bending moment)

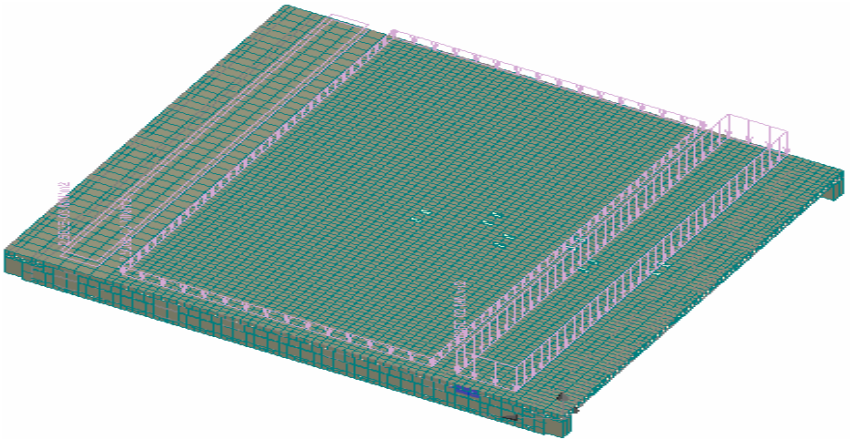

Fig 7. 5, ATENA model, lane loads for maximum longitudinal bending moment

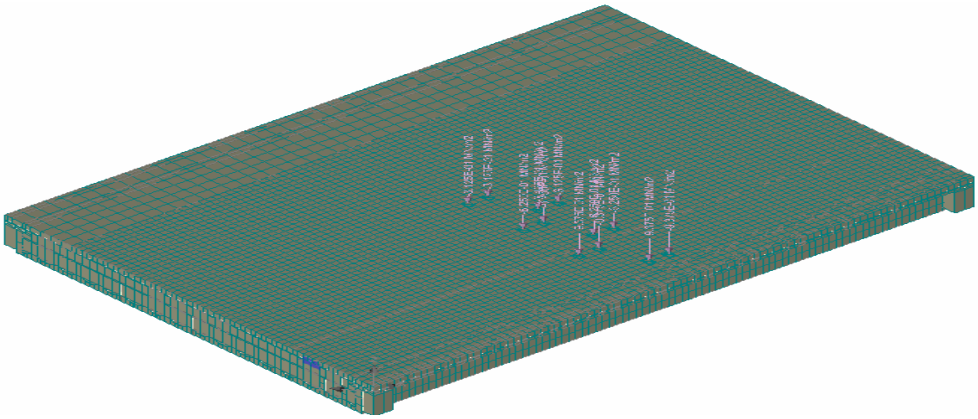

Fig 7. 6, ATENA 3D model, axle loads for maximum longitudinal bending

In the orthotropic plat model, different load cases and arrangements were tested to find the critical load case and position that generate maximum torque in the bridge. The following load arrangement was found to be critical, which is considered in this 3D model.

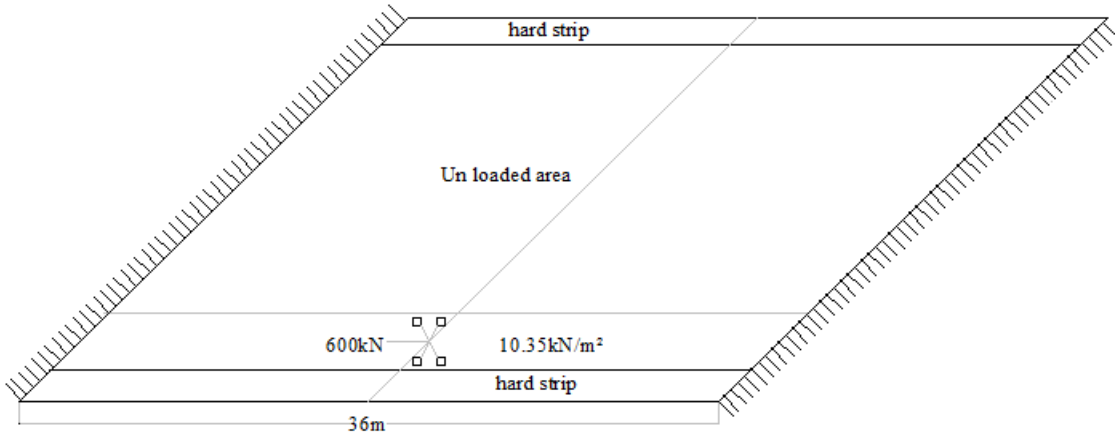

Fig 7. 7, Load case-2 (Load arrangements for maximum negative torsion moment)

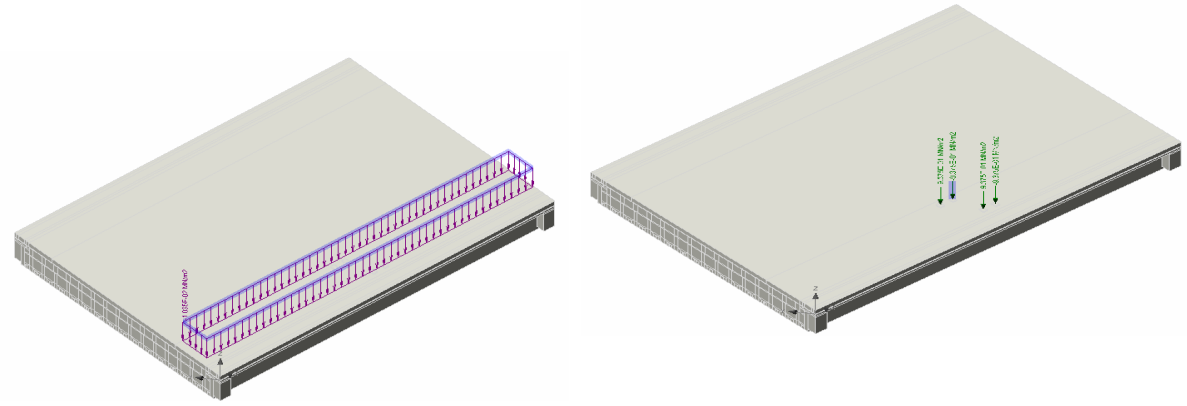

a) Lane load arrangement b) Axle load arrangement

Fig 7. 8, ATENA model, load arrangement for torsion moment

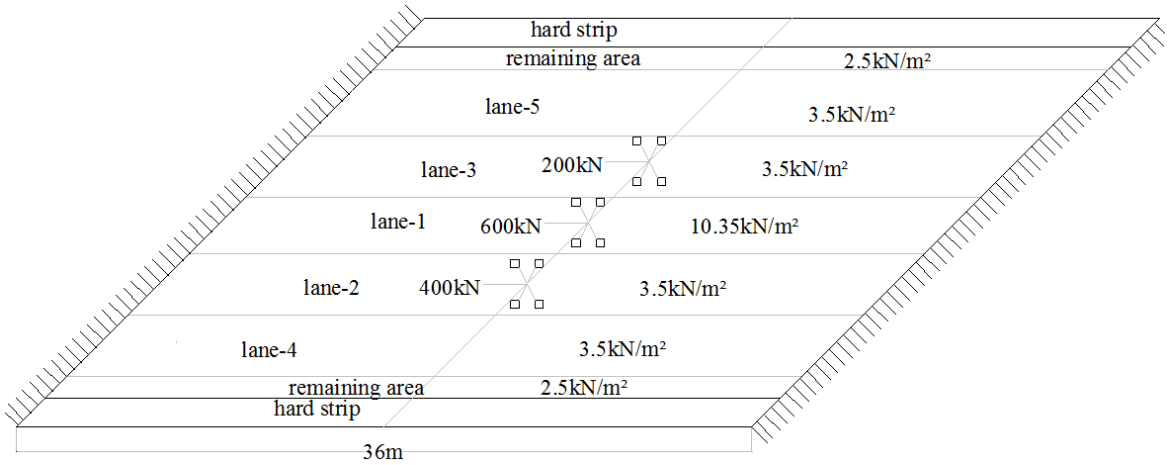

Fig7. 9, Load case -3 (load arrangement for maximum transverse moment in the deck)

7.2.2 Load combinations

Maximum bending moment in the longitudinal direction (M_y):

Asphalt layer + edge element loads + load case-1

Maximum torsion moment (M_x)

Asphalt layer + Edge element loads + load case-2

Maximum transverse positive moment in the deck

Asphalt layer + Edge element loads + Load case-3

7.3 Finite element model results

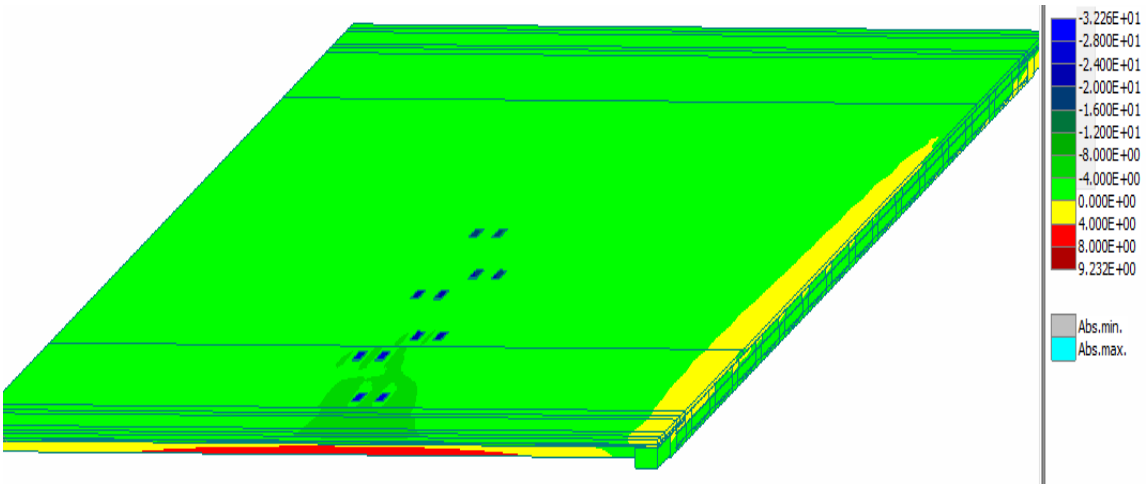

Fig 7. 10**,** Stress (σ_{xx}) in all structural members as a result of load combination 1

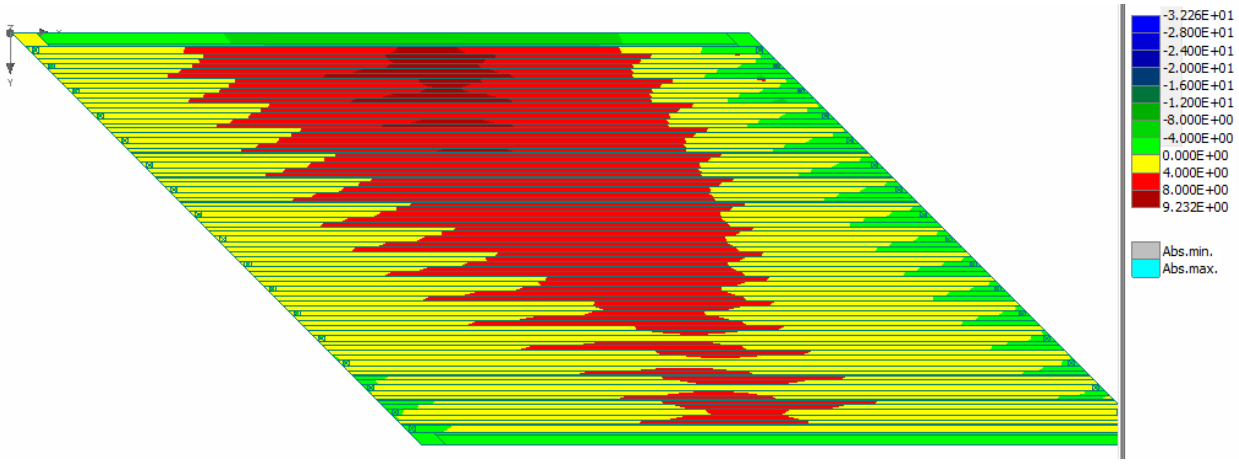

Fig 7. 11, Stress (σ_{xx}) in the longitudinal direction at the bottom fiber of the girders (comb-1)

The Figure 7.10 and Figure 7.11 show that there exist a large stress concentration at the loading and support steel plates. It is understandable, but this affects the colour scale that is automatically selected by the program such that it covers the whole stress range in the model. Very often this is not desirable, since it would be more interesting to learn about the stress distribution in the girders and deck slab only. With this scale setting, it is not possible since almost the whole deck is covered by a single color. Therefore, new color scale was selected and the stress in the first inverted T-girder and deck slab is shown in the subsequent figures.

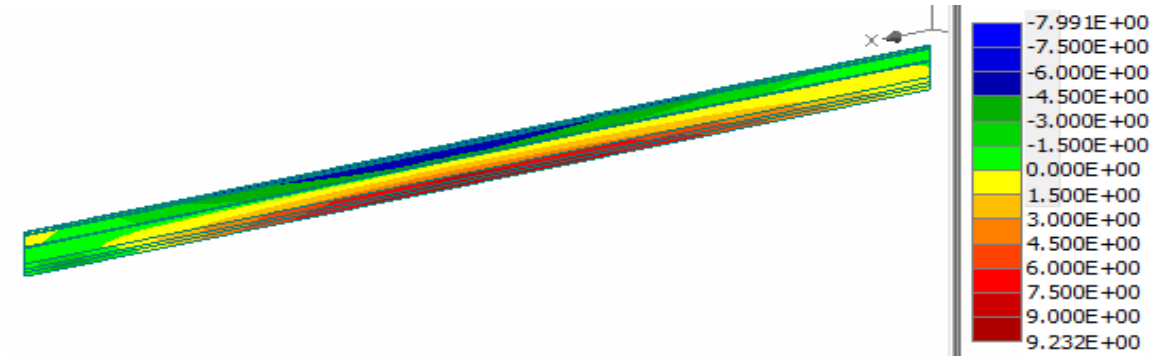

Fig 7. 12, Stress (σ_{xx}) in the x direction at the first inverted T-girder (Comb.1)

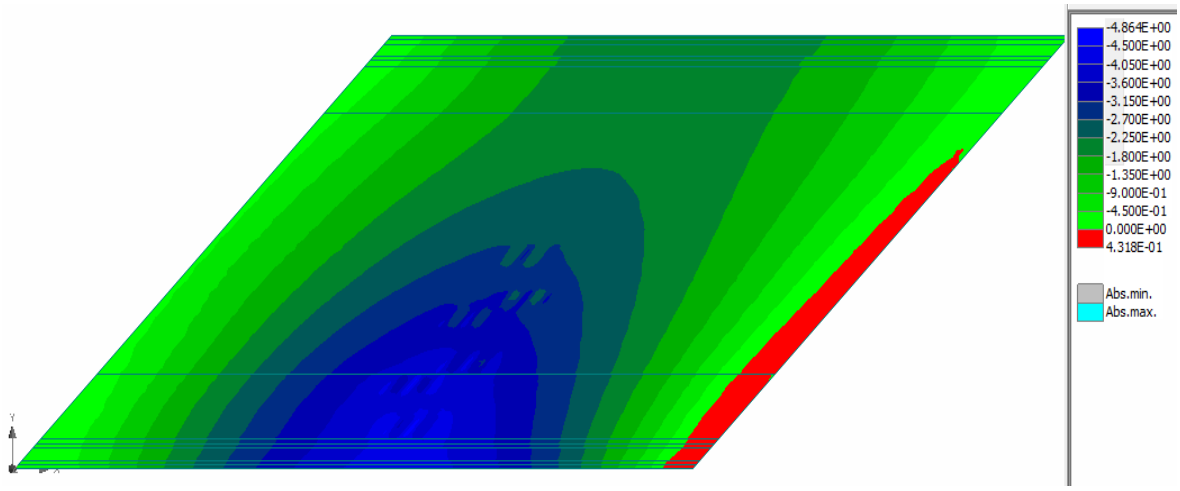

Fig 7. 13, Stress (σ_{xx}) in the deck in the longitudinal direction (load comb-1)

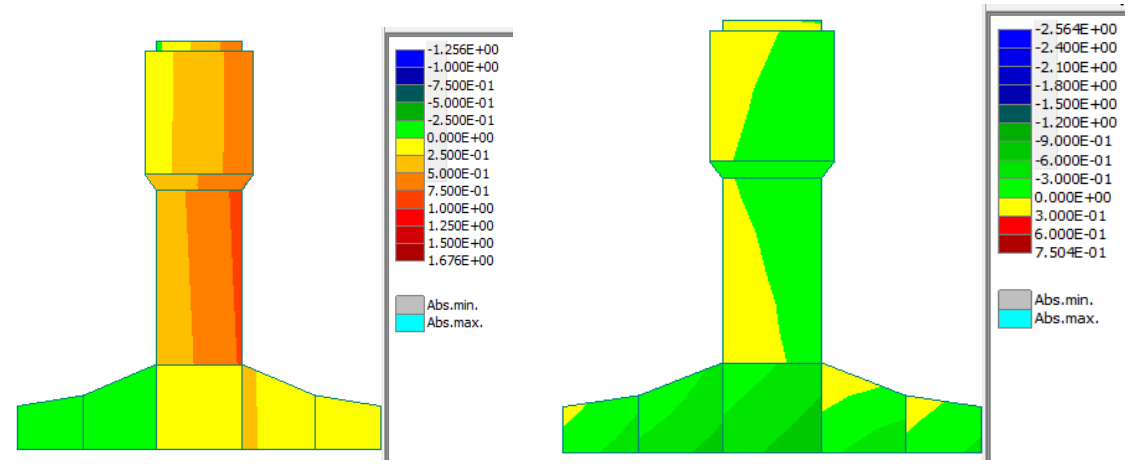

a) Shear stress σ_{xz} b) Shear stress σ_{xy}

Fig 7. 14, Shear stresses at face of end diaphragm in the first inverted T-girder

7.4 Post processing of results

In ATENA 3D one can define a section at a certain longitudinal distance and get stress distribution on that section. These stresses are very general and shown as a wide range of colours. Finding out the exact values of these stresses at a particular section is not possible in ATENA 3D. For finding the magnitude of normal and shear stresses at a particular section, the model has been exported to ATENA WIN. A model being examined can be depicted in its unreformed or deformed state using wire or rendered visualization of the structure. Here in ATENA WIN, it is possible to control direction of view and it is also possible to select one particular macro element to display the internal stresses.

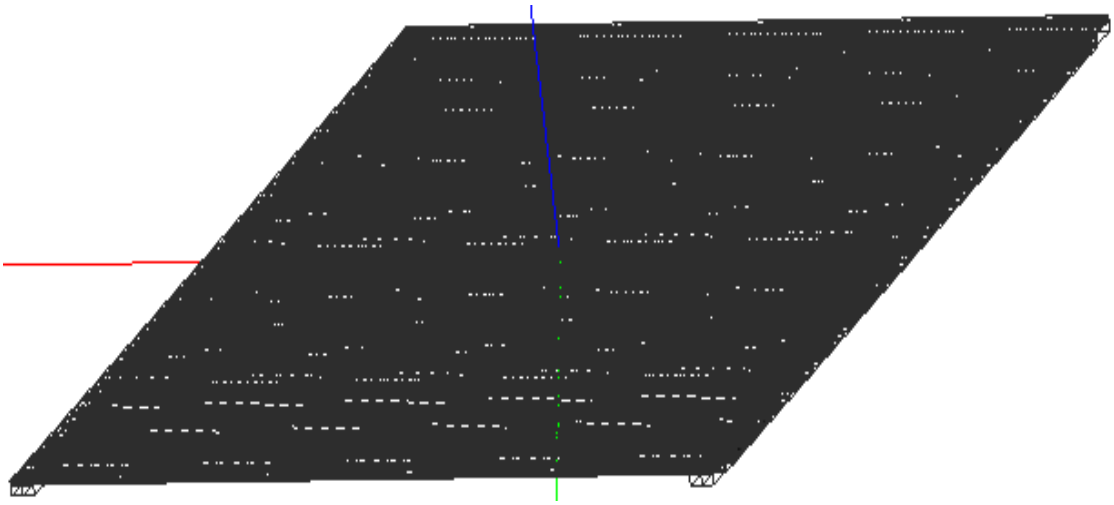

Fig 7. 15, Wire mesh geometry of the whole bridge

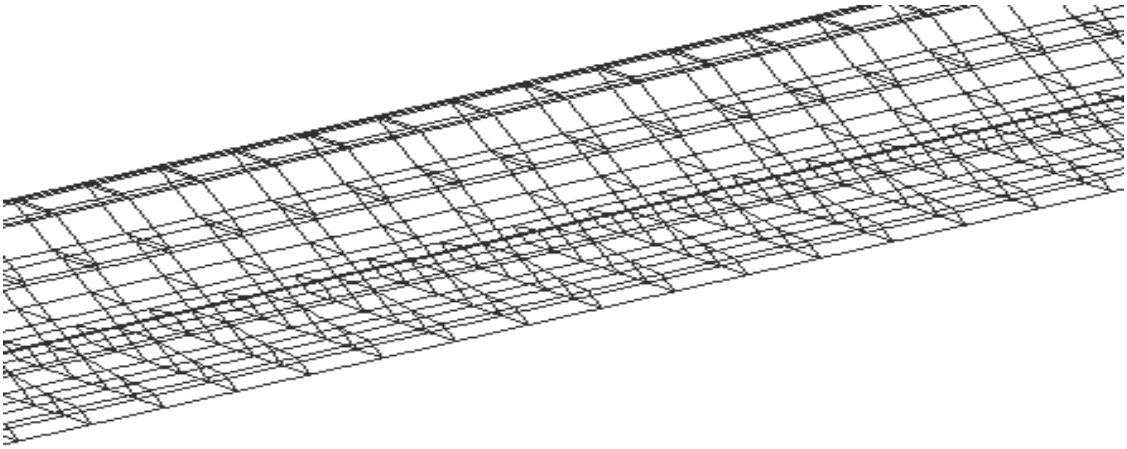

Fig 7. 16, Wire mesh geometry of part of the first inverted T-girder

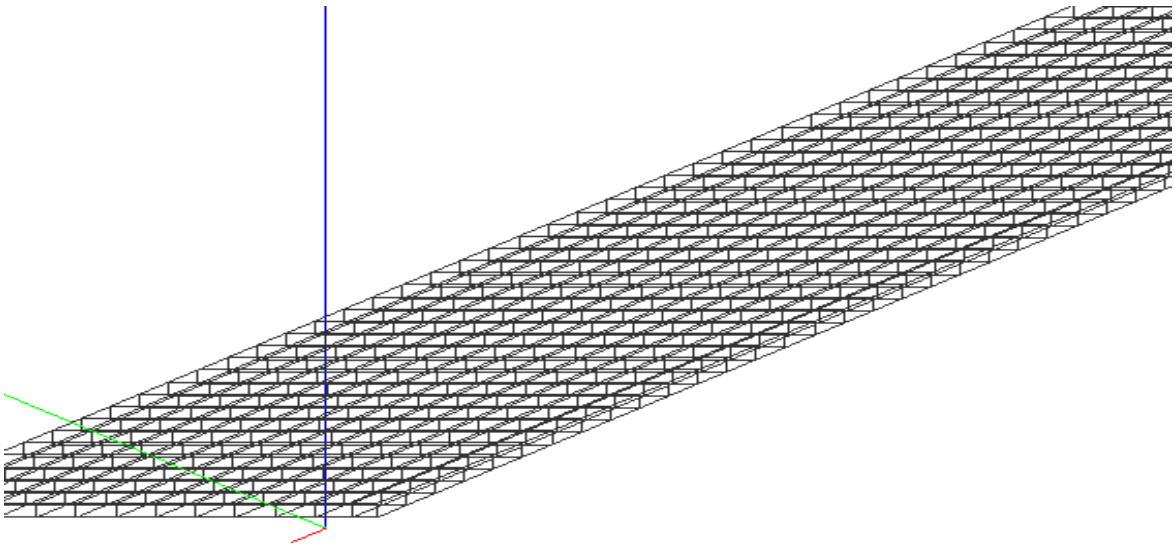

Fig 7. 17, Wire mesh of part of the deck slab

The maximum normal stresses near the middle of the bridge and the shear stresses in the obtuse corner of the bridge are the most interesting results in this research. Nodes have been selected in the first inverted T-girder at critical sections and stresses and nodal coordinates were printed from ATENA WIN output window. Twisting moment in the first inverted T-girder has been computed using shear stresses σ_{xy} and σ_{xz} at the face of the end transverse beam. The maximum bending moment in the major axis was calculated using normal stresses at the middle of the girder.

7.4.1 Integration of nodal stresses over a cross-section

The four nodal stresses obtained in one particular area shown in the figure below are not equal in magnitude. In order to get the moments and internal forces in a cross-section, stress functions for each area has been generated and these stresses have been integrated on their respective areas.

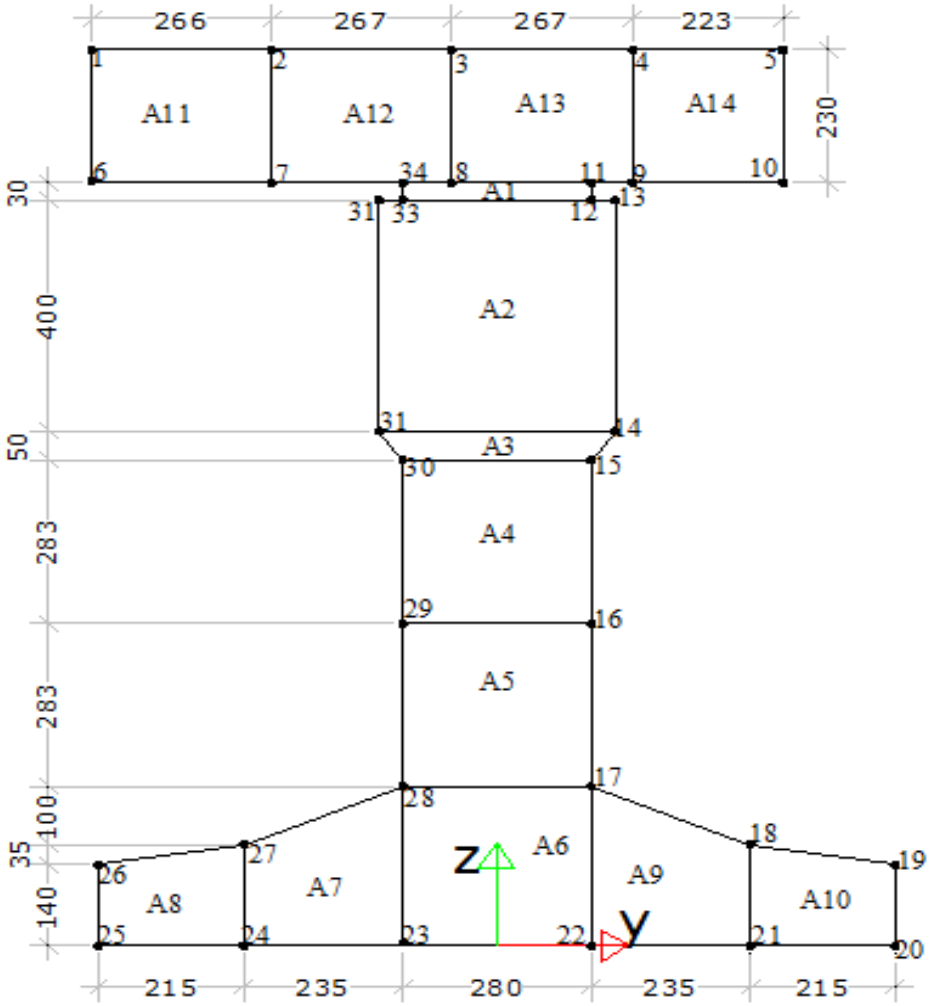

Fig 7. 18, Node and area names in a particular section at the first inverted T-girder

Node No.	y(m)	z(m)	Node No.	y(m)	z(m)	Node No.	y(m)	z(m)
1	-0.600	1.550	13	0.175	1.290	25	-0.590	0.000
2	-0.334	1.550	14	0.175	0.890	26	-0.590	0.140
3	-0.067	1.550	15	0.140	0.840	27	-0.375	0.175
4	0.200	1.550	16	0.140	0.558	28	-0.140	0.275
5	0.423	1.550	17	0.140	0.275	29	-0.140	0.558
6	-0.600	1.320	18	0.375	0.175	30	-0.140	0.840
7	-0.334	1.320	19	0.590	0.140	31	-0.175	0.890
8	-0.067	1.320	20	0.590	0.000	32	-0.175	1.290
9	0.200	1.320	21	0.375	0.000	33	-0.140	1.290
10	0.423	1.320	22	0.140	0.000	34	-0.140	1.320
11	0.140	1.320	23	-0.140	0.000			
12	0.140	1.290	24	-0.375	0.000			

Table7. 1, Nodal coordinates from the bottom of the girder

7.4.2 Stress functions and integration of stresses

For first order linear interpolation in both x and y directions, the stress functions in one particular area for quadrilateral finite elements would be written in the following form.

$$\sigma_i = a_i y + b_i z + c_i yz + d_i \text{ ..... [(15)]}$$

The stress values at each node and their respective coordinates are known and it is possible to write the stress functions in each area. Areas which are not rectangular are approximated to rectangles of equal area with the original ones. The systems of equation of four unknowns with four variables have been solved by Maple to determine constants a_i, b_i, c_i and d_i.
See [ANNEX D].
The bending moment in the major axis (M_y) is computed as follows:

$$M_y = \int z * \sigma_{xx} dA = \iint z * \sigma_{xx} dydz \text{ ,..... [(15)]}$$

Where: z is measured from the center of the composite system (girder and deck).
In the same way, the net internal in-plane force (normal force) in the composite system is:

$$N = \int \sigma_{xx} dA = \iint \sigma_{xx} dydz \text{ ,}$$

The summation of the bending moment about the composite centroid for 14 areas shown in the above figure would give total bending moment. And the summations of the normal forces give the net normal force in the whole cross-section.

After integration the total bending moment in the longitudinal direction and the net normal force for the composite system due to traffic load and edge element loading in the SLS has been found to be 2515kNm and 499kN. See [ANNEX D].
In the same way the torsion moment is calculated as follows

$$M_x = \int (y * \sigma_{xz} - z * \sigma_{xy}) dA = \iint (y * \sigma_{xz} - z * \sigma_{xy}) dydz$$

The total twisting moment at the face of the end diaphragm beam with critical combination in the first inverted T-girder was found to be -120kNm. See [ANNEX D].

7.5 Comparison of results in the SLS

The comparison of all the preceding models has been clearly explained in following chapter.

CHAPTER 8, COMPARISION OF RESULTS AND SELECTION OF THE BET MODEL

8.1 Limitations of each numerical model

It is always cost effective for the engineer to simplify the modelling approaches employed in order to estimate the structural responses of the components within the structure. However, these simplifications compromise one or more aspects of the real bridge deck behaviour. In this chapter, the kind of simplification and limitations of all the modelling techniques studied in the preceding chapters will be discussed in depth.

- **Orthotropic plate model:**

The orthotropic plate modeling method is a study of an equivalent plate system for an assembly of cast in-situ slab and precast girders. This modelling technique fails to deal with the following aspects of bridge deck behavior:

- Transverse and longitudinal in-plane forces
- Distortion of beam members
- Local bending effects

It is apparent that, the neutral axis for the entire bridge is not the same in the transverse direction. This is due to the fact that, the center-to-center spacing between girders is not the same for exterior and interior girders. Moreover, the cross sectional dimensions of the spandrel beam (End girders) is not the same as the inverted T-girders. However, in orthotropic plate modeling method, the transverse variation of this neutral axis should be taken into consideration in the hand calculation of stiffness parameters.

- **Centric beam element for girders and Isotropic plate for the deck:**

Like the orthotropic plate model, this model is planar (two dimensional) and the following things cannot be taken into account:

- Transverse variation in the level of the neutral axis
- Transverse and longitudinal in-plane forces

In addition to these limitations, this model failed to consider the eccentric distance between the center of the deck and center of the girders. The centers of the girders are concurred to the center of the deck slab. For this reason, it underestimates the flexural strength of the

composite system in the major axis. Hence, this model underestimates the bending moments in the longitudinal direction of the girders and overestimates the torsion moments.

The support system (bearings) in the real viaduct is under each girder. However, in orthotropic plate, centric beam and eccentric beam element models the support system is at the center of the deck slab. This implies that, the location of the support is moved vertically to the center of the deck in the numerical models. This is also the other limitations of the above models.

- **shell elements for the deck:**

In shell element model for deck and girder, SCIA Engineer failed to connect shell elements of the deck and girders using rigid links. As a result, an approximate method by extending the girder to the centre of the deck and sharing the same node with the deck shell element has been used. In addition to this, non prismatic shaped girders were approximated with equivalent prismatic sections.

In the following table all the above limitations for all modelling methods are summarized.

Different aspects of bridge deck	Orthotropic plate model	Isotropic plate with centric beam element	Isotropic plate with eccentric beam element	Shell element for deck and girders	3D model using volume elements
Transverse variation in the level of the neutral axis	✓	x	✓	✓	✓
Transverse and longitudinal in-plane forces	x	x	✓	✓	✓
Distortion of beam members	x	x	x	✓	✓
Flexural stiffness calculation	✓	x	✓	✓	✓
Correct location of the support	x	x	x	✓	✓
Local bending effects	x	✓	✓	✓	✓

Table 8. 1, Summery of limitations of each finite element modeling methods

8.2 Comparison of results

In chapters 3-6 different numerical models with different sophistication have been developed using SCIA Engineer. In addition a comparative study has been done in both service and ultimate limit state conditions in each chapter. However, none of those models has perfect similitude with the actual structure. As part of an effort to more accurately represent the bridge behavior a 3D model using volume elements has been created in chapter 7 using ATENA 3D. The development of the ATENA model and a summary of the internal forces and moment results were discussed in detail in the same chapter (Chapter 7). To make sure that those previous simplified models were applicable to the current bridge case, the results obtained from those simplified models have been compared to the results from the solid

model. The comparison was limited to bending in the longitudinal direction and torsion at the first inverted T-girder and bending moments in the transverse direction of the deck.

8.2.1 Summary all the five numerical models

As briefly described in each model, the reinforced concrete deck slab has been cracked in the transverse direction even in serviceability limit state conditions. On the contrary, it is fully effective to resist the longitudinal sagging moment in compression. In the three dimensional model using ATENA 3D, it is impossible to create an orthotropic deck having different stiffness in the transverse and longitudinal directions. Consequently, identical deck property (Isotropic) in both directions was required. In order to compare the results of the simplified models with the 3D one, it has been necessary to assign the same material property with the 3D model. To consider cracking for deck slab half of young's modulus was used in both directions for all finite element models.

When a structure is subjected to ultimate limit load condition, the structure would be cracked severely and the torsion stiffness would particularly decrease to a great extent. To consider this effect, the torsion stiffness of the section has decreased by 60% in the ultimate limit state for all simplified models described in chapter 3-6. The increase in bending in the longitudinal and transverse direction as a result of this reduction in torsion stiffness was also discussed in depth. However, decrease in torsion stiffness by decreasing the shear modulus keeping the modulus of elasticity unchanged in the ATENA 3D was not possible. Therefore, only serviceability limit state condition has been compared in this chapter.

8.2.2 Comparison in SLS

In the comparison only traffic loads, both concentrated and uniformly distributed, and edge element loads have been considered. The effect of self weight of the bridge was not taken into account. Bending in the longitudinal direction, bending in the transverse direction and torsion moments have been computed in their respective critical traffic load arrangements and load combinations. End transverse diaphragm beams have been taken in to account in all cases. Comparison results are presented in Tables 8.1 and Table 8.2 below.

Finite element modeling techniques	Bending moment (kNm)	Normal force (kN)	Torsion moment (kNm)	my-deck (kNm/m)	ny-deck (kN/m)
Orthotropic plate	2968	-	51	35	-
Isotropic plate for deck and Centric beam element for girders	2846	-	150	43	-
Isotropic plate for deck and Eccentric beam element for girders	2938	773	108	25	103
Shell element model for both deck and girder	2537	540	162	24	83
Volume element model (brick)	2515	499	120	20	67

Table8. 2, result of all finite element modeling methods in the SLS

As described in chapter 6, the twisting moments in the orthotropic plate model, shown in Table 8.2, should be multiplied by two to obtain the design values. Hence, it is imperative and reasonable to compare the modelling methods using design torsion moments in SLS conditions.

The required longitudinal and transverse reinforcement due to torsion should be calculated independently as per Euro-code of recommendations. The total longitudinal and transverse bending reinforcements and/or prestressing cables are the sum of the amount computed due to torsion and bending moments. Adding the part of torsion moments to the longitudinal and transverse moments in the reinforcement estimation will make the calculation inaccurate. Hence, in the table below, longitudinal and transverse moments are the result of the finite element models.

Finite element modeling techniques	Bending moment (kNm)	Normal force (kN)	Torsion moment (kNm)	my-deck (kNm/m)	ny-deck (kN/m)	% difference with 3D model (torsion)
Orthotropic plate	2968	-	102	35	-	-15%
Isotropic plate for deck and Centric beam element for girders	2846	-	150	43	-	+25%
Isotropic plate for deck and Eccentric beam element for girders	2938	773	108	25	103	-10%
Shell element model for both deck and girder	2537	540	162	24	83	+35%
Volume element model (brick)	2515	499	120	20	67	0%

Table8. 3, Comparison, SLS

In the table above particular attention was given for torsion moments at the obtuse corner of the bridge and the percentage difference obtained from each finite element model has been tabulated in the last column. The table discovered that, the percentage difference in the design torsion moments in the first inverted T-girder for orthotropic plate and eccentric beam element models are fairly similar and have close proximity to the 3D model. Orthotropic plate model underestimates the twisting moment by 15% and Eccentric beam element model by 10%.

It is theoretically apparent that the shell element model for deck and girders has a better similitude to the actual bridge than eccentric beam element and orthotropic plate models. In spite of this fact, as described in chapter 6, this modelling technique with SCIA Engineer was found to be impossible to accurately model the bridge geometry. This incorrect geometric modelling increases the relative torsion stiffness than the corresponding flexural one. This makes the torsion moment found in shell element model higher by 35% than the 3D model.

As clearly explained in chapter 4, the centric beam element model underestimates the flexural stiffness of the composite system about the major axis at large. This makes an increase in torsion moments by more than 25%, which makes it in appropriate modelling procedure.

8.3 Selection of the best modelling technique

The question of which modelling technique is appropriate for a given structure is typically answered by first considering the objectives of the analysis. Two critical and computing aspects in a particular structural analysis are: a desired level of accuracy in results and the time required. The decision of selection is a direct function of the economy behind the project, as well as the requirements of the project. In this particular case study the following important aspects have been considered to select the best modeling techniques out of the above models.

- The desired level of accuracy in results for daily practice in the construction industry.
- Time-efficiency of the analysis, which is a function of the modeling time for the engineer and the time needed for the computer to give results (waiting time).
- Application friendliness of the model and susceptibility in making errors. Simplicity of interpreting the results of the model, user friendliness of the software and the required educational level of the engineer can be considered in this aspect.

The following table shows the comparison of all the modeling methods tested.

Finite element Modelling techniques	Required Accuracy	Time efficiency		Simplicity of interpreting results	Required educational level of the Engineer
		Modelling time	Computational time		
Orthotropic plate(SCIA Engineer)	+	++	++	+	+
Isotropic plate with Centric beam element (SCIA engineer)	--	++	++	++	+
Shell elements with Eccentric beam element (SCIA Engineer)	+	++	++	++	+
Shell element for both deck and girder (SCIA Engineer)	0	-	+	-	+
Volume elementS (ATENA 3D)	++	--	--	--	-

++ Very good + good 0 -neutral - bad -- very bad

Table 8. 4, Summary of the selection procedure

From the table 8.4, one can see that, concentric beam element model has very bad accuracy and 3D model on the contrary has very good accuracy in results. However, the 3D model has very poor time-efficiency in modelling. On top of that, the outputs of this model are stresses and strains which are inappropriate for the design engineers. The same is more or less true for the shell element model for the deck and girders. The results are normal forces in kN/m and bending moments in kNm/m which needs integration to find the design moments and internal forces. The two remaining better modeling techniques are then orthotropic plate and Eccentric beam element models. From table 8.3 above, these two models have fairly similar torsion moment and have relatively smaller percentage difference with the 3D model. Comparing the modeling time, orthotropic plate model takes relatively long time to calculate the stiffness parameters than Eccentric beam element model. Eccentric beam element model allows the engineer to exploit the program ultimately. All the section properties of the prestressed girders and the deck slab are calculated automatically by the program. All what he or she needs to do is to define the cross section of the girders and desk only. Moreover, Eccentric beam element model can represent the 3D behavior of the bridge especially the transverse and longitudinal in-plane forces than the corresponding orthotropic plate model. In conclusion, a model with shell element for deck slab and eccentric beam element for girder can simulate the horizontally skew inverted T-girders on cast in-situ deck slab with reasonable accuracy and excellent time efficiency using SCIA Engineer.

CHAPTER 9, EFFECT OF SKEWNESS ON THE GENERAL BEHAVIOUR OF BRIDGES

9.1 Introduction

As already mentioned in the literature review part of this work, internal force distribution in skew bridges is affected by angle of skewness, span length of the bridge, girder spacing and number and arrangement of transverse beams. However, the skew angle of the deck is the most influential factor on live load distribution. In this chapter, the internal force flow of a particular bridge having different skew angles was tested using two finite element modeling techniques. The bridge analyzed in the previous chapters of span length of 36m and internal girder spacing of 1.2m was chosen for the subsequent study. Four skew angles of 0^o, 30^o, 45^o, and 60° were considered for each finite element model. Only two 900mm wide support transverse beams were provided in each case. SCIA Engineer commercial finite element program is adopted for this part of the work as well.

In the previous chapters it has been shown that in the transverse direction of the deck, tensile stress even in SLS condition is far above the tensile strength of the in-situ deck concrete. Therefore, the concrete would be cracked and this transverse cracking of the in-situ concrete was considered by taking half of the young's modulus in the transverse direction only. In the longitudinal direction deck slab is fully effective to take the longitudinal sagging moment in compression. Unlike the previous chapters, full stiffness was considered for the deck slab in the longitudinal direction. Girders were made up of high quality concrete and they are prestressed and full stiffness was assumed.

The following two finite element techniques were employed in this part

1. Orthotropic plate model (quadratic shell element)
2. Eccentric beam element for girders and orthotropic plate (quadratic shell element) for the deck

Detail investigation about the modeling techniques of skew bridges has been carried out in the preceding chapters, and it was made clear that eccentric beam element can represent the presteressed girders with practically accepted accuracy. In this part, it was sufficient to model the bridge deck using shell elements for the deck and eccentric beam elements for the girders. Nevertheless, current practice showed that many engineers are using planar (two dimensional)

orthotropic plate models. Hence, these two techniques were tested subsequently to understand the effect of skewness in the general behavior of the bridge deck.

9.2 load cases and load arrangements

To investigate the sensitivity of the bridge with angle of skewness, bending in the longitudinal direction of the girders, torsion near the obtuse corner of the bridge and bending in the transverse direction in the deck have been compared with right bridge of the same span. Having this in mind, three variable load arrangements were selected for longitudinal bending, transverse bending and torque in the obtuse corner of the bridge as shown in the following three figures.

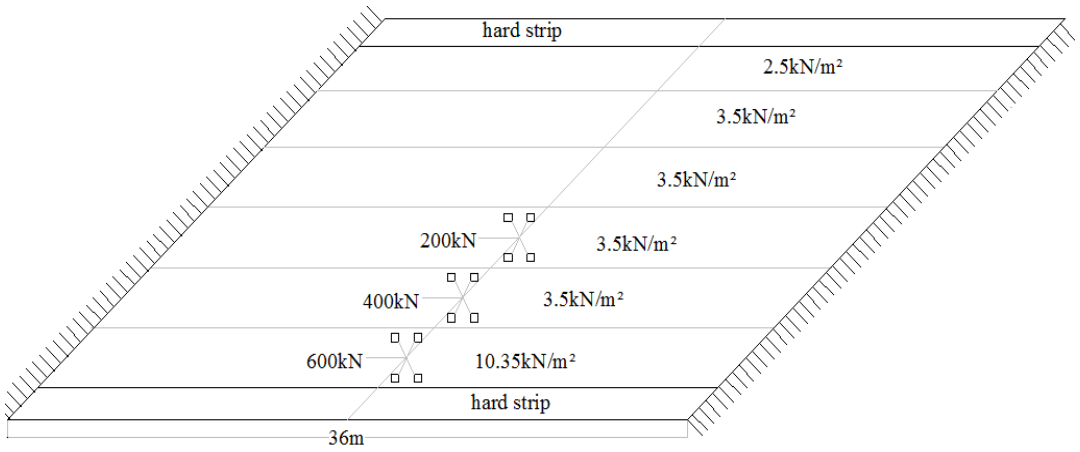

Fig9. 1, Load cases and arrangement for maximum longitudinal bending in the girders

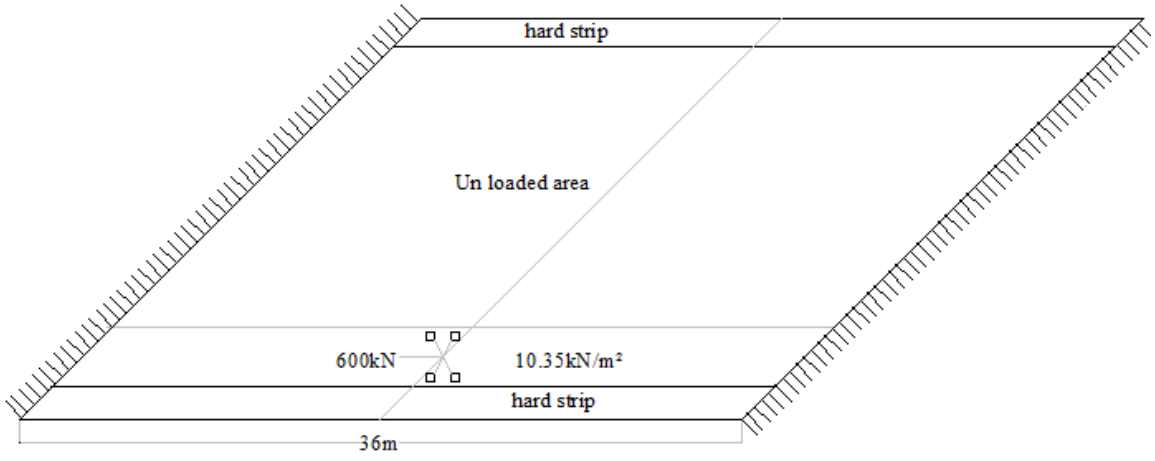

Fig9. 2, load case and arrangement for torsion moment near obtuse corner of the bridge

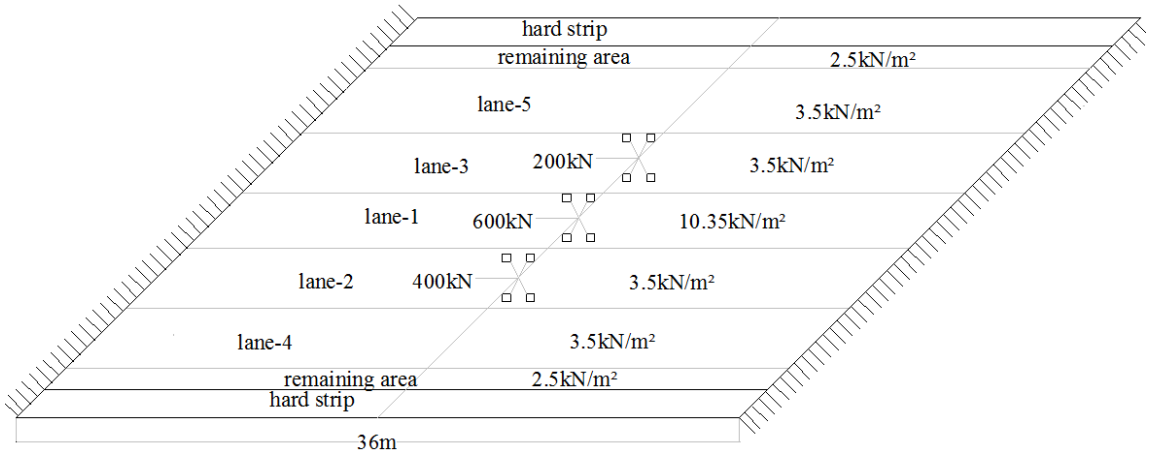

Fig9. 3, Load cases and arrangement for transverse bending moment in the deck

In addition to the live loads shown in the above three figures, the permanent load due to asphalt layer and edge elements were considered in the finite element models. Three different load combinations for longitudinal bending, torsion near obtuse corner and transverse deck was considered.

9.3 Result of the two finite element modes

The following tables show the result of orthotropic plate and Eccentric beam element models.

Orthotropic plate(shell elements) model with end diaphragms				
	Bending moment in the first inverted T-girder	Design torsion moment in the first inverted T-girder	Torsion in the end diaphragm Beam	Transverse moment in the deck
0^o	3158	58	186	27
15^o	3139	68	214	28
30^o	3119	76	240	28
45^o	3037	90	260	29
60^o	3017	124	290	37

Table 9. 1, Result of orthotropic plate model

In the above table, the torsion moment found in the finite element model was multiplied by two to get the design values. The locations of the maximum bending moments in the longitudinal direction for each angle of skewnesses are not the same. For high skewness the location of the maximum moment shifts towards the obtuse corner from the middle of the bridge. In the table above the locations at which the maximum moment obtained are not the same.

Eccentric beam element for girders and orthotropic plate(shell elements) for deck with end diaphragm beams					
	Bending moment in the first inverted T-girder	Torsion moment in the first inverted T-girder	Normal force in the first inverted T-girder	Torsion in the end diaphragm Beam	Transverse moment in the deck
0^o	3065	70	844	246	24
15^o	3055	82	827	266	25
30^o	3044	94	810	285	25
45^o	2989	103	772	290	26
60^o	2765	134	720	305	32

Table9. 2, Result of Eccentric beam element model

The longitudinal bending, torsion moment in the girders and transverse bending in the deck tabulated in the above two tables were with their respective different worst load combinations and in critical variable load arrangements.

9.3.1 Effect of skewness in bending moment in the longitudinal direction

The following graph shows the longitudinal bending moment results of the two finite element modeling techniques mentioned above.

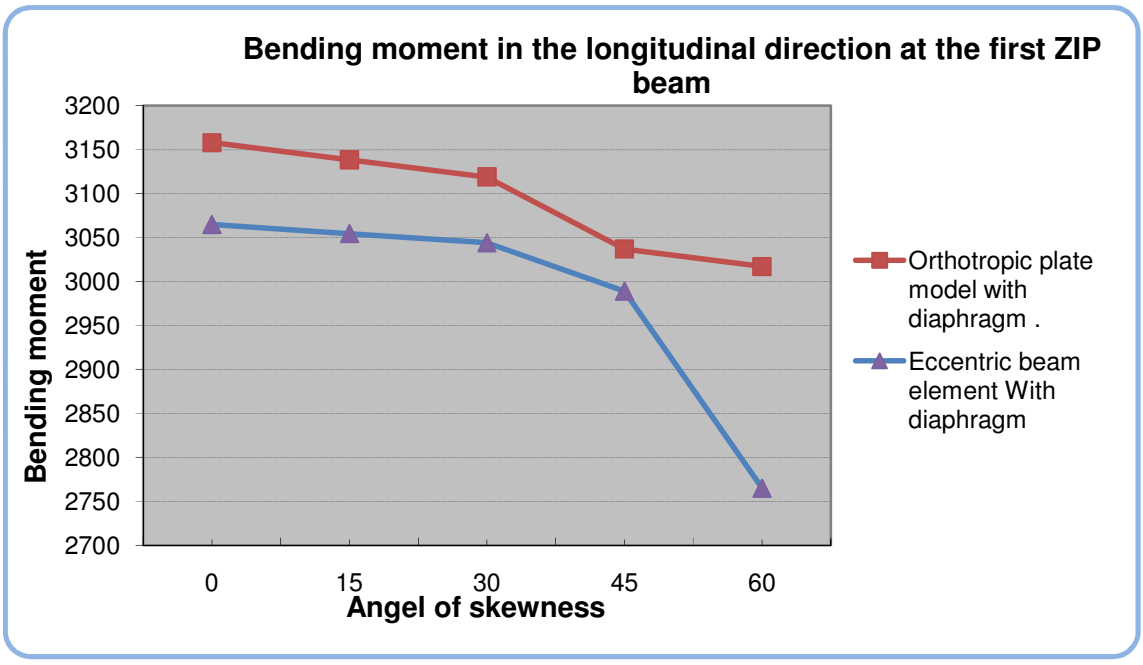

Graph9. 1, Longitudinal bending moment verse skew Angle

The skew angle of the bridges is the most critical parameter that affects the wheel-load distribution and is the focus of this study. Results from the 36m bridges investigated shown in

the above graph that skew bridges always have smaller design live-load longitudinal moments than right bridges with the same span and width. This result corroborates similar conclusions by all researchers mentioned in the literature review part of this work. From the above graph, for bridges with skew angle not exceeding 30^o the reduction in the longitudinal live load bending moment to the first inverted girder attains 1.5% in both finite element techniques considered. For skew angles between 30^o and 60^o the reduction attains 10% and 5% for eccentric beam element and orthotropic plate models respectively. As can be seen from the table9.2, for a 45^o skew bridge, the decrease in longitudinal bending moment is only 5%. For a 60^o skew bridge, however, the bending moment reduction increased to 10%.

9.3.2 Effect of skewness in Torsion moment in the First Inverted T-Girder

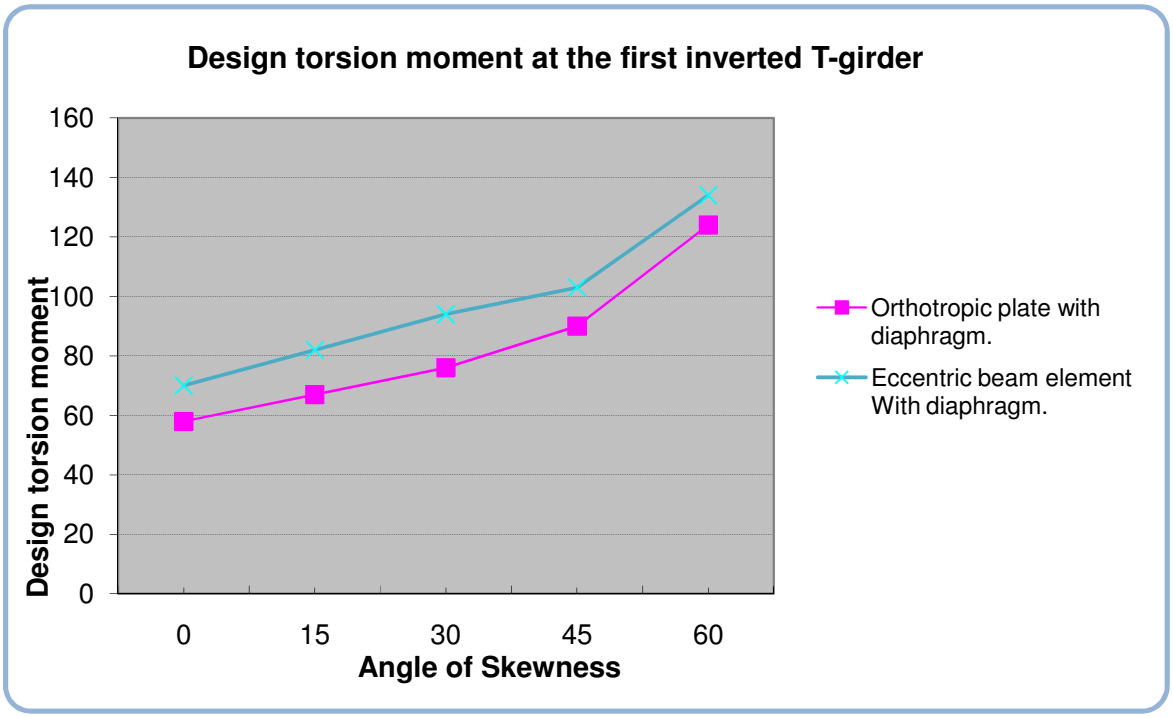

Graph9. 2, Torsion moment in the first Inverted T-girder

The decrease in longitudinal moment up to 10% in high skew bridges has been accompanied by a big increase in torsion moment in girders. As shown in graph9.2, for 60^o skewness, the torsion moment at the obtuse corner of the first inverted T-girder increases by more than 100% as compared with right bridge. For decks with skew angle up to 30^o, the increase in torsion moment attains 30%. Although percentage variation in results for angle of skewness less than 30^o seems larger, the actual difference between the results is very small. Therefore,

increase in twisting moment due to skewness less than 30^o is insignificant. Graph9.2 shows typically that the sensitivity of the rate of increase in torsion moment with respect to skew angle is high for decks with a skew angle more than 45^o. The above graph additional revealed that the two finite element models produced parallel lines and the difference in the design torsion was trivial.

9.3.3 Effect of skewness in bending moment in the transverse direction of the deck

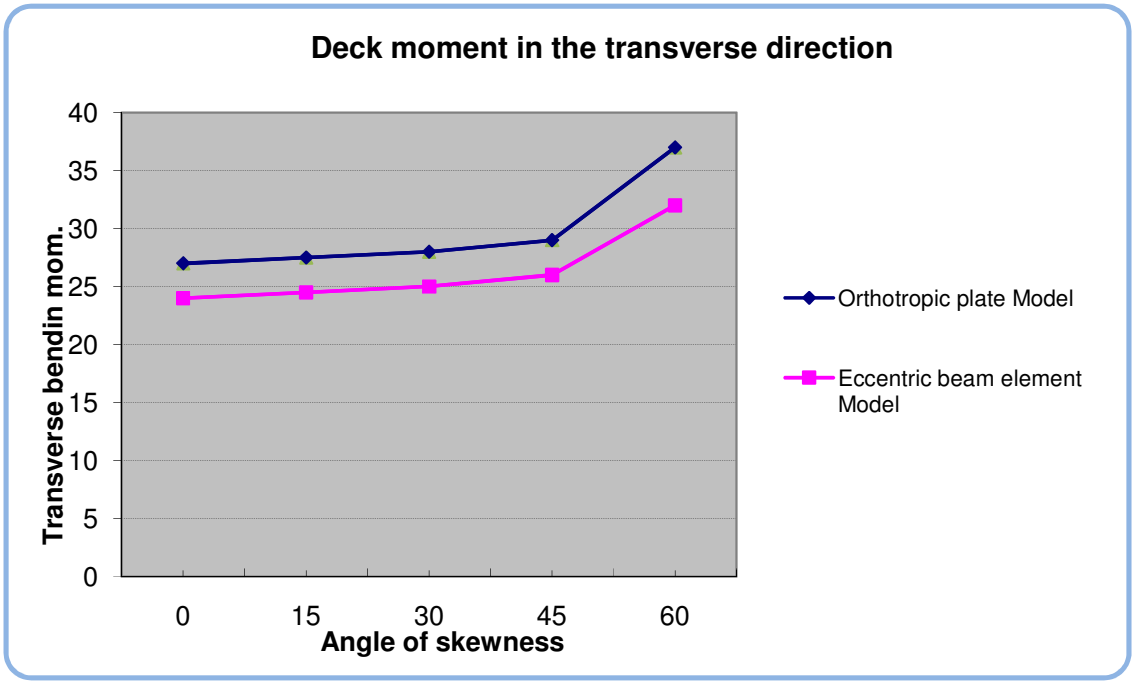

Graph9. 3, Transverse moment in the deck

As torsion moment of the girders, the transverse moment in the deck increases with increase in angle of skewness. For 60^o skewness, the transverse live load moment in the deck increases by more than 35% as compared with right bridge .Graph9.3 shows that, for decks with skew angle up to 45^o, the rate of increase in live load bending moment in the transverse direction is approximately constant. However, for skew angles more than 45^o this has found to be very sensitive. The same observation was made in torsion moment for angle of skew greater than 45^o. The transverse moment in eccentric beam element model is less than in magnitude than orthotropic plate model. This is due to the fact that in eccentric beam element model there is tension normal force in the deck in addition to bending moment, which makes the design tension stress will be more or less the same in both cases.

9.4 Summary and conclusion

The effects of skew angle in single-span multilane reinforced concrete deck slab on precast presteressed girders composite bridge were investigated and the FEA results are presented in this chapter of this thesis work. The study involved keeping the geometric characteristics of the bridges like span length and deck width unchanged and taking four distinct skew angles. The live load longitudinal bending moment, torsion moment near obtuse corner of the bridge, and transverse moment in the deck were compared with the reference straight bridge to clearly understand the effect of skewness on this kind of viaducts.

The ratio between the FEA longitudinal moments in the first inverted T-girder for skewed and straight bridges was almost one for bridges with skew angle less than 30°. As the askew angle of the bridge increases to 60^{o} the longitudinal bending moment in the reference girder decreases by 10%. This decrease in the longitudinal moment is offset by an increase by up to 35% in the maximum transverse moment in the deck and by up to 100% in torsion moment in the girders as the skew angle increases from 0^{o} to 60°.

It can be concluded that large skew angles always reduce the longitudinal bending moment and increases the torsion moment at the obtuse corner of the bridge and the transverse bending in the deck. This might be due to the fact that some of the wheels of trucks on skew bridges are closer to the supports than on right bridges. Another reason may be that in short spans with large skew angle bridges, the slab tends to bend along a direction perpendicular to the abutments. This action can transfer part of the load from deck slabs directly to the supports, rather than through the girders as in right bridges.

CHAPTER 10, ADVANTAGE AND DISADVANTAGE OF CONSIDERING THE END DIAPHRAGM BEAMs IN THE FE MODEL

10.1 Introduction

Diaphragms are intended to tie girders together to facilitate construction and maintenance, transfer lateral loads and improve traffic load distributions. Therefore, this element may be one of the important structural components for bridge load capacity. Nevertheless, in the calculation of live load distribution and capacity verification, many codes of recommendations and researches recommends to exclude the effect of diaphragms in the model.[24] As the result, it is a common practice to ignore the contribution of end diaphragms in the analysis. However, providing wide full depth diaphragm beams thinking that it will help load distribution between girders is questionable.

As part of this case study, the load distribution of 36m long and 20m wide skew bridge was tested with and without considering the stiffness of the end diaphragm beam in the serviceability limit state. For models with end diaphragm beams, 900mm wide cast in place reinforced concrete diaphragm beams were added at both supports of the bridge. 0^o, 30^o, 45^o and 60^o skewness were examined. In all cases cracked stiffness, half of the young's modulus of the in-situ concrete, in the end diaphragm and in the transverse direction of the deck is considered. However, full stiffness is assigned in presteressed girders and in the longitudinal direction of the deck. Material properties for both deck and girders were identical to the previous chapters. All four angle of skewness were tested using orthotropic plate and eccentric beam element modeling methods using SCIA Engineer general purpose commercial finite element package.

In orthotropic plate model, the end diaphragm beam was modelled as an isotropic plate having same property in all directions. However, in eccentric beam element, the diaphragms were modelled as a space truss element connecting the girders in the transverse direction. The end diaphragm beams and the longitudinal girders were eccentrically connected to the deck slab.

Three variable load arrangements for longitudinal bending, torsion and transverse deck bending, which were considered in chapter 9 was taken up in this part. Permanent loads such as asphalt layer and edge element loads were also added in the finite element model.

10.2 Model results

Orthotropic plate(shell element) model				
Without end diaphragm beams				
Angle of skew	Bending moment in the first inverted T-girder	Design torsion in the first inverted T-girder	Transverse moment in the deck	Design torsion in the end diaphragm beam
0^o	3237	94	29	-
15^o	3207	104	30	-
30^o	3177	112	31	-
45^o	3124	142	32	-
60^o	3102	170	38	-
With end diaphragm beams				
0^o	3158	58	27	186
15^o	3139	68	28	214
30^o	3119	76	28	240
45^o	3037	90	29	260
60^o	3017	124	37	290

Table10. 1, Results of orthotropic plate model with and without end diaphragm beams

Orthotropic plate(shell element) for deck and Eccentric beam element for girders model					
Without end diaphragm beams					
Angle of skew	Bending in the first inverted T-girder	Design torsion in the first inverted T-girder	Normal Force in the first inverted T-girder.	Transverse moment in the deck	Design torsion in the end diaphragm beam
0	3150	73	922	26	-
15	3141	87	905	27	-
30	3132	101	888	28	-
45	3100	123	870	30	-
60	2929	148	833	35	-
With end diaphragm beams					
0	3065	70	844	24	246
15	3055	82	827	25	266
30	3044	94	810	25	285
45	2989	103	772	26	290
60	2765	134	720	32	305

Table10. 2, Result of Eccentric beam element model with and without end diaphragm beams

10.2.1 Effect of considering end diaphragm beams in the longitudinal bending moment of the first inverted T-girder

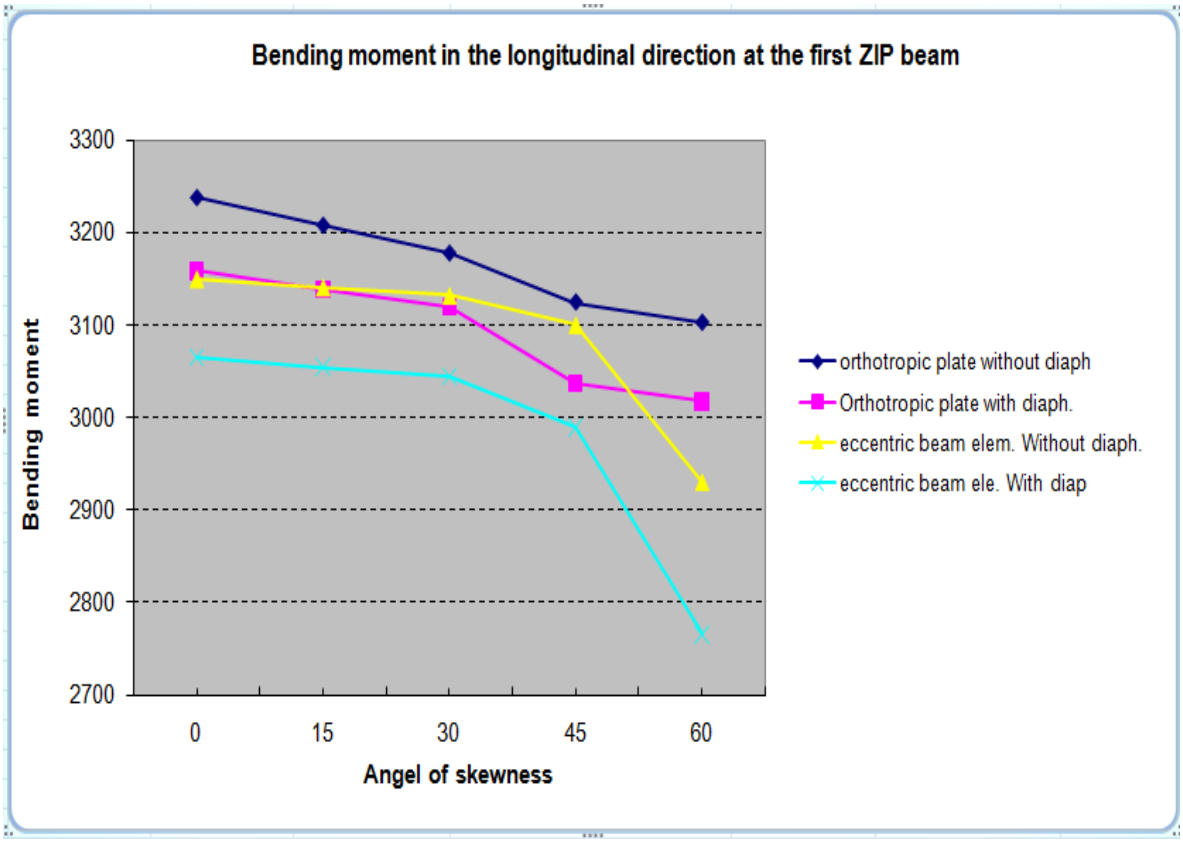

Graph10. 1, Longitudinal bending moment with and without end diaphragm beam

1. Orthotropic plate model:

In orthotropic plate model, considering the stiffness of the end diaphragm beam in the analysis has small decrease in longitudinal bending moment in the girders. As shown in graph 10.1, the blue and the pink lines are almost parallel. This implies effect of end diaphragm beam in the longitudinal bending moment of the girders is barely affected by the skew angle. For 60^{o} skew angle, a 3% reduction in bending moment at the first inverted T-girder is observed. This is more or less true in all angle of skewness considered in this work.

2. Eccentric beam element for girders and orthotropic plate (shell element) for deck:

Graph-10.1 clearly shows that the bending moment in the longitudinal girders is predominantly affected by the angle of skewness. The effect of end diaphragm beam in the model is very minimal. For bridges with skew angles not exceeding 45^{o} the reduction in the longitudinal live load bending moment to the first inverted girder due to the stiffness of end diaphragm attains 4%. However, for skew angles between 45^{o} and 60^{o} the reduction increases

to 6%. Due to longitudinal in-plane tension force at loaded area of the girders, the longitudinal bending moment in eccentric beam element model is always less than the corresponding bending moment in the orthotropic plate model.

10.2.2 Effect of considering end diaphragms in Torsion moment in the girders

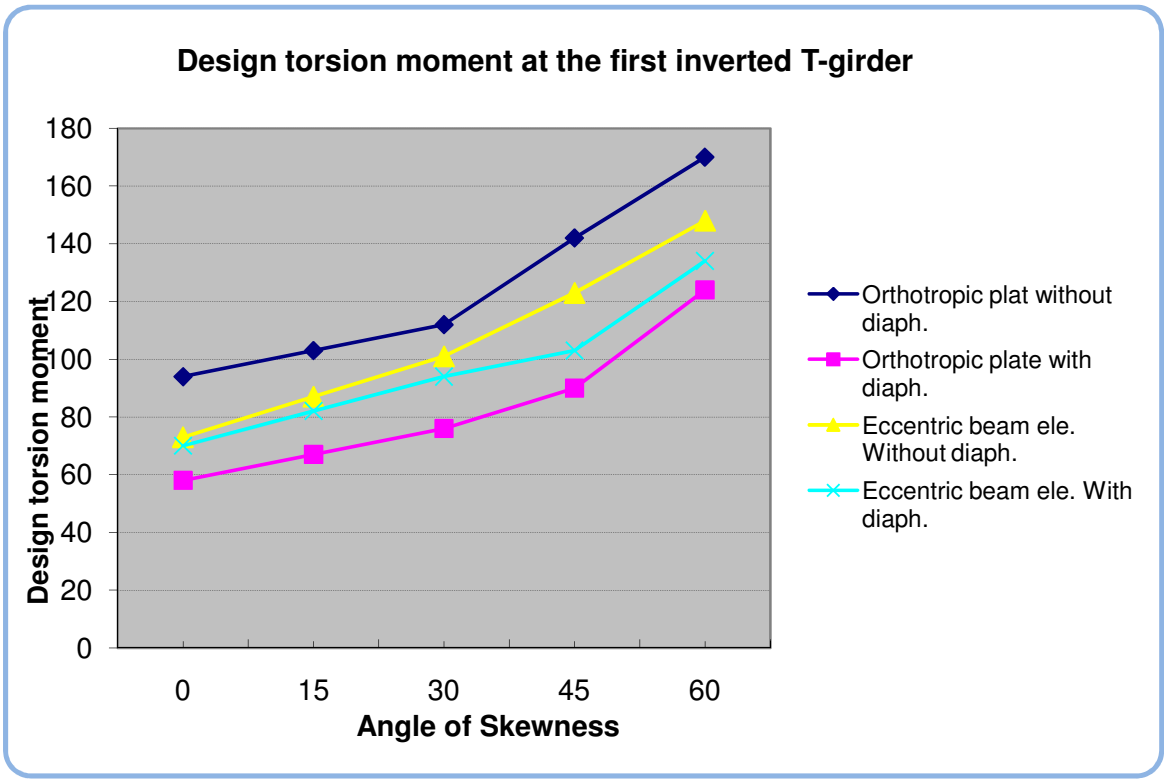

Graph10. 2, Torsion moment in the first inverted T-girder at the obtuse corner of the bridge

For bridges having angle of skewness less than 30^{o}, the stiffness's of end diaphragms have approximately 35% decrease in the torsion moment at the reference girder in orthotropic plate model. In eccentric beam element model, however, this reduction in torsional moment due to end diaphragm beams was found to be lower than 5%. In the plate model, for bridges with 60^{o} angle of skewness, the introduction of transverse end beam decreases the torsion moment at the first inverted T-girder by up to 20%. As a matter of fact, the amount of decrease in torsional moments at the reference girder due to the introduction of end diaphragm beam in orthotropic plate was found to be similar for all angle of skewness. The percentage difference is due to increase in torsion moment at high skew angles. With the same change in torsion moment, higher values have small percentage difference.

Graph10.2 additionally shows that, the change in torsion moment in the girders due to the presence of end transverse beam in the model is high in orthotropic plate model than in eccentric beam element model.

10.2.3 Torsion moment in the end diaphragm beam

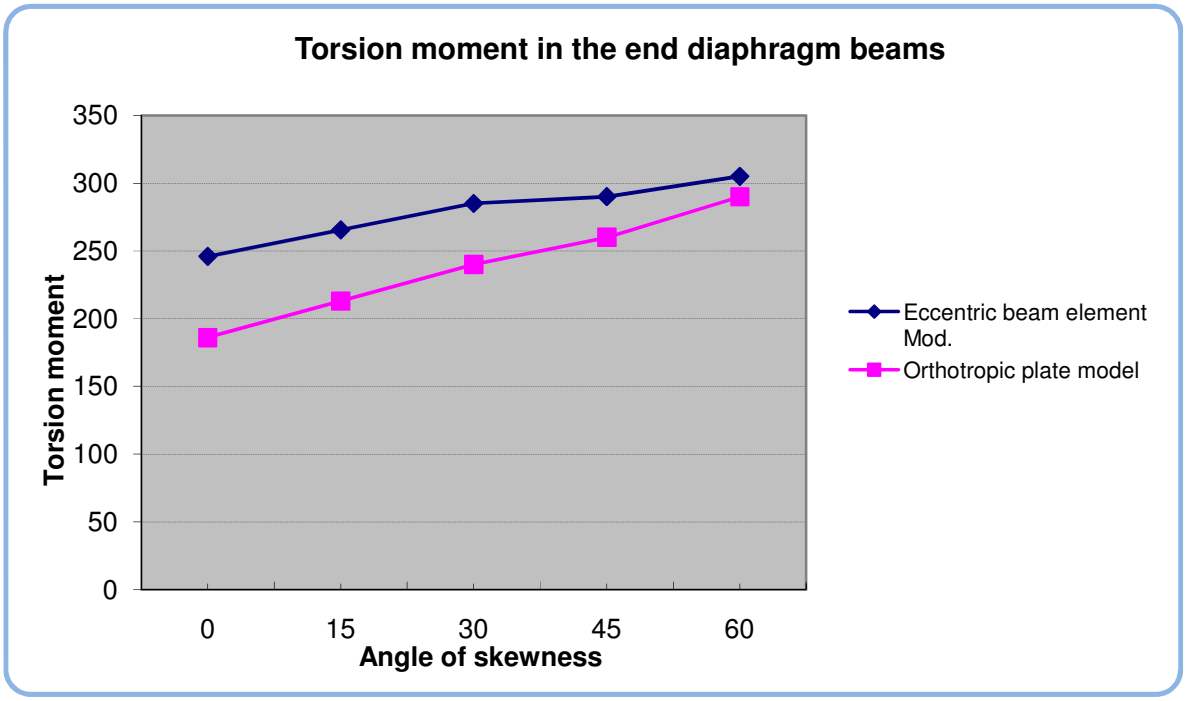

Graph10. 3, Torsion moment in the end diaphragm beam

In both finite element models examined, due to the occurrence of end transverse beam in the FE model, a small decrease in longitudinal bending and torsion moment in the girders has been observed. This decrease in bending and twisting moment is as the expense of very high torsion moment in the end diaphragm beams. The magnitude of the torsion moment in the transverse beams exceeds 300kNm in both models. From graph 10.3 shown above, the torsion moment in the end transverse beam increase linearly with skew angles in both models. The above graph further made clear that, the two models have equivalent torsion moments in the transverse end beams.

10.2.4 Effect of considering end diaphragm in the transverse bending moment of the deck

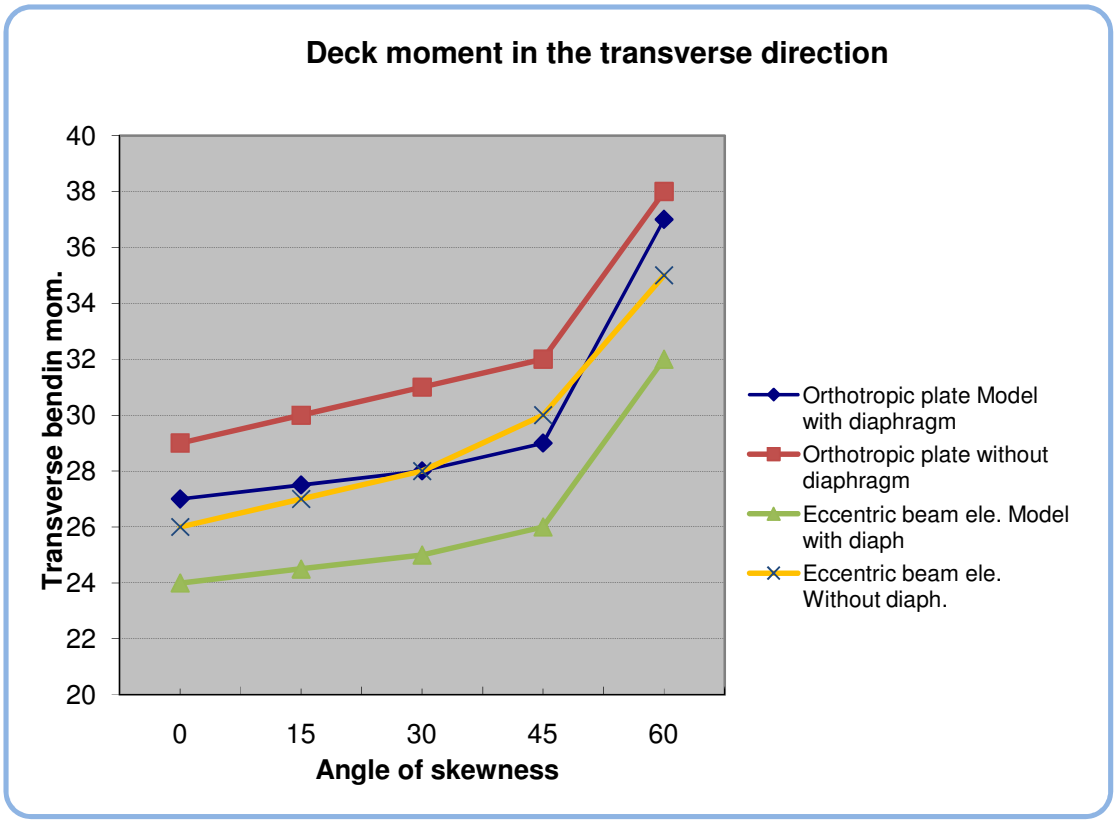

Graph10. 4, Transverse bending moment in the deck

Like longitudinal bending and twisting moment, the transverse bending moment in the deck decreases when the transverse support beams were taken in to account in the FE model. From graph10.4, in orthotropic plate model the decrease in transverse moment in the deck is in the order of 1-2kNm/m. This decrease varies from 2-4kNm/m in eccentric beam element model. Due to the presence of transverse in-plane tension force in the deck at the middle of the deck, the transverse bending in the deck for eccentric beam element model is smaller than the corresponding plate model.

10.3 Summary and conclusion

The effects of introducing the stiffness of end transverse beam in the finite element model in a single-span multilane cast in-situ reinforced concrete deck on precast prestressed girders composite bridge were investigated. Two finite element modeling techniques were examined and the results of the two models were presented. 36m long and 20m right width bridge with four different skew angles with and without end transverse beams were analyzed to look into the sensitivity of the bridge performance on the diaphragm stiffness. The live load longitudinal bending moment, torsion moment near obtuse corner of the bridge in the girders, edge transverse beam torsion moment and transverse bending in the deck were compared with and without diaphragm beams to evidently understand the effect of considering the stiffness of end transverse beams in the model.

In this part of this thesis work it has been made clear that taking the stiffness of end diaphragm beam in the analysis results in up to 4% decrease in live load bending moment and up to 35% live load torsion moment in the presteressed girders. Very small reduction in transverse bending is also observed in the cast in-situ deck slab. These decreases in span bending moments and torsion moments have been accompanied by a high live load torsion moment in the transverse end beams. The percentage decrease in variable load longitudinal bending moment is a very small portion of the whole bending moment when the self weight of the bridge is included.

Practices showed that placing reinforcement and constructing diaphragms used in prestressed girder bridges on skewed viaducts are difficult. As the skew angle increases and girder spacing decreases, the connection and the construction become more intricate. In spite of this fact, in very skew bridges the presence of end diaphragm beams in the FE model decreases especially the torsion moments in some extent. At high angle of skewnesses, the shear stresses as the result of torsional moments and shear forces might be large and excessive stirrups would be required. To optimize the required stirrups in the inverted T-girders the introduction of the end diaphragm beams in the FE model is advantages. However, in small angle of skewnesses, the presence of end diaphragms in the finite element model would be additional labour work and could be eliminated.

CHAPTER 11, CONCLUSIONS AND RECOMMENDATIONS

The main goal of this research study was to develop a numerical modelling technique capable of predicting the three dimensional behavior of skew bridges consisting of cast in-place concrete deck on precast prestressed inverted T-girders. Different finite element modelling methods were tested and compared with a 3D volume element model. The Torsional moments in the skew bridge was the most fascinating part of this work. This is due to the fact that, the torsion moments near the obtuse corner of skew bridges are generally high. Concentrated and uniformly distributed variable loads, which covers most of the effect of the traffic of Lorries and cars as per Euro code of recommendations was consulted. To determine the worst scenario in the particular bridge under consideration, different variable load arrangements were investigated. Based on this study the following conclusions are consolidated.

1. For the particular bridge considered, the maximum torsional moment is near the obtuse corner of the bridge. It was obtained by putting the axle load close to the edge of the bridge in the middle of the span. [Refer- Fig3.16] It was remarkable that the extra design axle loads reduce this torsion moment. For UDL, placing the first design lane load at the first notional lane and leaving unloaded for the others creates maximum effect. This simple rule has been obtained by studying all possible load configurations for all variable load cases.
2. Five structural models have been developed and analyzed for the particular bridge. Comparison shows that the model consisting of shell elements for the deck and Eccentric beam elements for the girders is best choice for engineering practice [Table8.4]. This recommendation is based on accuracy in results, the modelling time, and the post processing effort.
3. The orthotropic plate model failed to predict the transverse and the longitudinal in-plane forces (n_y and N). The other result, m_x, m_y and m_{xy} are sufficiently accurate for engineering design.
4. Analysis has been made with the orthotropic plate modelling method where the contribution of the girders to the torsion stiffness had been ignored. This had very little influence on the maximum bending moments. This shows that for ultimate limit state equilibrium, it is possible to leave out the torsional reinforcement. However, Euro-code detailing rules to avoid excessive cracking should be consulted.

5. A centric beam element model for girders is not suitable for modelling the bridge considered. This is because, this modelling technique is unable to calculate the flexural stiffness of the composite system about the major axis correctly and it was found to be the most erroneous model to capture the three-dimensional behavior of the real bridge.
6. All three of the 3D models developed in this study showed that for linear elastic analysis, a tension normal force in the transverse direction of the deck was occurred under vertical loading. This result is carefully checked and considered to be correct. However, hand calculations and experimental results showed that when cracking is included this tensile membrane force becomes compressive. This compressive force is advantages to increase the shear capacity of the deck. Therefore linear elastic analysis is not appropriate to determine the membrane force in the lateral direction of the deck. Consequently, the shear capacity of the deck is underestimated.
7. Live-load maximum bending moments in girders of skew bridges are generally smaller than those in right bridges of the same span and deck width. The larger the skew angle, the smaller the live load bending moments of the girders. On the contrary, the torsional moments in the obtuse corner of the bridge and the transverse moments in the deck increases with skew angels. These effects have been negligible for skew angles less than 30^{o}.
8. The bridge at hand with different skew angles was analyzed to investigate the sensitivity to the presence of diaphragm beams. End diaphragm beams decreases the bending and twisting moments in the girders and the deck. However, this reduction was insignificant as compared to the torsional moments occurring in the diaphragm beams.

RECOMMENDATIONS

a. It would be convenient to model skew bridge with skew angle larger than 30^o as an equivalent right bridge. As explained in the conclusion part, the predicted bending moment would be large and the torsion moments would be small. The resulting reinforcement could be still sufficient. More research on this area is recommended.
b. End diaphragm beams could be excluded from the finite element model. This has only very small effects on the internal forces and moments due to vertical loading of the other structural elements of the bridge. In this case, the end diaphragm beams can be designed with minimum reinforcement according to Euro-code of recommendation.

c. For small angle of skewnesses the presence of end diaphragm beams gives only a small reduction of the longitudinal bending moments and the torsions for vertical loading. For the purpose of fast construction and economy the wide reinforced concrete diaphragm beams could be replaced by simple non structural elements. However, detail investigation of the consequences is required.

d. Presence of end diaphragm beams in the bridge restraint the horizontal expansion of the deck slab. This lateral restraint increases the strength of the deck slab in excess of those predicted by Eurocode of recommendations. This strength enhancement is the result of compressive membrane action. The degree of membrane action is strongly dependant on the magnitude of the lateral restraint and in reality the contribution of the end diaphragm beams to this lateral restraint can't be easily defined. Additional study to predict the contribution of the end diaphragm beams to the compressive membrane action in the considered bridge type is required.

REFERENCES

1. **C.HAMBLY, E.** *BRIDGE DECK BEHAVIOUR.* London : Clays Ltd. St Ives plc, 1991.

2. **M.J. Ryall, G. A. R. Parke and J. E. Harding.** *The Manual of Bridge Engineering.* 2000.

3. *LIVE LOAD MOMENT FOR CONTINUOUS SKEW BRIDGES.* **Mohammad, Khaleel and Rafik.** September 1990, Journal of Structural Engineering, pp. 1-13.

4. *Finite Element Analysis of Steel Girder Highway Bridges.* **al., Mabsout. et.** s.l. : Journal of Bridge Engineering,1(3), 1997.

5. *Load Distribution Factors in Simply Supported Skew bridges.* **Mirzabozorg, Khaloo and.** s.l. : JOURNAL OF BRIDGE ENGINEERING © ASCE, July/August 2003, Vols. 8, No-4.

6. *Load Distribution for a Highly Skewed Bridge.* **Huang, Shenton, and Chajes.** s.l. : Journal of Bridge Engineering, , November, 2004, Vols. Vol. 9, No. 6.

7. *Influence of Skew Angle on Reinforced Concrete Slab Bridge.* **Menassa, Mabsout, Tarhini and Frederick.** s.l. : the Journal of Bridge Engineering, March 1, 2007, Vols. Vol. 12, No. 2.

8. *EFFECT ON SUPPORT REACTIONS OF T-BEAM SKEW BRIDGE DECKS.* **Misra, Trilok Gupta and Anurag.** s.l. : ARPN Journal of Engineering and Applied Sciences, FEBRUARY 2007, Vols. VOL. 2, NO. 1.

9. *Influence of Diaphragms on Load Distribution in P/C I-girder Bridges.* **Griffin.J.J.** s.l. : PhD Dissertation, University of Kentucky, 1997.

10. *Non-destructive test of field bridges in Florida.* **Cai. C.S., Shahawy. A.M. and El-Saad. A.** Texas : s.n., 1998.

11. *Live-Load distribution factors in prestressed concrete girder bridges.* **F., Barr P. J. Eberhard M. O. and Stanton J.** s.l. : Journal of Bridge Engineering, September/October 2001.

12. *Effectiveness of Continuity Diaphragm for Skewed Continuous Prestressed Concrete Girder Bridges.* **Aziz Saber, Freddy Roberts, Walid Alaywan and Joseph Toups.** s.l. : PCI JOURNAL, March–April 2007.

13. *Shear resistances of concrete slabs at concentrated loads close to supports.* **P.E.Regan.** 1982

14. *Bridge Engineering Lecture Note.* s.l. : Technical University of Delft, 2008.

15. **Hoefakker, J. Blaauwendraad and J.H.** *THEORY OF SHELLS.* s.l. : Delft University of Technology, September 2003.

16. **Blaauwendraad, Prof.dr.ir.J.** *Plate Analysis, Theory and Application* . s.l. : Technical University of Delft, November 2006.

17. **Mahmoud E. Kamara, Ph.D., and Basile G. Rabbat, Ph.D., S.E.** *Torsion Design of Structural Concrete Based on ACI 318-05.* September 2007.

18. **EUGENE. J and DAMIEN L. KEOGN,** BRIDGE DECK ANALYSIS, Dublin, Ireland1999

19. European standard (2005), Euro-code 1" Actions on structures-part 2 traffic loads on bridges.

20. European standard (2005), Euro-code 2: Design of concrete structures –part 1-1: General rules and rules for buildings

21. European standard (2005), Euro-code 2: Design of concrete structures –concrete bridges – Design and detailing rules.

22. European standard (2005), NEN-EN 1337-3 (Structural bearings-Part3-Elastomeric bearings)

23. American Association of State Highway and Transportation Officials (AASHTO), "Standard specification for highway bridges," Washington, DC. 2002.

24. American association of State Highway and Transportation Official (AASHTO), "LRFD Bridge Design Specification," Washington, Dc 2004.

25. Old design reports from Spanbeton prefab company

26. SCIA Engineer finite element software manual

27. ATENA 3D and ATENA WIN finite element software manuals

28. Serviceability of Bridge Deck Slabs with Arching Action. **Susan E. Taylor, Barry Rankin, David J. Cleland, and Jim Kirkpatrick**: ACI structural Journal, Title no. 104-S05